

**Genomic approaches to dorsoventral patterning and
functional studies of epithelial morphogenesis in
the short-germ beetle *Tribolium castaneum***



Inaugural-Dissertation

zur

Erlangung des Doktorgrades

der Mathematisch-Naturwissenschaftlichen Fakultät

der Universität zu Köln

vorgelegt von

Nadine Frey

aus Lindau (Bodensee)

Köln, 2017

Berichterstatter:

Herr Professor Dr. Siegfried Roth

Herr PD Dr. Michael Kroiher

Vorsitzender der

Prüfungskommission:

Frau Professor Dr. Ute Höcker

Tag der mündlichen Prüfung:

19.12.2017

Table of contents

Zusammenfassung.....	7
Abstract	9
CHAPTER I	
Reconstructing the dorsoventral gene regulatory network of <i>Tribolium castaneum</i>	10
1 Introduction.....	10
1.1 Gene regulatory networks (GRNs).....	10
1.2 <i>Tribolium</i> as an emerging model organism	11
1.3 The evolution of dorsoventral patterning	13
1.3.1 Formation of the dorsoventral axis in <i>Drosophila melanogaster</i>	14
1.3.2 The dorsoventral gene regulatory network of <i>Tribolium castaneum</i>	15
1.4 Identification of new DV-patterning genes by differential expression analysis	17
1.4.1 Generation of knockdown embryos lacking key DV patterning genes	17
1.4.2 Validation of the knockdown efficiency	20
1.4.3 Identification of differentially expressed genes.....	20
1.5 Aims of the study.....	22
2 Results	23
2.1 Verification of the RNA-seq data by an <i>in-situ</i> hybridization screen	23
2.1.1 Detailed analysis of two subgroups of differentially expressed genes	24
2.1.2 Identification of genes regulated by Dpp	24
2.1.3 Expression patterns of genes regulated by Toll and/or Twist.....	26
2.2 Functional analysis of genes potentially involved in the DV-GRN of <i>Tribolium</i>	28
2.2.1 Functional analysis of Sog/Dpp targets	29
2.2.2 Functional analysis of Toll and Twist targets.....	31
3 Discussion.....	36
3.1 Verification of the RNA-sequencing data.....	36
3.2 Expression patterns of some candidates suggest an involvement in DV patterning	37
3.2.1 <i>Tc-uninflatable</i> knockdown affects the formation of abdominal segments	38
3.2.2 <i>Tc-tartan</i> is an early regulator in neurogenesis	38
3.2.3 Involvement of the FGF pathway in formation of mesodermal derived tissue	39

3.2.4	Extracellular matrix components (ECMs) and their role in mesoderm formation.....	40
3.2.5	Zfh1 - A new essential regulator maintaining late <i>Tc-twist</i> expression	41
3.3	Possibilities and limitations of comparative analysis by RNA-sequencing.....	42
3.3.1	Stronger influence of <i>Tribolium</i> homologs on early embryonic development	42
3.3.2	Comparative analysis for de novo identification of DV-GRN components	43
3.3.3	Reasons for the detection of false positives	44
3.4	Conclusion	45
3.5	Outlook.....	46

CHAPTER II

	Fog signaling and its role in epithelial morphogenesis in <i>Tribolium castaneum</i>	47
1	Introduction.....	47
1.1	The role of cell shape changes in embryonic development.....	47
1.2	The Fog signaling pathway	49
1.2.1	The Pathway components and their interaction.....	49
1.2.2	Regulation of Fog signaling.....	52
1.2.3	Fog and T48 - Two distinct mechanisms of myosin localization	52
1.3	Conservation of Fog signaling in insect morphogenesis	54
1.4	Different modes of mesoderm internalization.....	55
1.5	Morphogenetic movements during <i>Tribolium</i> gastrulation.....	56
1.6	Aims of the study.....	59
2	Results	60
2.1	Expression patterns of the Fog signaling key components in <i>Tribolium castaneum</i>	60
2.2	Knockdown of Fog signaling components in <i>Tribolium</i> results in a variety of defects	65
2.3	Fog signaling is required for primitive pit formation	66
2.4	Mesoderm invagination is delayed upon <i>Tc-fog</i> knockdown	70
2.5	Positioning of the primordial germ cells is controlled by Fog signaling.....	75
2.6	Regulation of Fog signaling in <i>Tribolium</i>	77
2.7	Serosa spreading - A novel function of Fog signaling.....	81
2.8	Knockdown of smog does not result in morphogenetic defects	83
2.9	T48 does not contribute to mesoderm internalization in <i>Tribolium castaneum</i>	85

3	Discussion	86
3.1	Fog and its conserved role in tissue internalization during gastrulation	86
3.2	Genes with less influence on apical constrictions in <i>Tribolium</i> compared to <i>Drosophila</i>	88
3.3	The importance of posterior amniotic fold formation by Fog signaling	89
3.4	Positioning of the primordial germ cells is influenced by Fog signaling	90
3.5	The regulatory network underlying Fog signaling.....	92
3.6	Serosa spreading and cellularization - A novel function of Fog signaling	93
3.6.1	Fog signaling regulates flattening of the serosa cells.....	93
3.6.2	A role of Fog signaling in the blastoderm.....	95
3.7	Conclusion	97
	Material &Methods.....	98
1	Strains.....	98
2	Animal keeping and embryo collection.....	98
3	Total RNA isolation	99
4	cDNA synthesis	99
5	Primer design.....	100
6	Standard Polymerase Chain Reaction (PCR).....	100
7	Gel electrophoresis.....	101
8	<i>In-situ</i> hybridization (ISH)	101
8.1	Generation of mRNA probes	101
8.1.1	Two-step Polymerase Chain Reaction	101
8.1.2	Probe synthesis.....	102
8.2	Embryo fixation	103
8.3	Detection of mRNA expression	103
9	Double <i>in-situ</i> hybridization (dISH)	104
10	Fluorescence staining	106
10.1	Phalloidin staining	106
10.2	Nuclear staining.....	107
10.2.1	DAPI staining.....	107
10.2.2	Sytox staining.....	107
11	Generation of knockdown embryos by RNA interference (RNAi).....	108
11.1	Production of double-stranded RNA (dsRNA)	108

11.1.1	2. PCR for amplification of a dsRNA template.....	108
11.1.2	dsRNA synthesis	108
12	Adult or pupal injections (pRNAi).....	109
13	Embryonic injections (eRNAi).....	110
14	Cuticle preparation.....	111
15	Cryosections	111
16	Microscopy	112
17	Live-imaging.....	112
	References.....	113
	Appendix A: Primerlist RNA-Seq.....	123
	Appendix B: Genes differentially expressed upon <i>Tc-dpp</i> kd and <i>Tc-sog</i> kd	124
	Appendix C: Genes differentially expressed upon <i>Tc-twist</i> vs <i>Tc-Toll</i> knockdown	125
	Appendix D: Marker gene expression in <i>Tc-sog</i> and <i>Tc-dpp</i> knockdown embryos	127
	Appendix E: Marker gene expression in <i>Tc-Toll</i> and <i>Tc-twist</i> knockdown embryos	128
	Appendix F: Varsity in knockdown strength of <i>Tc-LanB1</i>	129
	Appendix G: Primerlist Fog signaling.....	130
	Appendix H: Movies	130
	Acknowledgements.....	131
	Erklärung zur Dissertation	132
	Lebenslauf	133

Zusammenfassung

Ein entscheidender Schritt in der frühen Embryonalentwicklung ist die Festlegung verschiedener Zellschicksale entlang der dorsoventralen (DV) Achse. Das Zellschicksal wird durch die räumliche und zeitliche Expression bestimmter Gene festgelegt, die durch genregulatorische Netzwerke (GRN) reguliert werden. Diese Arbeit befasst sich mit der Evolution des DV-GRN von Insekten. In der Gruppe der stark spezialisierten Drosophiliden ist die dorsoventrale Musterbildung durch den Toll Signalweg reguliert, welcher den BMP Signalweg kontrolliert. Während das dorsoventrale Netzwerk in *Drosophila melanogaster* gut untersucht ist, ist nur wenig über das genregulatorische Netzwerk bekannt, welches die Bildung der dorsoventralen Achse des Roten Reismehlkäfers *Tribolium castaneum* reguliert. Das Ziel dieser Arbeit war es neue potentielle Dorsoventral-Gene in *Tribolium* zu identifizieren. Um dieses Ziel zu erreichen, wurde eine vergleichende Transkriptom-Analyse nach der Herunterregulierung verschiedener Bestandteile des Toll und BMP Signalwegs durch RNAi durchgeführt. Ich habe die Expressionsmuster ausgewählter Gruppen der 796 differentiell exprimierten Genen untersucht. Des Weiteren, wurden funktionelle Untersuchungen für Gene durchgeführt, die ein typisches dorsoventrales Expressionsmuster aufweisen. Die Ergebnisse weisen darauf hin, dass einige der konservierten Dorsoventral-Gene (z.B. Tartan) einen stärkeren Einfluss auf die dorsoventrale Musterbildung in *Tribolium* haben als ihre *Drosophila* Homologe. Zusätzlich unterscheiden sich die Expressionsdomänen von einigen Notch Signalweg Bestandteilen erheblich von denen ihrer Homologe in *Drosophila*. Interessanterweise wird Zfh-1 anders als in *Drosophila*, für die Aufrechterhaltung der *Tc-twist* Expression während der Keimbandstreckung benötigt und ist daher essenziell für die Entwicklung des Mesoderms in *Tribolium*.

Neben der Bildung der Körperachsen, tragen auch morphogenetische Bewegungen von Epithelien erheblich zur Entwicklung komplexer Embryonalstrukturen bei. In *Drosophila* ist der Fog Signalweg an der Kontrolle morphogenetischer Bewegungen beteiligt. Fog induziert apikale Zellkonstruktionen, welche die Invagination von Epithelien ermöglichen. Die Inaktivierung des Fog Signalwegs führt zu Defekten in der Internalisierung des Mesoderms und des hinteren Mitteldarms. Bisher wurde davon ausgegangen, dass der Fog Signalweg ausschließlich während Gastrulation einiger stark abgeleiteter Fliegen eine Rolle spielt. Im zweiten Teil dieser Arbeit wird die Funktion des Fog Signalwegs im *Tribolium* Embryo untersucht, welcher eine im Vergleich zu *Drosophila* ursprünglichere Form der Embryonalentwicklung aufweist. Interessanterweise führt die Herunterregulierung wichtiger Fog Signalwegbestandteile in *Tribolium* zu einer verzögerten Mesoderminternalisierung und einem vollständigen Verlust der Internalisierung des Hinterdarms und posterioren Endoderms. Dies weist auf eine Konservierung des Fog Signalwegs für die Gewebeinternalisierung während der Gastrulation außerhalb von höheren Dipteren hin. Zusätzlich werden in dieser Arbeit bisher unbekannt Funktionen

des Fog Signalwegs bei der Bildung der posterioren Amnionfalte, bei der Positionierung der primordialen Keimzellen und in der Ausweitung der extraembryonalen Serosa erläutert. Auch deuten die Ergebnisse auf eine weitere konservierte, allgemeinere Rolle von Fog für die Koordinierung von Zellformveränderungen im Blastoderm hin.

Abstract

A crucial step in early embryonic development is the determination of different cell fates along the dorsoventral (DV) axis. These cell fates are defined by the spatially and temporally restricted expression of gene sets, controlled by complex gene regulatory networks (GRN). Here, we address the evolution of the DV-GRN within insects. In the highly derived group of the drosophilids, dorsoventral patterning is dominated by Toll-signaling, which directly controls BMP-signaling. Whereas the DV-GRN of *Drosophila melanogaster* is well understood, little is known about the GRN that acts during establishment of the DV axis in more basally branching insects like the red flour beetle *Tribolium castaneum*. This work aimed to identify new potential DV patterning genes in *Tribolium*. To achieve this goal, a comparative transcriptome analysis after knockdown of Toll signaling and BMP signaling components by RNAi was performed. I analyzed the expression patterns of selected subgroups of the 796 differentially expressed genes. Furthermore, functional studies for genes exhibiting typical dorsoventral expression patterns were performed. The results suggest that some of the conserved DV-GRN components (e.g. Tartan) have a stronger and earlier influence on DV patterning in *Tribolium*. In addition, the expression of Notch signaling components clearly differs from the expression pattern of their *Drosophila* homologs. But the most striking finding was the identification of Zfh-1, which is required for maintaining *Tc-twist* expression during germ band extension and is thus essential for mesoderm development in *Tribolium*.

Besides the establishment of the body axis, morphogenetic movements of epithelial sheets significantly contribute to the development of complex embryonic structures. The Fog signaling pathway is one of the best studied processes in initiating early morphogenetic movements by cell shape changes. Modifications of the acto-myosin cytoskeleton by Fog signaling result in apical cell constrictions which enable bending of epithelial sheets. In *Drosophila*, loss of Fog signaling causes defects in mesoderm and posterior midgut internalization. So far, it was assumed that Fog signaling is exclusively involved in gastrulation in some highly derived flies. In the second part of this work the role of Fog signaling was analyzed in *Tribolium*, which possesses a more ancestral mode of embryogenesis. Interestingly, knockdown of important Fog signaling components in *Tribolium* cause similar defects in ventral furrow formation and internalization of the posterior endoderm. This indicates the conservation of Fog signaling in tissue internalization during gastrulation outside of higher dipterans. In addition, this work presents so far unknown functions of the Fog signaling pathway in formation of the posterior amniotic fold, positioning of the primordial germ cells and spreading of the serosa. Furthermore, the results suggest another conserved more general role of Fog in coordinating cell shape changes in the blastoderm.

CHAPTER I

Reconstructing the dorsoventral gene regulatory network of *Tribolium castaneum*

1 Introduction

1.1 Gene regulatory networks (GRNs)

Pathways are a simple way to visualize gene interactions. In a pathway each component acts upon a substrate or another gene product. Nevertheless, a pathway is often limited in describing the various complex gene interactions. In fact, genes or gene products are not only affecting single targets, but are also influenced by numerous gene products, deriving from multiple pathways. This complex system of interaction between different pathways can be best described as networks (Stern, 2010). Gene regulatory networks (GRNs) consist of various regulatory inputs like binding of gene products to enhancers, silencers and insulators (cis-regulatory elements) (Levine and Davidson, 2005). The diversity of cis-regulatory elements establishes compartmentation by enabling the independent control of gene transcription in different body parts (Carroll, 2005).

Transcription factors (TFs) are often the most essential parts of GRNs and act as key regulators. Different transcription factors can concurrently bind to one enhancer. Depending on the set of bound TFs at a specific time, the enhancer activates the expression of a specific gene set, thus resulting in functional output (Levine and Davidson, 2005). Furthermore, gene expression can be influenced by genetic circuits. By feed-forward loops components of a network can modify their own expression by either enhancing or repressing it. These circuits act directly by negative or positive self-regulation or indirectly via regulation of target genes (Peter and Davidson, 2011).

Embryogenesis is controlled by large gene-regulatory networks, which generate spatially and temporally refined patterns of gene expression, enabling progressive restriction of cell fates from pluripotent fields of cells to complex organs and tissues. (Sandmann et al., 2007). Evolutionary alterations of the functional organization of the gene regulatory networks that control development of the body plan cause changes in animal anatomy (Peter and Davidson, 2011). In fact, instead of changes in protein structure, evolutionary changes in morphology occur primarily through changes in regulatory sequences (Carroll, 2005). The dorsoventral gene regulatory network (DV-GRN) of *Drosophila* was already intensively studied (Bonn and Furlong, 2008; Stathopoulos and Levine, 2002, 2005). However, elucidating the genes and their interlinkage in the DV-GRN of more ancestral insects like *Tribolium* or *Oncopeltus*, might provide insights in the integration of Toll signaling in the regulation of early developmental processes like cell-fate determination.

1.2 *Tribolium* as an emerging model organism

Due to their diversity and the easy husbandry conditions, insects are suitable for evolutionary comparative analysis. *Drosophila* is a member of the evolutionary relatively young order of Diptera, and many aspects of its embryogenesis are highly derived. *Tribolium castaneum* (*Tc*) is a more basally branching member of the insect lineage, with ~300 million years of independent evolution from *Drosophila* (Rousso et al., 2010). Thus, it shares many features with other insects, particularly a more ancestral mode of embryonic development, compared to *Drosophila*. In long germ-type embryos, like those of *Drosophila melanogaster*, the segments are formed synchronously in the blastoderm. In short germ-type insects, like *Tribolium castaneum*, only head and thorax segments are generated in the blastoderm stage, while the abdominal segments derive from a posterior segment addition zone (Fig. 1.1) after gastrulation. In addition, *Tribolium* embryos develop two distinct extraembryonic membranes: amnion and serosa. The fruit fly possesses only a reduced amnioserosa (Tautz and Sommer, 1995). However, the localization of the three germ layers (mesoderm, neurogenic ectoderm and dorsal ectoderm) along the DV axis does not differ between both insects.

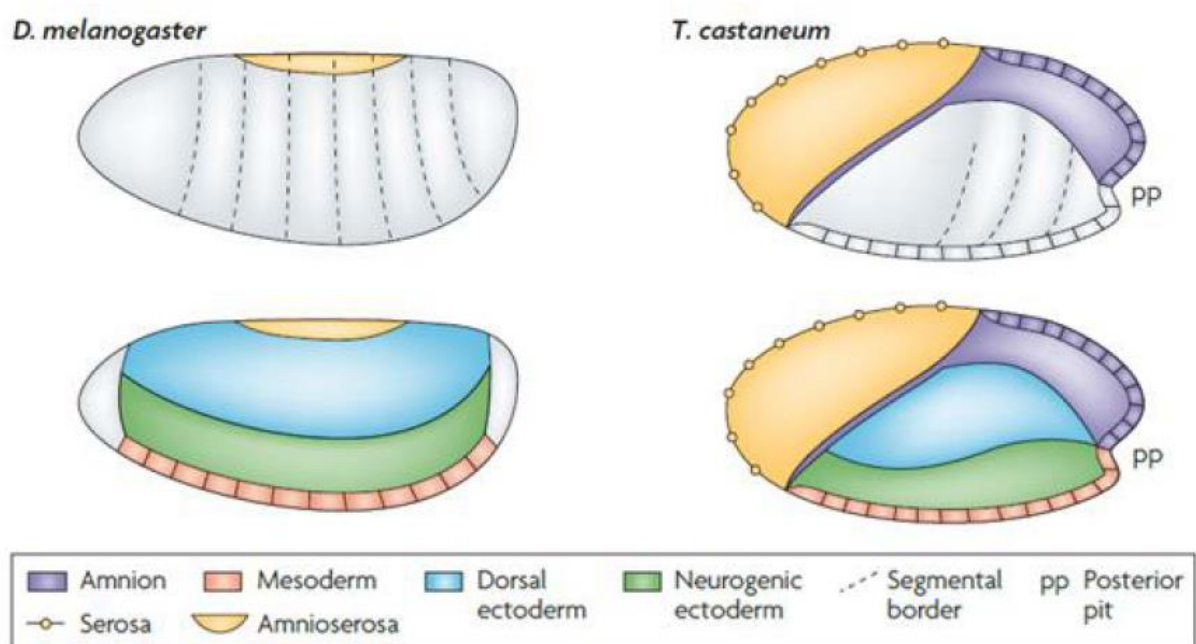


Figure 1.1: Fate determination and segmentation in *D. melanogaster* and *T. castaneum*

Drosophila as well as *Tribolium* mesoderm, neurogenic ectoderm and dorsal ectoderm are specified in the blastoderm. In long germ-type embryos like *Drosophila*, all segments are formed synchronously in the blastoderm. In short germ-type embryos, like *Tribolium castaneum* the segments are successively added at the posterior end after gastrulation. Only the most anterior segments are formed in the blastoderm. *Drosophila* possesses a single extraembryonic tissue, the amnioserosa. *Tribolium* has two extraembryonic membranes: amnion and serosa. modified from (Sommer, 2009)

Many tools for functional analysis are available in *Tribolium castaneum*. Diverse methods for generation of transgenic lines (Berghammer et al., 2009; Gilles and Averof, 2014; Gilles et al., 2015; Lorenzen et al., 2003; Pavlopoulos et al., 2004) and for transient gene expression (Benton et al., 2013) could be established, enabling advanced techniques like live-imaging. In addition, *Tribolium* shows a strong RNAi response (parental as well as embryonic) (Bucher et al., 2002; Posnien et al., 2009), providing many possibilities for functional studies. Furthermore, the availability of a well annotated genome (Tcas 5.2/OGS 3) as well as various transcriptomic data (different embryonic stages) and a database, containing functional information on genes based on a genome-wide RNAi screen (iBeetleBase, Schmitt-Engel et al., 2015), qualify *Tribolium* as a perfect candidate for comparative analysis. Although the DV-GRN of *Tribolium* shows some regulatory differences compared to the *Drosophila* DV-GRN, the flour beetle has still an evolutionary intermediate position compared to other insects. For example, the jewel wasp *Nasonia vitripennis* (Hymenoptera), or the milk weed bug *Oncopeltus* (Hemiptera) show both a stronger reliance on BMP signaling (Lynch and Roth, 2011; Ozuak et al., 2014; Sachs et al., 2015). The evolution of the insect DV-GRN will be described in detail in the next section.

1.3 The evolution of dorsoventral patterning

The formation of the two body axes, the anterior-posterior (AP) axis and the dorsoventral (DV) axis is a crucial early step in establishing the body of any animal (Wilson et al., 2014). Though, early embryogenesis and corresponding formation of the axes varies in different species. BMP (bone morphogenetic protein) signaling and its role in dorsoventral patterning is highly conserved (De Robertis and Kuroda, 2004). However, in the model organism *Drosophila melanogaster* the Toll pathway plays the major role in dorsoventral patterning, whereas BMP acts downstream and only on the dorsal side of the embryo (Lynch and Roth, 2011) (Fig. 1.2). Although, Toll signaling has a conserved function in innate immunity of almost all bilaterians (Caamano and Hunter, 2002; Lemaitre et al., 1996; Rosetto et al., 1995), its role in axis formation appears to be an evolutionary novelty in insects (Leulier & Lemaitre 2008). This leads to the conclusion that Toll was integrated into an existing patterning pathway during insect evolution. Regarding its evolutionary changing role in DV-patterning, the Toll-NFκB/Dorsal pathway is an interesting subject that promises insights into evolution of gene regulation and into functional constraints, underlying gene regulatory network (GRN) evolution. Comparative studies using more basally branching insects might help to understand the mechanisms of such modifications. The emerging model organism *Tribolium castaneum* is an insect with more ancestral features of embryogenesis and is thus, a perfect candidate for comparative analysis. The following section concentrates on *Drosophila* in order to highlight the best understood DV patterning system, which is the foundation for comparative studies in this thesis.

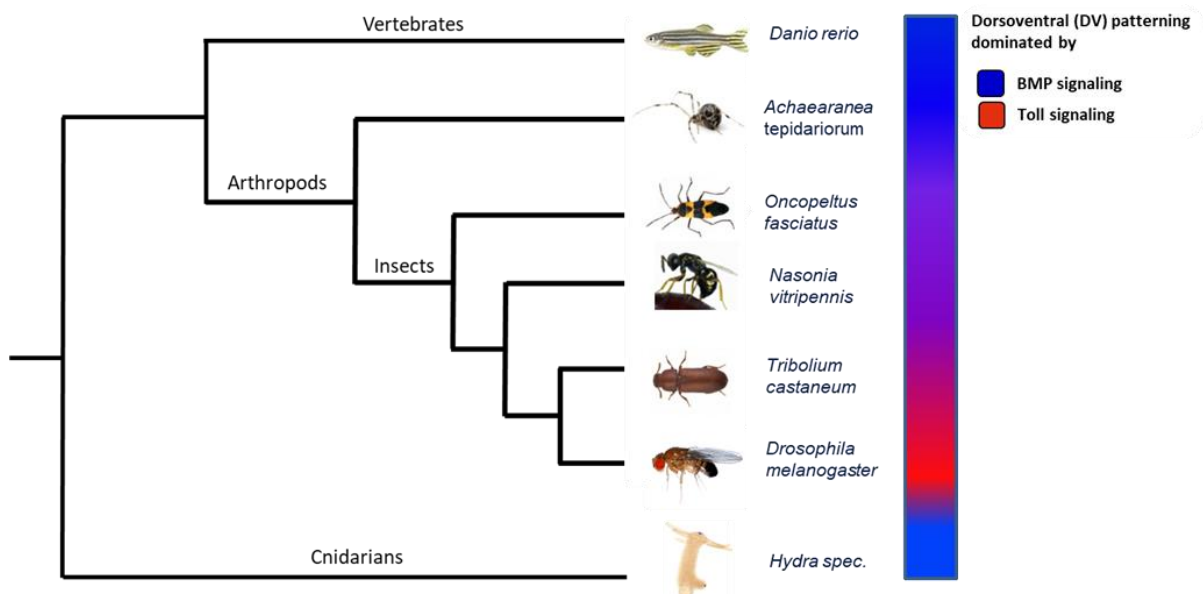


Figure 1.2: Evolution of dorsoventral patterning

The BMP pathway (blue) plays a conserved role in the establishment of dorsoventral polarity in vertebrates as well as in arthropods. However, during insect evolution the Toll pathway (red) which has a conserved role in innate immunity, became dominant in establishing the DV axis.

1.3.1 Formation of the dorsoventral axis in *Drosophila melanogaster*

One of the best studied developmental processes is the dorsoventral axis formation of *Drosophila melanogaster*. Multiple former studies uncovered the fine-tuned, spatio-temporal gene expression which leads to the determination of different cell fates.

The DV-axis is established by migration of the oocyte nucleus from a central-posterior towards an anterior-cortical location (Peri and Roth, 2000; Roth, 2003; Roth and Lynch, 2009). The maternal mRNA of the TGF α -like ligand Gurken is located around the nucleus and activates upon translation, the EGF receptor (Roth, 2004) in the overlying follicle cells (Schupbach and Roth, 1994). EGFR signaling restricts the expression of the sulfotransferase Pipe to the ventral side where it modifies several components of the vitelline membrane (Nilson and Schupbach, 1998; Roth, 2003). This dorsoventral polarity of the egg chamber is transmitted to the early embryo via an extracellular proteolytic cascade in the perivitelline space (Fig. 1.3).

The final step of the protease cascade is the cleavage of Spätzle. After cleavage, Spätzle binds and activates the Toll receptor. Probably, the cleaved Spätzle protein is present in a concentration gradient. Cleavage of the Toll-ligand Spätzle generates a gradient of Toll receptor activation on the ventral side of the embryo (Morisato, 2001; Moussian and Roth, 2005). The activation of the Toll receptor leads to the phosphorylation and degradation of Cactus. Usually Cactus binds the NF- κ B transcription factor Dorsal, which is consequently retained in the cytoplasm. Upon degradation of Cactus, Dorsal can translocate into the nuclei which leads to the establishment of a nuclear Dorsal gradient (Fig. 1.3) with peak levels at the ventral midline (Moussian and Roth, 2005; Roth et al., 1991). The nuclear Dorsal gradient in *Drosophila* is stable and leads to the transcriptional regulation of 60-70 different target genes (Type I, Type II, Type III) which are activated or repressed by Dorsal in a concentration-dependent manner (Reeves and Stathopoulos, 2009) (Fig. 1.3). Genes like *twist* and *snail* are expressed, due to high nuclear Dorsal levels (Type I), on the ventral-most side of the embryo and specify the presumptive mesoderm (Jiang et al., 1991; Leptin, 1991). In more lateral regions of the egg circumference, intermediate nuclear Dorsal concentrations activate the transcription of genes like *ventral nervous defective (vnd)* (Type II), which trigger formation of the neuroectoderm.

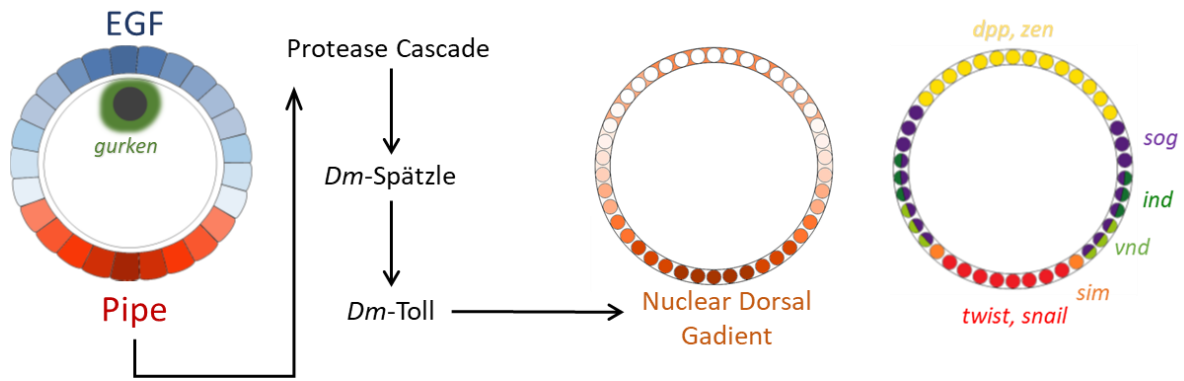


Figure 1.3: Establishment of the dorsoventral axis in *Drosophila melanogaster*

Activation of EGF signaling (blue) in the dorsal ovary follicle cells by Gurken (green) restricts Pipe (red) to the ventral side. Pipe activates a protease cascade in the perivitelline space. The cleaved and thus active ligand Spätzle binds to Toll receptors which finally results in the establishment of a nuclear Dorsal gradient with peak levels at the ventral midline (brown). Dependent on the nuclear Dorsal concentration, different target genes are expressed along the dorsoventral axis.

Two subgroups of Type III genes are regulated by low nuclear dorsal concentrations. Type III+ genes like *short gastrulation (sog)* are activated, while Type III- genes like the BMP homolog *decapentaplegic* are repressed (Hong et al., 2008; Reeves and Stathopoulos, 2009). *dpp* is expressed on the dorsal most side, where no nuclear Dorsal is present. Sog acts as an inhibitory modulator for BMP signaling and antagonizes the BMP2/4-like ligand Decapentaplegic (Dpp) in lateral regions (Reeves et al., 2012). Dpp gets bound and transported to the dorsal side, where it is cleaved by the metallo-protease Tolloid. Released Dpp can then bind to its receptors (Nunes da Fonseca et al., 2008). This mechanism restricts the activation of BMP signaling to the dorsal side, which is necessary for the specification of the dorsal non-neurogenic ectoderm and the amnioserosa (Nunes da Fonseca et al., 2008). The differences of the DV-GRN of *Tribolium* will be discussed in the following section.

1.3.2 The dorsoventral gene regulatory network of *Tribolium castaneum*

DV patterning in *Tribolium* shows many similarities to DV-patterning in *Drosophila melanogaster*. However, the mRNA of the *Tribolium* TGF α homolog is not localized in the ovaries. Thus, the process of DV polarity transmission from the ovary to the embryo remains unclear (Lynch and Roth, 2011). Former studies showed that Toll is also a key component in DV patterning of *Tribolium castaneum*. Like in *Drosophila*, the activation of *Tc*-Toll by binding of *Tc*-Spätzle leads to nuclear uptake of *Tc*-Dorsal. But in contrast to *Drosophila*, the resulting *Tc*-Dorsal gradient is spatio-temporally dynamic (Chen et al., 2000; Nunes da Fonseca et al., 2008). The *Tc*-Dorsal gradient refines from a broad domain in the early blastoderm to a narrow stripe along the ventral midline (Fig. 1.4). Finally, it disappears from the germ rudiment before the onset of gastrulation (Chen et al., 2000). In addition, *Toll* and *cactus* are zygotically expressed genes in *Tribolium*, whereas they are maternally expressed in the fruit fly (Lynch and Roth, 2011). Thus, the dynamism of the Dorsal gradient is caused by several negative and positive feedback mechanisms that act on zygotic level (Nunes da Fonseca et al., 2008). Previous studies (Lynch

and Roth, 2011; Nunes da Fonseca et al., 2008) showed that *Tc-Cactus* is activated by *Tc-Dorsal* itself and in addition by the *Tc-Dorsal* target *Tc-Twist*. This Dorsal-/Twist-dependent activation of *Tc-Cactus* simultaneously leads to an enhanced repression of *Tc-Dorsal*. In addition, *Tc-Dorsal* regulates its own activator *Tc-Toll* in a positive feedback loop (Fig. 1.4). Furthermore, ChIP sequencing experiments revealed a potential self-regulative input of *Tc-Dorsal* and a positive regulation of *Tc-Dorsal* on the Toll ligand *Tc-Spätzle* (Stappert, PhD Thesis 2014).

Another difference is that the BMP pathway plays a more important role in DV-patterning of *Tribolium castaneum*, and that the Toll pathway influences less target genes compared to the derived patterning system of *Drosophila*. It was shown, that loss of *sog* in *Drosophila* results in weaker defects than the *Tc-sog* kd, which leads to a strong dorsalization of the embryo, indicating that *Tc-Dorsal* is not a direct repressor of *Tc-dpp* (Nunes da Fonseca et al., 2010). Moreover, *dpp* knockout in *Drosophila* does not affect the mesoderm, while knockdown of *dpp* in *Tribolium* results in a slight expansion of the mesoderm (Nunes da Fonseca et al., 2008). These results strengthen the presumption that Toll's role in DV patterning is derived, and that the DV-GRN changed since the last common ancestor of flies and beetles. The approach to elucidate these changes is described in the following sections.

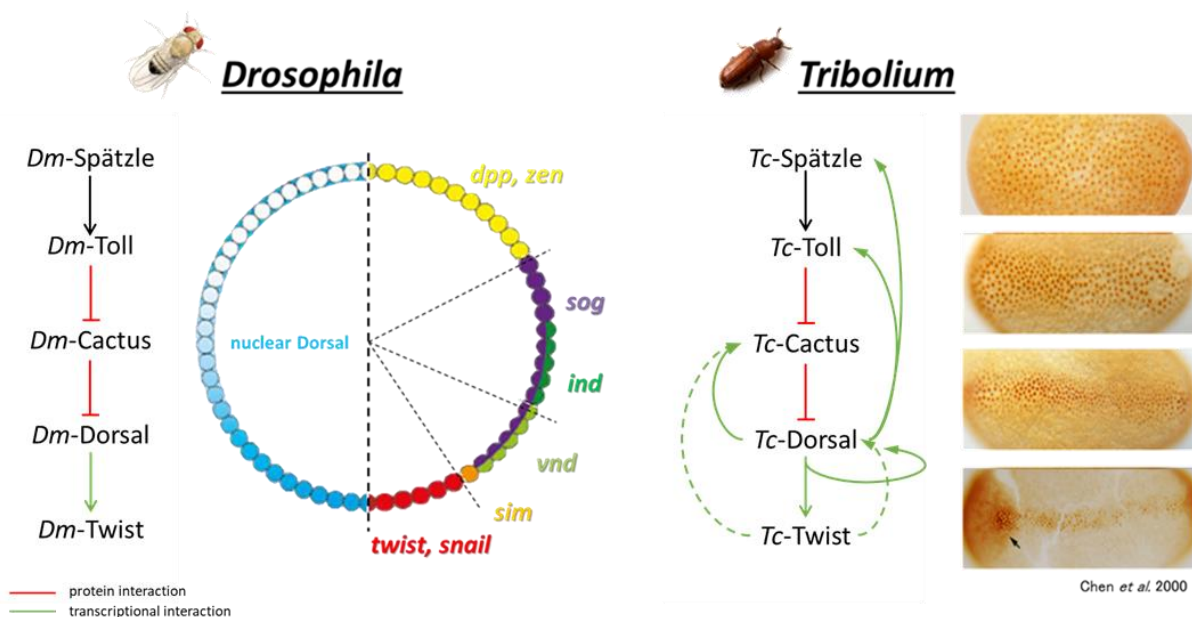


Figure 1.4: Regulation of dorsoventral patterning genes

The *Drosophila* nuclear Dorsal-gradient is stable and regulates the transcription of ~ 50 target genes in a concentration-dependent manner. The same signaling cascade initiates the expression of *Tc-twist* and other DV patterning genes in *Tribolium castaneum*. However, in contrast to *Drosophila* the nuclear *Tc-Dorsal* gradient is dynamic due to feedback mechanisms. *Tc-cactus* is regulated by Dorsal and by the Dorsal target gene *twist*. This activation establishes a negative feedback loop, as Cactus has a negative influence on the nuclear uptake of Dorsal. In addition, *Tc-Dorsal* regulates its own activator *Tc-Toll* in a positive feedback loop.

modified from (Chen et al., 2000; Nunes da Fonseca et al., 2008; Stappert, PhD Thesis 2014)

1.4 Identification of new DV-patterning genes by differential expression analysis

Comparative studies are often performed by candidate gene approaches, requiring sequence identification of already known pathway components in the organism of interest by DNA or protein BLAST. Many important evolutionary studies are based on this approach. However, analyzing evolutionary changes in gene regulatory networks by a candidate gene approach depends on the presence of the respective pathway components, rendering discovery of new genes involved in a GRN impossible. Modern techniques like whole genome sequencing, identification of binding regions by ChIP-sequencing or generation of transcriptomes by RNA-sequencing (RNA-seq), facilitate new opportunities in the wide field of evolution and development. To get more insights into the DV-GRN of *Tribolium castaneum* and the differences in composition and wiring of the genes to the DV-GRN of *Drosophila melanogaster*, I performed a genome wide comparative differential expression analysis after RNAi. The establishment of this modern technique for comparative studies in *Tribolium* was performed together with Dominik Stappert (Frey, Master Thesis 2013; Stappert, PhD Thesis 2014).

1.4.1 Generation of knockdown embryos lacking key DV patterning genes

To identify new potential target genes, transcriptomes of *Tc-Toll*¹, *Tc-twist*, *Tc-sog* and *Tc-dpp* knockdown (kd) embryos were generated by parental RNA interference (pRNAi). Wildtype embryos derived from uninjected mothers served as control. Considering possible false positive results by genes activated via the injection procedure itself (e.g. inflammatory genes, RNAi machinery genes), an additional control was used. Therefore, female pupae were injected with dsRNA for *dsRed* which is derived from *Discosoma spec.* and is not present in the *Tribolium* genome. Thus, *dsRed* knockdown embryos should not show differential gene expression.

The RNA for transcriptome analyses was isolated from embryos derived from dsRNA injected mothers and staged to 7.5h to 11.5h AEL. At that stage, the embryo proceeds from the early differentiated blastoderm stage to the horseshoe stage. The carefully selected time window captures a critical time in DV patterning. During the differentiated blastoderm numerous direct target genes of the key regulators Dorsal and Twist are expressed. These genes are especially important for tissue specification and early tissue differentiation during the gastrulation of the embryo. The embryos were stained with DAPI and surveyed for phenotypic penetrance (Fig. 1.5).

¹ Knockdown of *Tc-dorsal* results in a higher death rate of the injected females and to a reduced number of eggs. *Tc-Toll* RNAi is upstream of *Tc-dorsal* and thus phenocopies *Tc-dorsal* with regard to its dorsoventral phenotype.

dsRed kd embryos do not show any morphological defects and look similar to embryos from untreated wildtype control females (Fig. 1.5 A-A'). Although knockdown of *Tc-twist* results in complete loss of the mesoderm (Stappert et al., 2016), the visible defects in DAPI-stained *Tc-twist* kd embryos are rather mild. Older embryos show characteristic finger-like structures at the posterior end (Fig. 1.5 B-B''). These structures are the malpighian tubules which are usually wrapping the connection of the hindgut and the midgut. Compared to wildtype (WT) blastoderm stage embryos (Fig. 1.5 A'), which show an oblique borderline between the big anterior serosa cells and the more compact posterior germ band cells, the border becomes straight and is shifted towards the posterior pole after knockdown of *Tc-Toll* (Fig. 1.5 C'). Elongating germ bands look like a thin tube which is interrupted at different places (Fig. 1.5 C''). Due to their respective defects, *Tc-sog* kd and *Tc-dpp* kd embryos show antagonistic phenotypes. Whereas the knockdown of *Tc-sog* results in loss of the neurogenic ectoderm and the head structures (Fig. 1.5 D), *Tc-dpp* kd embryos lack the dorsal ectoderm (Fig. 1.5 E). Similar to *Tc-Toll* kd, *Tc-sog*-RNAi and *Tc-dpp*-RNAi embryos reveal already strong DV-defects in the differentiated blastoderm stage. *Tc-sog* kd embryos have a straight serosa-germ band border. Furthermore, the border shifts towards the posterior pole (Fig. 1.5 D'). Also, the serosa-embryo border of *Tc-dpp*-deficient embryos loses its obliqueness, but shifts to a more anterior position (Fig. 1.5 E'), compared to wildtype embryos. Furthermore, extending germ bands show the typically reduced head upon loss of *Tc-sog* and tube-shaped remaining segments (Fig. 1.5 D''). The tube-like shape of the germ band was also seen for *Tc-dpp*-deficient embryos. In addition, some tissue at the posterior end does not get invaginated and is thus not covered by the serosa (Fig. 1.5 E'').

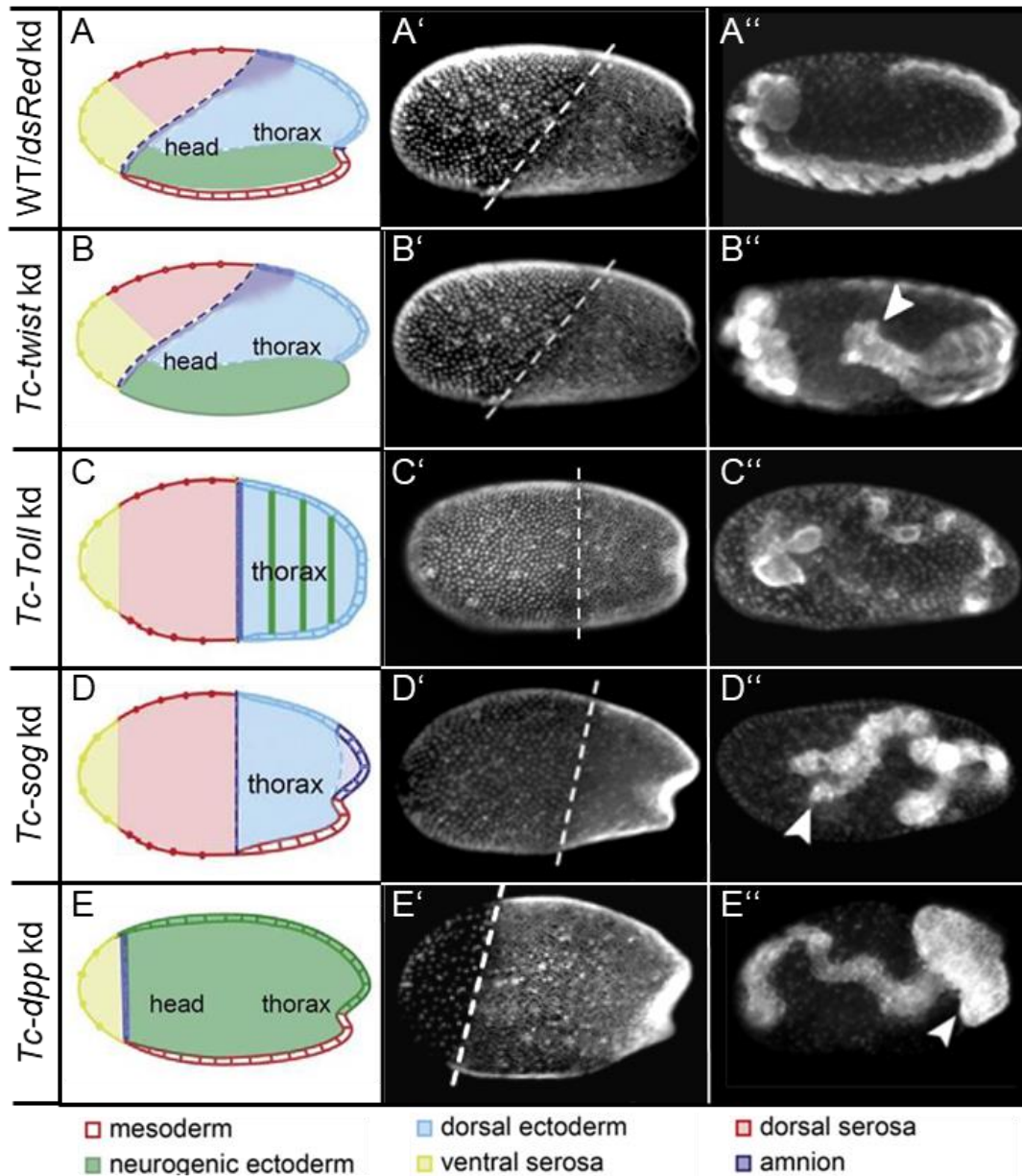


Figure 1.5: Fate maps of dorsoventral phenotypes

(A-E) Fate maps of *Tribolium* embryos at the beginning of gastrulation². The different colors indicate different cell fates as displayed in the legend. (A'-E') DAPI stained embryos corresponding to A-E. The dashed lines represent the embryo-serosa border. (A''-E'') DAPI stained elongated germ bands of the respective knockdowns shown in (A-E). Anterior to the left; kd = knockdown. (A) Fate map of a wildtype embryo or of embryos from mothers injected with dsRNA of *dsRed*. The embryo-serosa border at beginning of gastrulation is oblique (A'). (A'') Fully extended germ band stage wildtype embryo. (B) Fate map of *Tc-twist* knockdown embryos in which the mesoderm is lost. In *Tc-twist* kd embryos, the embryo-serosa border is not affected (B'), while germ bands show a misplacement of the malpighian tubules (B''). (C) Fate map of dorsalized *Tc-Toll* knockdown embryos. The dorsal serosa is expanded and its border becomes straight (C'). The mesoderm is lost and the neurogenic ectoderm is also affected. (C'') Germ band embryos after *Tc-Toll* kd have a tube-like morphology. (D) Fate map of dorsalized *Tc-sog* knockdown embryos. The mesoderm is present, but the neurogenic ectoderm is lost and the dorsal serosa is expanded. Similar to *Toll* kd embryos, the serosa is shifted towards the posterior pole (D') and the elongated germ band forms a tube with reduced head structures (D''). (E) Fate map of ventralized *Tc-dpp* knockdown embryos. The dorsal serosa is lost and the neurogenic ectoderm is expanded. (E') The embryo-serosa border is shifted towards the anterior pole and germ band embryos show a typical tissue ball at the posterior end, which is not surrounded by serosa (E''). modified from (Fonseca et al., 2009)

² In former schemes the amnion comprised the whole dorsal-most side reaching to the primitive pit. Due to unpublished results by Matthew A. Benton, the borders of the amnion were modified in A.

1.4.2 Validation of the knockdown efficiency

Before the isolated RNA was sequenced, the knockdown efficiency of the samples was analyzed by qRT-PCR (Stappert et al., 2016). Five replicates of wildtype, *Tc-Toll* kd and *Tc-twist* kd and 3 replicates of each *dsRed* kd, *Tc-sog* kd and *Tc-dpp* kd were chosen due to the best results for phenotypic penetrance; analysis of the knockdown efficiency by qRT-PCR and quality of the isolated RNA and send to the Cologne Center for Genomics (CCG)³. After an additional quality control, the samples were sequenced by Illumina sequencing (HiSeq 2000, paired end mode, read size of 100 bp) (Stappert, PhD Thesis 2014).

1.4.3 Identification of differentially expressed genes

The bioinformatic analysis of the RNA-sequencing data was performed by Dominik Stappert. In this study, only genes which showed up as differentially expressed upon analysis with two different programs, DESeq2 and edgeR were considered. Details about the used pipeline and algorithms are described in the PhD Thesis of Dominik Stappert, 2014 and in our corresponding paper (Stappert et al., 2016). A comparison of the transcriptomes of uninjected wildtype embryos compared to embryos derived from mothers injected with *dsRed* dsRNA revealed that the injection procedure itself has no influence on gene regulation in the embryos. For future generation of *Tribolium* transcriptomes it is thus sufficient to use control embryos from uninjected mothers.

To identify differentially expressed genes, the sequenced transcriptomes of the respective knockdown embryos were first compared to the transcriptomes of control embryos (WT and *dsRed-kd*). The identified genes should be regulated either by *Tc-Toll* and/or *Tc-twist* or by BMP signaling. The comprehensive transcriptome analysis revealed in total 796 genes (Fig. 1.6 A, table), which were differentially expressed in the knockdown embryos compared to the control with a false discovery rate (FDR) of 1%. The data set identified 310 differentially expressed genes in *Tc-Toll* kd embryos compared to the control, 347 upon *Tc-twist* kd compared to the control. 377 genes showed up as potentially regulated by Dpp. However, only 18 differentially expressed genes could be identified by comparing the transcriptomes of *Tc-sog* knockdown embryos and the control (detailed list in the supplement of (Stappert et al., 2016)). Although the fate shift seen in *Tc-sog* kd embryos is severe (massive expansion of the neuroectoderm), the effect on more downstream components is restricted. Sog is an inhibitory modulator of BMP signaling (van der Zee et al., 2006) and might not have as many target genes as a transcription factor. A heat map (Fig. 1.6 B) shows the 222 genes up- or downregulated in more than one knockdown condition.

³ 6 samples were then send to GATC (Konstanz) and 18 samples to the Cologne Center for Genomics (CCG) for sequencing (in total 24 RNA samples). Due to a first test of the procedure, the first six samples were produced and sent separately from the other samples.

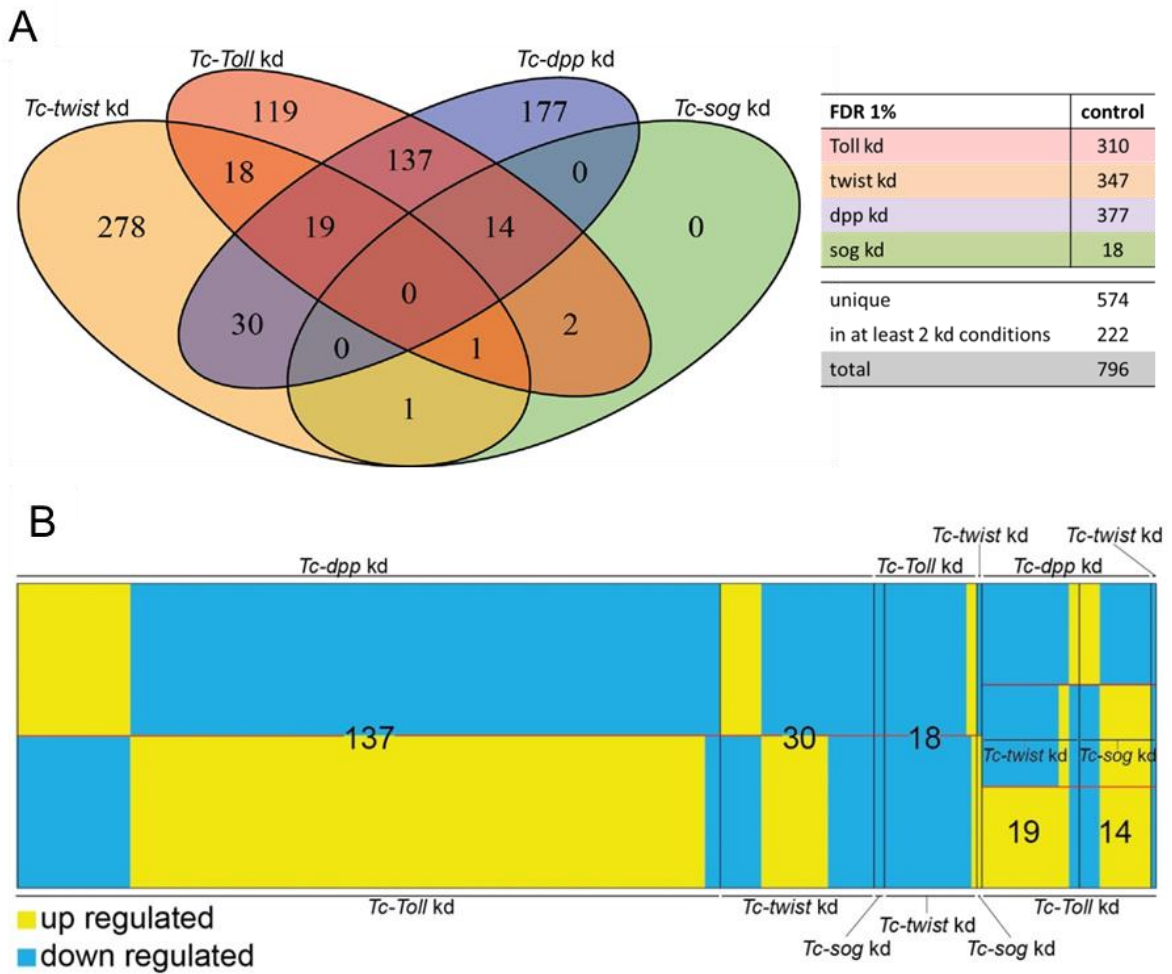


Figure 1.6: 222 genes are differentially expressed in more than one knockdown condition

(A) Venn diagram depicting the number of genes which are differentially expressed upon kd of *Tc-twist*, *Tc-Toll*, *Tc-dpp*, *Tc-sog* as compared to wildtype embryos. Each field in the Venn diagram shows the number of genes that are exclusively found in the overlap of conditions indicated by the diagram. (B) Heat map showing if genes that are found in the overlapping fields of the Venn diagram are up regulated (yellow) or down regulated (blue). The numbers in the figure correspond to the numbers in the fields of the Venn diagram.

(Stappert et al., 2016)

1.5 Aims of the study

Although they interact differently, the transcription factors Dorsal and Twist are key regulators of dorsoventral patterning in *Tribolium* and *Drosophila*, and likely control major parts of the DV-GRN in both organisms. However, BMP signaling has a stronger influence on DV patterning in *Tribolium*, while Toll signaling seems to control less genes compared to *Drosophila*. Since little is known of the components involved in the *Tribolium* DV-GRN, a simple candidate gene approach might not be sufficient to reveal all evolutionary changes compared to the DV-GRN of *Drosophila*.

The goal of this study was to identify new potential DV patterning genes via unbiased comparative differential transcriptome analysis after knockdown via pRNAi of (*Tc-Toll*, *Tc-twist*, *Tc-short gastrulation* and *Tc-decapentaplegic*) followed by high-throughput RNA sequencing. Providing direct information on differential gene expression, this approach facilitates analysis of GRNs. Based on the RNA-sequencing data, two subgroups of potential DV patterning genes will be chosen and further investigated by *in-situ* hybridization, concerning their mRNA expression domains. A selection of these genes will be functionally analyzed by the generation of knockdown embryos via pRNAi. The identified differences in the DV-GRNs of *Tribolium* and *Drosophila* will be discussed in an evolutionary context.

2 Results

2.1 Verification of the RNA-seq data by an *in-situ* hybridization screen

For the identification of genes involved in the dorsoventral gene regulatory network (DV-GRN), the transcriptomes of *Tc-Toll*, *Tc-twist*, *Tc-sog* and *Tc-dpp* knockdown embryos were compared to a control (Stappert et al., 2016).

201 genes showed up as upregulated upon *Tc-Toll* kd compared to the control. To verify the bioinformatics analysis, the expression patterns of a random selection of them was investigated. I analyzed the mRNA expression for some of the genes in wildtype embryos and compared it to *Tc-Toll* deficient embryos. The expression patterns in *Tc-Toll* knockdown embryos reflect the data of the differential transcriptome analysis. As the serosa expands after knockdown of *Tc-Toll* 8 of 10 the genes are strongly expressed in the serosa (Fig. 2.1). *TC008197* is only expressed in the dorsal serosa (Fig. 2.1 I). Especially this part is strongly expanded in *Toll* knockdown embryos (Fig. 2.1 I'). The verification of the RNA-sequencing data correlates well with the RNA-seq data set. Thus, subgroups of potential dorsoventral patterning genes had to be chosen for further analysis.

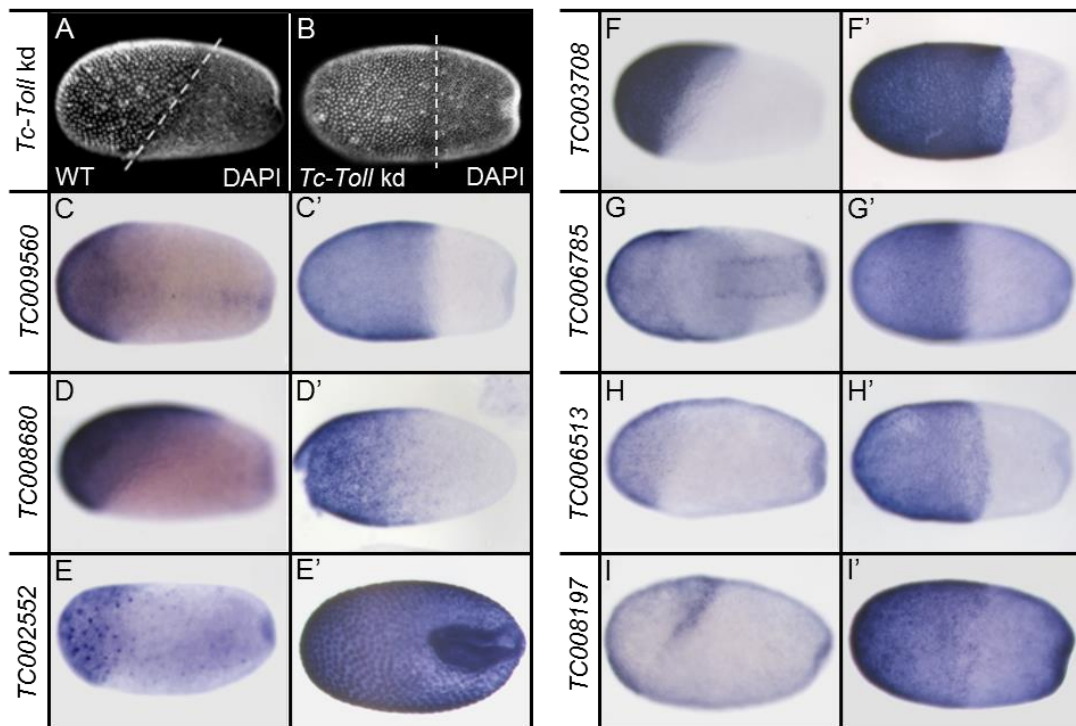


Figure 2.1: Expression patterns of genes differentially expressed upon knockdown of *Tc-Toll*

The expression pattern of selected genes which were upregulated in *Tc-Toll* kd embryos compared to the control. (A) DAPI staining of a wildtype embryo in the differentiated blastoderm stage. The dashed line indicates the oblique border between the serosa (anterior) and the embryo proper (posterior). (B) In *Tc-Toll* knockdown embryos, the embryo-serosa border is straight and shifted towards the posterior. (B-I) Expression patterns as identified by ISH; (B'-I') Expression of the same gene as depicted in pictures labeled with corresponding capital letters in *Tc-Toll* kd embryos. All embryos shown in lateral view – with exception to G, which is shown in a ventral view. Anterior to the left. All genes are expressed in the serosa. Note that *TC008197* (I) is just expressed in the posterior-dorsal part of the serosa and that *TC006785* (G) is also expressed in two ventral stripes. The expression pattern in *Tc-Toll* knockdown embryos reflects the data from the differential transcriptome analysis. As the serosa expands upon knockdown of *Tc-Toll* most of the genes show a wider expression domain.

2.1.1 Detailed analysis of two subgroups of differentially expressed genes

Facing a large numbers of potential target genes (796, FDR of 1%), it was necessary to reduce the data set for screening. Thus, I concentrated on those 222 genes which were differentially expressed in more than one knockdown condition (Fig. 1.6 B). The mesoderm is missing in *Tc-Toll* and *Tc-Twist* knockdowns, hence this comparison should predominantly reveal genes specifying the mesodermal fates of the embryo (Fig. 1.5 B and C). The opposing influence of *Tc-sog* and *Tc-dpp* kd is especially affecting the ectoderm. Thus, the comparisons of their transcriptomes should result in a list of genes mainly expressed in the ectoderm (Fig. 1.5 D and E). According to the resulting fate shift of the respective knockdown conditions, differentially expressed genes after knockdown of both *Tc-Toll* and *Tc-twist* (Fig. 2.2 A), as well as after knockdown of *Tc-dpp* and *Tc-sog* (Fig. 2.2 B) were most interesting for first analysis.

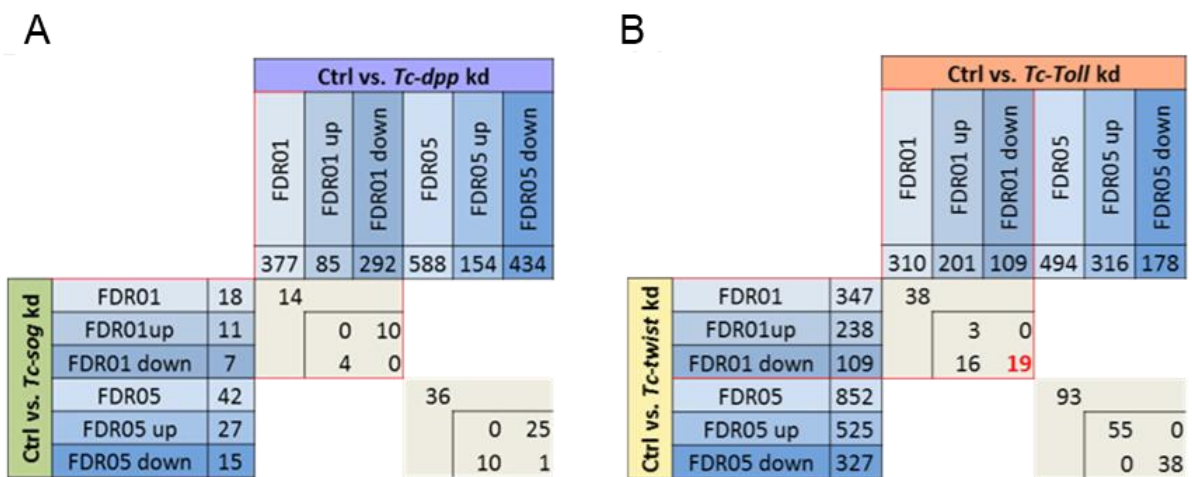


Figure 2.2. Genes differentially expressed upon *Tc-Toll* kd vs. *Tc-twist* kd and *Tc-sog* vs. *Tc-dpp* kd

ctrl - control embryos; kd - knockdown; FDR - false discovery rate; up - upregulated; down - downregulated. Transcriptomes of different knockdown conditions were first compared to the transcriptome of control embryos. The number of significantly differentially expressed genes was detected with a FDR of 1%. To increase the dataset, also genes with a FDR of 5% were included. (A) Number of genes differentially expressed between *Tc-sog* kd and *Tc-dpp* kd. (B) Number of genes differentially expressed between *Tc-twist* kd and *Tc-Toll* kd. For the identity of corresponding genes see Appendix B and C.

2.1.2 Identification of genes regulated by Dpp

The first group consists of all genes which were differentially expressed in *Tc-dpp* and *Tc-sog* knockdown embryos with a FDR of 1% (Fig. 2.2 A). As expected, the identified 14 genes which were up- or downregulated in *Tc-dpp* knockdown embryos are regulated in the opposite direction after *Tc-sog* knockdown. Out of this group of 14 genes, 10 are downregulated in *Tc-dpp* kd embryos compared to knockdown of *Tc-sog*. Thus, these genes should be expressed either in the serosa or in ectodermal regions of the embryo.

An *in-situ* hybridization screen revealed that 5 of these 10 genes are strongly expressed in the extraembryonic serosa (Fig. 1.5 A-E). The other 5 genes did not show a localized mRNA expression pattern. This finding can be explained by the prominent shift of the embryo-serosa border in different directions (Fig. 1.5 D' and E'). The remaining 4 genes showed up as being upregulated upon *Tc-dpp* kd, whereas they are downregulated in *Tc-sog* deficient embryos. These 4 genes are likely acting in the neurogenic ectoderm of the embryo and are therefore interesting candidates. Among these genes, *Tc-patched* (TC004745) is expressed mainly in the head anlagen of differentiated blastoderm stage embryos (Fig. 2.3 F). This expression domain is also visible for *Tc-tartan* (TC014658), but in addition *Tc-tartan*, as well as *Tc-prospéro* (TC010596), show an additional broad neuroectodermal expression (Fig. 2.3 G and H). To enlarge the data set and to increase the chances to identify promising candidates, also the 14 genes (exclusively on this list) which showed up as differentially regulated with a false discovery rate of 5% were analyzed. 7 of them showed a localized expression pattern: 4 are expressed in the serosa, 2 are expressed in segmental stripes and one shows mRNA expression in the neuroectoderm (see Appendix B).

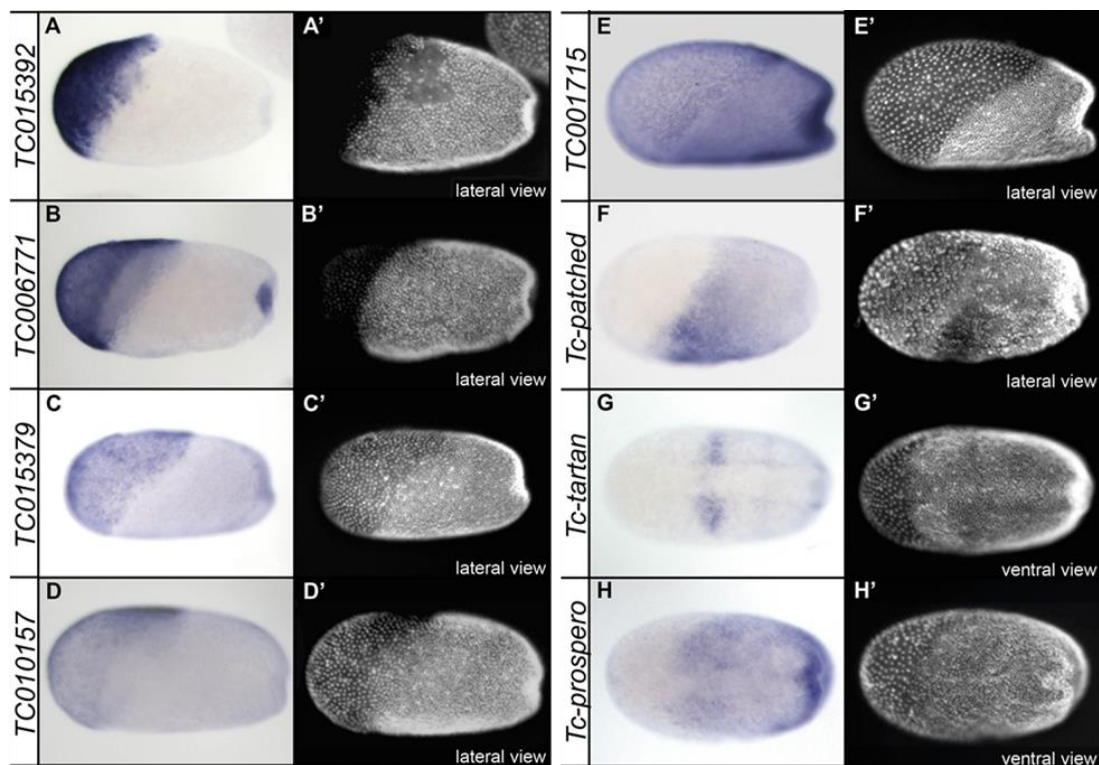


Figure 2.3: Expression patterns of genes differentially expressed upon knockdown of *Tc-sog* and *Tc-dpp*

(A-H) Expression patterns as identified by ISH; (A'-H') Same embryo as depicted in pictures labeled with corresponding capital letters, nuclei stained with DAPI for staging; Embryos in A-D in primitive pit stage; Embryos in E-H are gastrulating; Embryos in A-E: lateral view; embryos in F-H ventral view; Anterior to left. A - D) *TC015392*, *TC006771*, *TC015379*, and *TC010157* are expressed in the serosa. Note that *TC015392* is just expressed in part of the serosa and that *TC006771* is also expressed in the primitive pit. E) *TC001715* is expressed in the serosa, but also in the germ rudiment. F) *TC004745/Tc-patched* is not expressed in the serosa, but in the embryo proper. A DV stripe of strong expression posterior to the presumptive head lobes is visible. G) *TC014658/Tc-tartan* is expressed in the same domain in which strong expression for *TC004745/Tc-patched* is detected. The expression is absent from the mesoderm. H) *TC010596/Tc-prospéro* is not expressed in the serosa, but inside the germ rudiment, in which the expression is absent from the future mesoderm, although the expression borders are not well defined.

2.1.3 Expression patterns of genes regulated by Toll and/or Twist

The second subgroup of 38 genes showed up as differentially expressed after knockdown of both, *Tc-Toll* and *Tc-twist* with a false discovery rate of 1% (Fig. 2.1 A).

As the mesoderm is missing in both knockdown conditions, the 19 genes which are downregulated in both *Tc-Toll* and *Tc-twist* kd, are of special interest. The 14 genes which showed a specific mRNA expression domain, include already known dorsoventral patterning genes like *Tc-twist* itself, *Tc-cactus* and *Tc-snail* (Fig. 2.4 A, B and C). Also, the known *Drosophila* Twist targets *heartless* (Fig. 2.4 G) and *downstream-of-fgf (dof)* (Fig. 2.4 H) showed up as downregulated in *Tc-Toll* and *Tc-twist* kd embryos. Like the remaining genes, both show a clear ventral expression domain in the presumptive mesoderm of blastoderm *Tribolium* embryos (Fig. 2.4 A-D and G-L). Furthermore, I could identify *Tc-Delta* (Fig. 2.4 D). In *Drosophila*, *Delta* is expressed in the neuro-ectoderm, whereas it is repressed in the presumptive mesoderm (Vassin et al., 1987). However, in *Tribolium* *Tc-Delta* seems to be positively regulated by Toll and Twist in the mesoderm. Its expression is furthermore co-localized with two other components of the Delta/Notch pathway: *Tc-E(spl)1* and *Tc-E(spl)3*. Both *enhancer of split* homologs of *Tribolium* are expressed in a mesodermal domain with enhanced levels at its lateral borders (Fig. 2.4 E and F). Similar to *Delta*, *E(spl)1* and *E(spl)3* are expressed in the neurogenic ectoderm in *Drosophila* (Knust et al., 1992; Wech et al., 1999). The only gene showing a typical antero-posterior (AP) expression pattern was *TC008064 (sloppy paired/slp)*. *Tc-slp* is a pair-rule gene (Choe and Brown, 2007) which is expressed in segmental stripes along the AP axis (Fig. 2.4 M). Some of the candidates from this group (*TC003461*, *TC003606*, *TC007056*, *TC009862*, *TC010195* and *TC013142*), did not show a specific mRNA expression pattern (data not shown). Of the remaining 19 genes which are upregulated in *Tc-Toll* kd embryos and downregulated in *Tc-twist* embryos, only two showed a distinct expression pattern. Interestingly, they are expressed in the serosa, which is expanded after loss of *Tc-Toll*. Similar to the analysis of potential *Tc-Sog* vs *Tc-Dpp* targets, the expression patterns of 20 genes (exclusively on this list) which showed up as differentially expressed with a FDR of 5% were also analyzed. 5 of them are expressed in the mesoderm, 3 in the serosa and 2 are expressed in segmental stripes (see Appendix C).

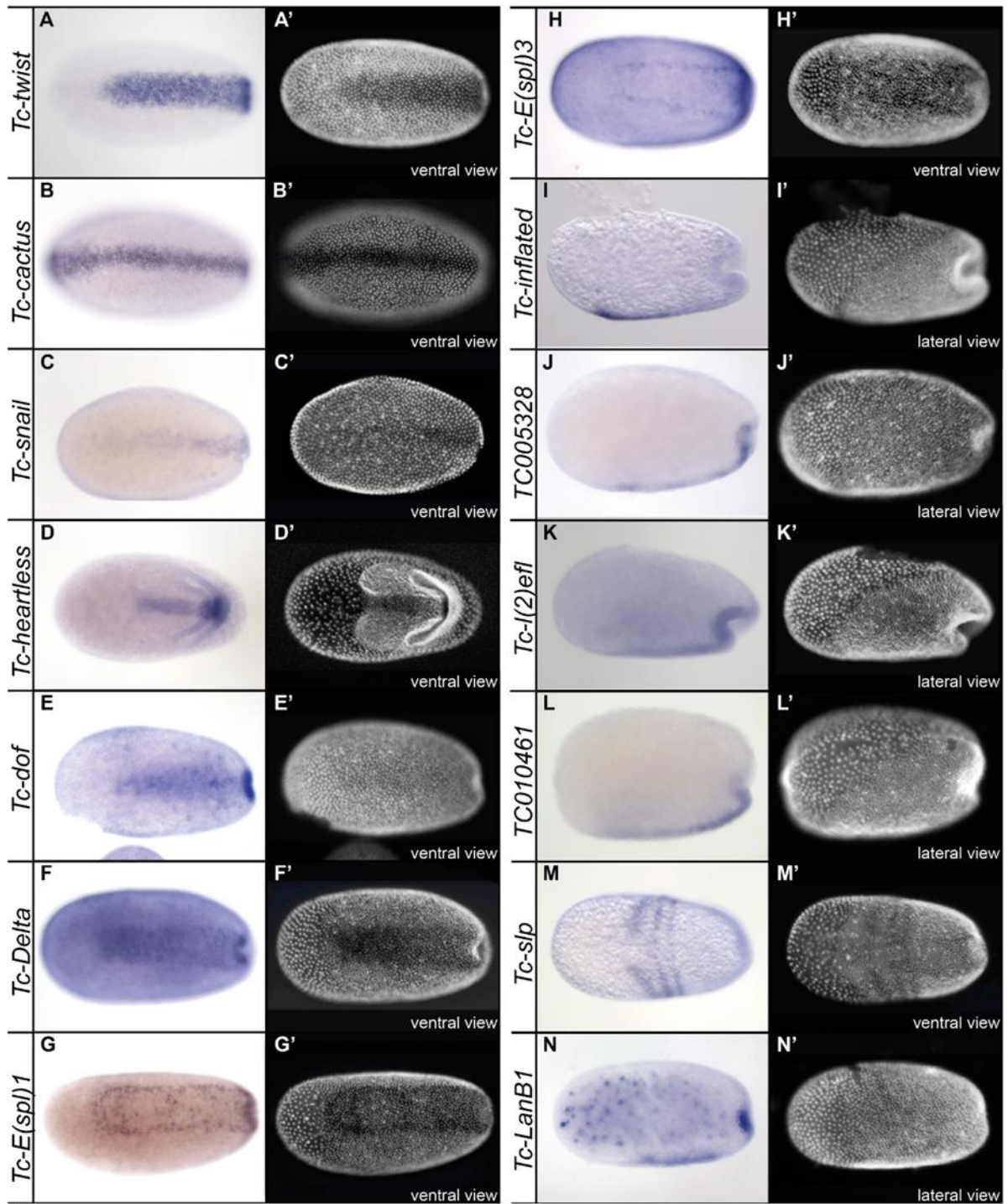


Figure 2.4: Expression patterns of genes downregulated upon knockdown of *Tc-Toll* and *Tc-twist*

(A-N) Whole-mount ISH of embryos at blastoderm stage. (A-C) Primitive pit stage (E-H, J, L, M, N) or early gastrulation stage (D, I, K). (A'-N') DAPI staining of the respective embryos. (A-H, M) Ventral surface views. (I-L, N) Lateral views with dorsal side pointing upwards. The anterior pole points to the left. All genes (except in G, H and M) are expressed in the presumptive mesoderm. Note that *Tc-cactus* (B) is also expressed in ventral parts of the serosa. *Tc-E(spl)1* (G) and *Tc-E(spl)3* (H) are expressed in narrow lateral stripes at the border of the mesoderm.

2.2 Functional analysis of genes potentially involved in the DV-GRN of *Tribolium*

To further investigate the role of selected candidate genes in the DV-GRN of *Tribolium castaneum*, functional studies using pRNAi were performed. The survival of the mothers injected with the respective dsRNA, the phenotypic penetrance in the embryos derived from these mothers and analyzed the expression of different marker genes in the knockdown (see Appendix D and E) were determined for each kd condition. *Tc-twist* was used as mesodermal marker, *Tc-achaete-scute homolog* (*Tc-ash*) as neuronal marker (Wheeler et al., 2003), *Tc-pannier* as marker for the amnion and the dorsal ectoderm (van der Zee et al., 2005) and *Tc-engrailed* (Brown et al., 1994) (not shown in Fig. 2.5) or *Tc-gooseberry* (Davis et al., 2001) as segmental markers (Fig. 2.5).

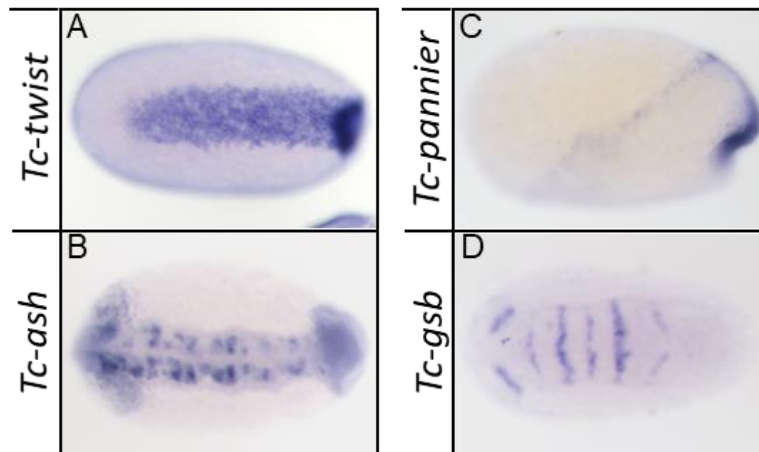


Figure 2.5: Expression of marker genes

(A-D) Expression of *Tc-twist*, *Tc-achaete-scute homolog* (*Tc-ash*), *Tc-pannier* and *Tc-gooseberry* (*Tc-gsb*) in wildtype embryos. (A) *Tc-twist* is expressed in a strong mesodermal stripe in differentiated blastoderm embryos. (B) Amniotic *Tc-pannier* expression along the embryo-serosa border and in the dorsal ectoderm around early gastrulation. (C) Expression of neuronal precursor marker *Tc-achaete-scute homolog* during germ band extension. (D) Expression of segmental marker *Tc-gooseberry* during germ band extension.

2.2.1 Functional analysis of Sog/Dpp targets

2.2.1.1 Neuroectodermal expression of *Tc-uninflatable*

A candidate showing an interesting neuroectodermal expression pattern could be identified among the differentially expressed genes with a false discovery rate of 5% (see Appendix B). *Tc-uninflatable* (*TC000871*) is a potential candidate, as it is known to be involved in Notch signaling in *Drosophila* (Xie et al., 2012; Zhang and Ward, 2009).

Tc-uif is upregulated in *Tc-dpp* kd and downregulated in *Tc-sog* kd embryos. In blastoderm embryos, it is expressed in a broad neuroectodermal domain, while it is absent from the mesoderm on the ventral side (Fig. 2.6 A). Shortly before gastrulation the expression becomes enhanced in two stripes flanking the mesoderm (Fig. 2.6 B). In elongating germ bands, *Tc-uif* is expressed uniformly with exception of the mesoderm (data not shown). Interestingly, *uif* also shows an early expression in ectodermal cells in *Drosophila* embryos (Zhang and Ward, 2009). No changes in the early expression of the marker genes in *Tc-uif* kd embryos could be detected (see Appendix D). However, the neuroectodermal expression domain is expanded to the ventral side after *Tc-twist* knockdown (Fig. 2.6 C). This result suggests a negative regulation of *Tc-uif* by either Twist itself, or by a Twist target gene.

Knockdown of *Tc-uninflatable* results in a consistent phenotype with a high phenotypic penetrance (61.45%; N=182). The knockdown embryos show thinner abdominal segments compared to wildtype embryos (Fig. 2.6 D and E). In addition, the posterior segments were often bended. Although, the mRNA shows an early localization before gastrulation, the defects are restricted to the segment addition zone of extending germ band embryos. However, affecting the segment addition zone indicates an important role of *Tc-uif* in embryonic development.

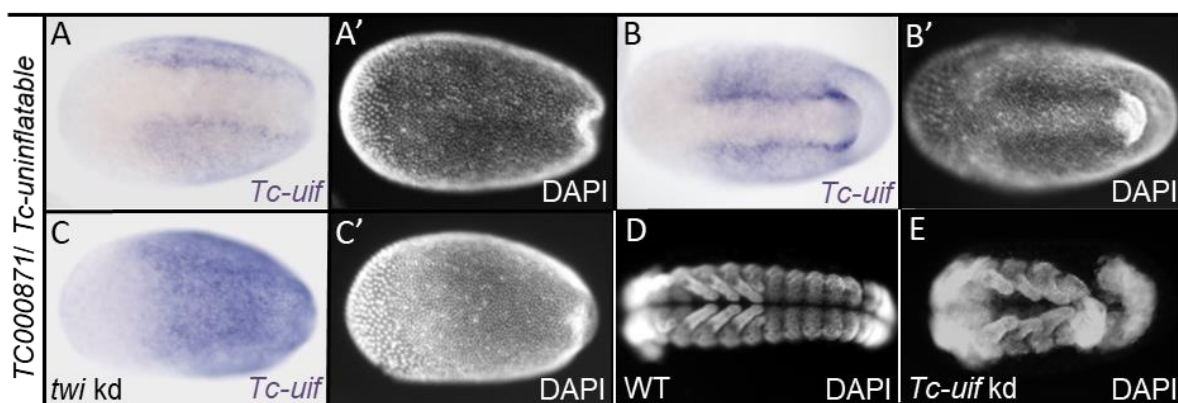


Figure 2.6: Functional analysis of *Tc-uninflatable*

(A-C) Expression patterns detected by ISH. (A'-C') Corresponding embryos, nuclei stained with DAPI for staging; All embryos in ventral view; Anterior to left. (A-C) Expression of *TC000871/Tc-uninflatable* (*Tc-uif*) in wildtype embryos. (A) In primitive pit stage embryos, *Tc-uif* is expressed in broad lateral domains. (B) When gastrulation proceeds, expression of *TC000871* enhances in stripes flanking the mesoderm. (C) In *Tc-twist* kd embryos the neuroectodermal expression domain expands towards the ventral side. E shows DAPI staining of older embryos (~24h-48h AEL) after *Tc-uif* knockdown via pRNAi. The abdominal segments of these embryos are thinner and often bent compared to WT (D).

2.2.1.2 *Tc-tartan* is involved in neurogenesis of *Tribolium castaneum*

The second candidate Tartan, is a transmembrane protein with extracellular leucine-rich repeats (LRRs) and is expressed in proneural clusters and sensory mother cells of *Drosophila* embryos (Chang et al., 1993). The weak neuroectodermal expression of *Tc-tartan* which is visible in blastoderm stage embryos (Fig. 2.7 A) becomes more enhanced and segmental in elongating germ bands, whereas expression is still absent from the mesoderm along the ventral midline (Fig. 2.7 B and C). Matching the fate shift upon *twist* knockdown, the neuroectodermal expression domain of *Tc-tartan* shows an expansion towards the ventral side, where the mesoderm is missing (Fig. 2.7 D). This indicates that *Tc-tartan* is repressed in the mesoderm similar to *Tc-uif*.

Although I could not observe morphological defects in DAPI-stained *Tc-tartan* knockdown embryos, changes in marker gene expression were observed. In contrast to wildtype embryos which express *Tc-ash* in proneural clusters cells (Fig. 2.7 E), *Tc-tartan* kd embryos lack expression of the neural marker, except in the pregnathal head region (Fig. 2.7 F). This result suggests a strong involvement of *Tc-tartan* in the neurogenesis of *Tribolium castaneum* embryos.

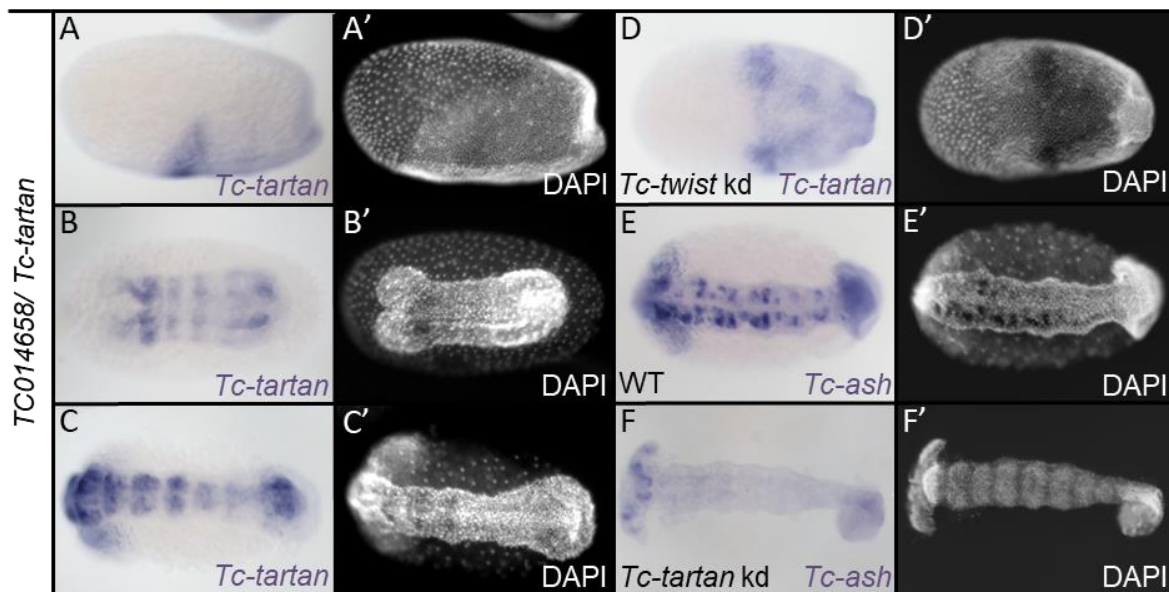


Figure 2.7. Functional analysis of *Tc-tartan*

(A-K) Expression patterns detected by ISH. (A'-K') Corresponding embryos, nuclei stained with DAPI for staging; All embryos in ventral view; with exception of A and A' which show the embryo in a lateral view; Anterior to left.

(A-C) Wildtype expression of *TC014658/Tc-tartan* in different stages of embryonic development. (A) Shows high expression levels of *Tc-tartan* in the head anlagen and weak expression in the more lateral neuroectoderm, while it is absent from the mesoderm. (B and C) In the elongating germ band the neuronal expression of *TC014658* becomes more segmental. (D) Knockdown of *Tc-twist* results in lateral expression of *Tc-tartan* expands towards the ventral side. (E and F) The knockdown of *Tc-tartan* results in loss of the neural cells (E), indicated by the absence of the *Tc-achaete-scute homolog (Tc-ash)* compared to wildtype (F).

2.2.2 Functional analysis of Toll and Twist targets

2.2.2.1 FGF pathway components mimic the *Tc-twist* knockdown phenotype

Four of the candidate genes showing mesodermal expression were chosen for further functional studies. *Tc-heartless* (TC004713, *Tc-htl*), which encodes a FGF receptor and is known to be a target of Twist in *Drosophila*, is expressed in a *Tc-twist* like mesodermal domain (Fig. 2.8 B and C) in the blastoderm. The loss of *Tc-htl* expression in *Tc-twist* knockdown embryos (data not shown) indicates that it is also a target of Twist in *Tribolium*. In addition, *Tc-heartless* deficient embryos have the same abnormal structure of the hindgut and the malpighian tubules as *Tc-twist* kd embryos (Fig. 2.8 A', B' and C'). Furthermore, using the G04609 line or "heart-GFP-line" (Koelzer et al., 2014), I was able to show that the knockdown of *Tc-htl* frequently (70.91%; N=115) results in loss of the cardioblast cell row (Fig. 2.8 A'', B'' and C''), similar to the knockdown of *Tc-twist*. Using the muscle enhancer line pBA19 (Lorenzen et al., 2003), I could also show a complete loss of the somatic muscles in *Tc-twist* kd embryos (Fig. 2.8 B''), as well as upon loss of *Tc-htl* (Fig. 2.8 C'''). However, the marker genes do not show changes in their expression (see Appendix E).

A second component of the FGF pathway was identified. *Tc-downstream-of-fgf* (TC0113239/*dof*) is a known Twist target gene in *Drosophila* and is involved in the FGF-dependent migration of tracheal and mesodermal cells. In *Tribolium*, *Tc-dof* is first expressed in a mesodermal stripe in the blastoderm (Fig. 2.8 D). I was not able to observe defects in DAPI-stained embryos (Fig. 2.8 D') or in the expression of marker genes after *Tc-dof* knockdown (see Appendix E). Although, the knockdown does not lead to complete loss of the cardioblast cell row, like in *Tc-twist* or *Tc-htl* deficient embryos, the loss of *Tc-dof* results in a clear reduction of the cardioblasts (Fig. 2.8 D''). This is in line with a reduction of the somatic muscles after knockdown of *Tc-dof* in embryos of the pBA-19 line (Fig. 2.8 D'''). It is likely that *Tc-dof* has a similar, but also slightly weaker role in DV patterning of *Tribolium* compared to *Drosophila*.

The fact that knockdown embryos of both, *Tc-heartless* as well as *Tc-dof* mimic the knockdown of *Tc-twist*, indicates that FGF signaling is most likely a direct and highly important target of Twist in *Tribolium*. The strong defects in heart precursor cells and the somatic muscles suggest, that FGF signaling has a strong influence on development of the mesodermal derived tissues.

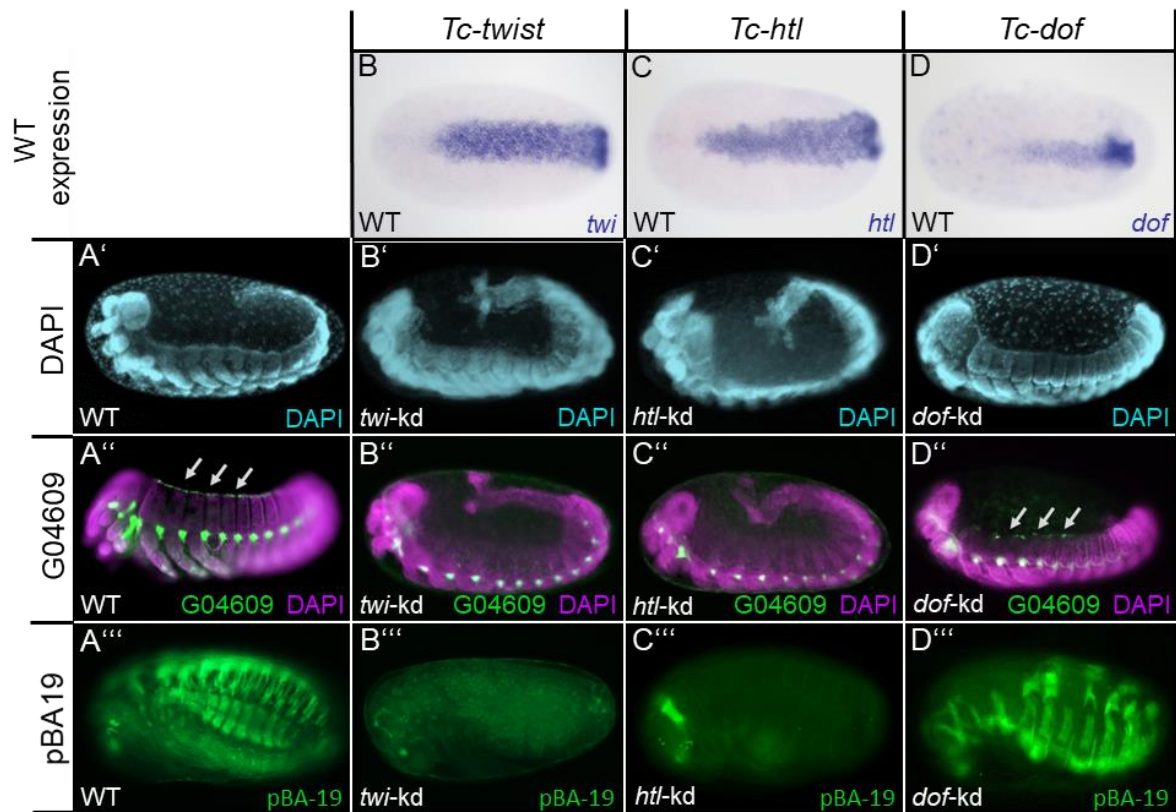


Figure 2.8: Functional analysis of FGF signaling components

The FGF-receptor *heartless (htl)* and *downstream-of-fgf (dof)* are involved in the formation of the heart, the visceral mesoderm and somatic muscles. (B-D) Both expressed in a *twist*-like stripe in the mesoderm. Knockdown embryos were created in transgenic lines in which mesodermal derived tissue is labeled by GFP: the heart-GFP line G04609 (Koelzer et al., 2014) (A''-D'') and muscle-GFP line pBA-19 (Lorenzen et al., 2003) (A'''-D'''). The results were compared to embryos after *twist* kd. (B'-C') Interestingly, upon *htl* knockdown the embryos showed fingering at the posterior end similar to *twist* kd embryos. They also show loss of the mesodermal derived cardioblasts (A''-C'') and complete loss of the somatic muscles (A'''-C'''). In comparison *dof* kd embryos show a weaker phenotype. The knockdown embryos lack the fingering (D'). Furthermore, the cardioblasts as well as the somatic muscles are not missing but strongly reduced (D'' and D'''). It seems that in *Tribolium* loss of a FGF ligand leads to weaker defects than the loss of the FGF receptor.

2.2.2.2 Laminin B1 – A regulator of heart and muscle development

Besides its enhanced mesodermal expression, *Tc-Laminin B1* (*TC005184*, *Tc-LanB1*) showed also a weaker expression in the whole embryo proper, but it is absent from the serosa (Fig. 2.9 A and B). The mesodermal expression is maintained during the elongation of the germ band (Fig. 2.9 C). After knockdown of *Tc-LanB1* via pRNAi, I observed fully elongated germ bands with a thinner and irregular shaped abdomen compared to WT (Fig. 2.9 D and D'). The defects in embryogenesis occurred in 71.83% (N=116) of the knockdown embryos. However, expression of the selected marker genes did change neither in the early nor in the late stages (Appendix E). While the cardioblast cell row is always completely lost (Fig. 2.9 E and E'), the knockdown of *Tc-LanB1* results only in partial loss and disorganization of the mesoderm derived somatic muscles (Fig. 2.9 F and F'). Furthermore, the muscle effect strongly varies in terms of strength (Appendix F). Compared to loss of *LanB1* in *Drosophila*, the effects seem to be more severe during *Tribolium* embryogenesis (Urbano et al., 2009).

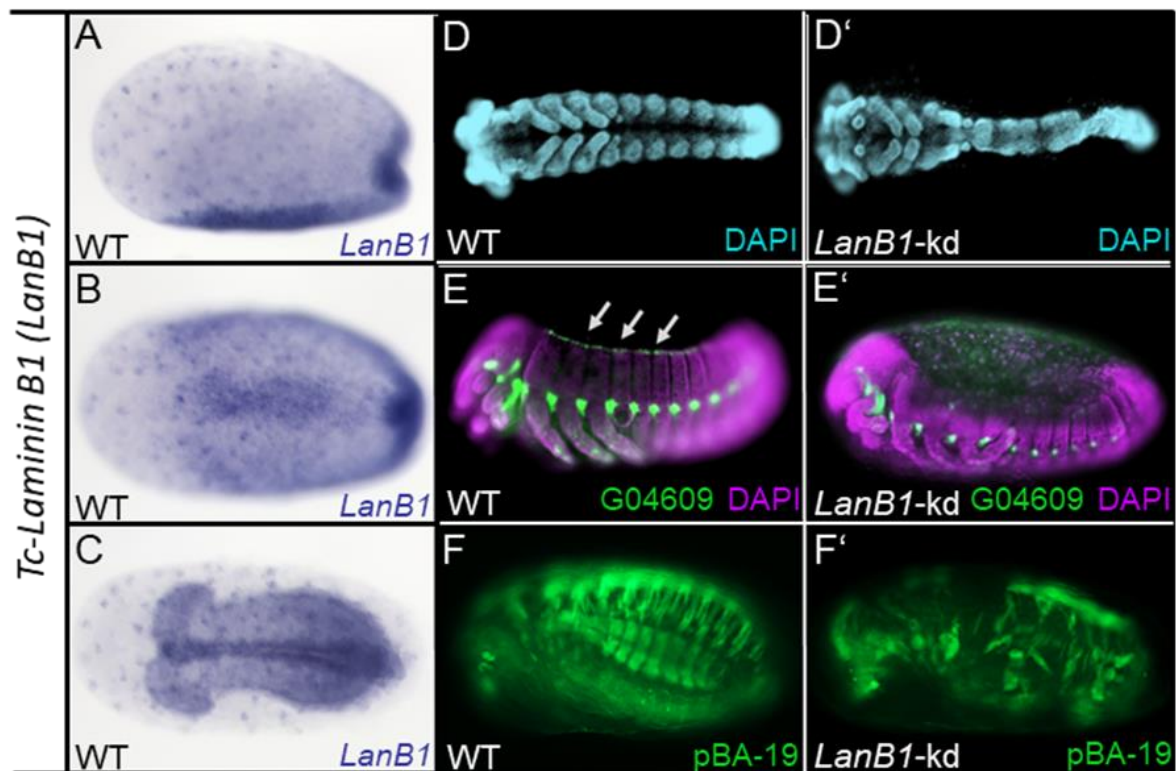


Figure 2.9: Knockdown of *Tc-LanB1* leads to loss of mesodermally derived tissues

(A-C) *Tc-LanB1* is expressed in the whole germ rudiment and upregulated in the presumptive mesoderm in differentiated blastoderm embryos. (D and D') *Tc-LanB1* knockdown. DAPI-stained germ band stage embryo shows defects in posterior segments. (E-E') Embryos of the enhancer trap line G04609. The cardioblast cell row (the presumptive heart) expresses EGFP (magenta counterstaining is DAPI). (E) Wildtype embryo of the G04609 line. (E') G04609 embryo after *Tc-LanB1* kd shows loss of the cardioblast cell row. (F and F') pBA19 enhancer trap line which expresses EGFP in muscles. (F) Wildtype pBA19 embryo. The body wall muscles are labeled by EGFP. (F') *Tc-LanB1* knockdown in pBA19, which shows GFP expression in somatic muscles. The somatic muscles are partially lost and severely disorganized.

2.2.2.3 Zfh1 – A transcription factor regulating late *Tc-twist* expression

Tc-zincfinger homeodomain 1 (TC011114; *Tc-zfh1*) is an unusual transcription factor combining zinc fingers and a homeodomain (Fortini et al., 1991). Transcription factors are often main regulators of GRN, thus it appears to be an interesting candidate which might be involved in DV patterning of *Tribolium*. *Zfh1* was identified as differentially expressed with a FDR of only 5%. Expression of *Tc-zfh1* appears firstly in early blastoderm embryos in a posterior located spot (Fig. 2.10 A). When the extraembryonic serosa separates from the embryo proper (differentiated blastoderm), *Tc-zfh1* expression expands to a ventral *twist*-like stripe (Fig. 2.10 B). This mesodermal expression also persists after gastrulation and is visible along the ventral midline (Fig. 2.10 C and D). The knockdown of *Tc-zfh1* results in high mortality of the injected mothers (72%; N=200). In addition, the survivors showed a reduced egg lay rate (data not shown). However, 94% of the embryos derived from these females (N=16) showed severe morphological defects (Fig. 2.10 E and F). A reduction of the dsRNA concentration from 1 µg/µl to 0.1 µg/µl reduced the sterility but did not affect the phenotypic penetrance of the embryos (data not shown). Surprisingly, the investigation of the marker gene expression shows only changes in the expression of *Tc-twist*. While the early expression of *Tc-twist* seems to be unaffected (Fig. 2.10 G), *Tc-twist* expression is completely absent from the developing abdominal segment during germ band elongation (Fig. 2.10 H and I). These findings indicate that *Tc-zfh1* is not only a target gene of *Tc-Twist*, but that it also regulates the maintenance of *Tc-twist* expression during germ band development.

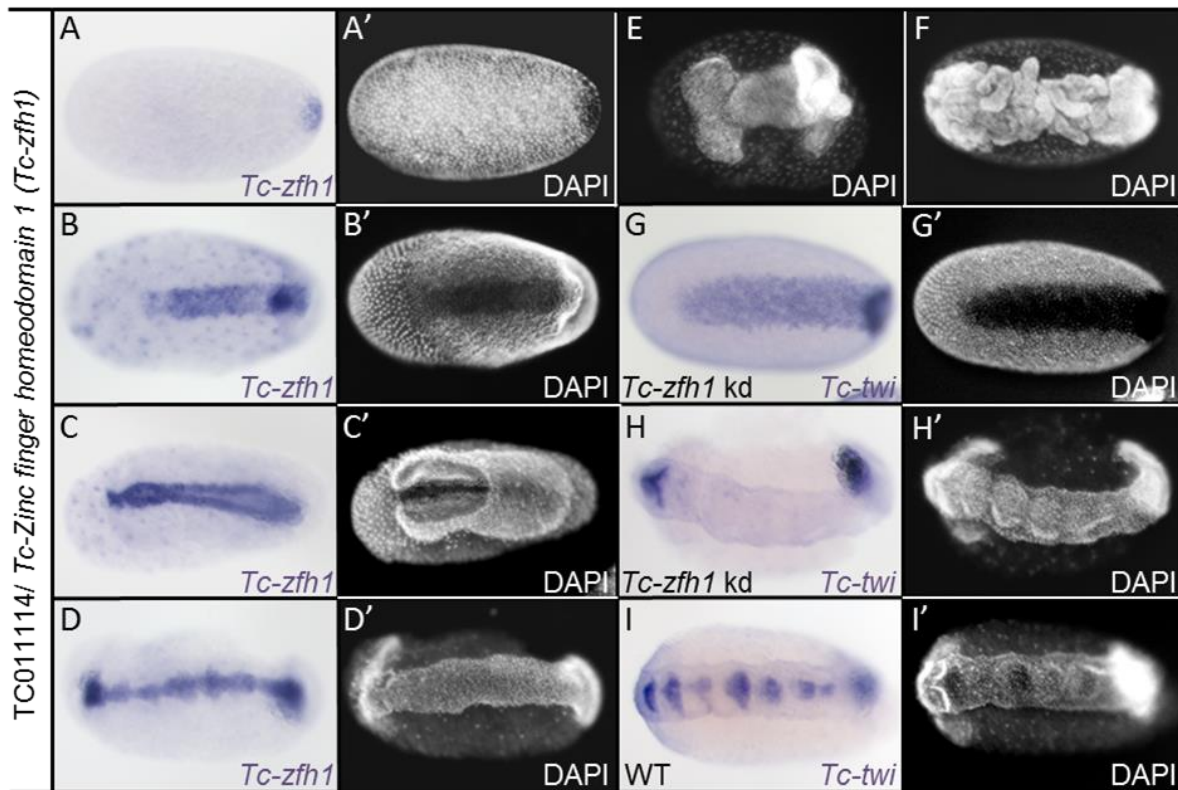


Figure 2.10: Analysis of mRNA expression and functional relevance of *Tc-zfh1*

(A-D) Wildtype expression of *TC011114/Tc-Zinc finger homeodomain 1 (Tc-zfh1)* in different stages. (A'-I') Same embryo as depicted in pictures labeled with corresponding capital letters, nuclei stained with DAPI for staging; all embryos in ventral view; Anterior to left. (A) Initially, *Tc-zfh1* is expressed in blastoderm embryos in spot at the posterior pole. (B) In the differentiated blastoderm around gastrulation, expression additionally arises in a ventral domain similar to the mesodermal expression of *Tc-twist*. (C and D) In the elongating germ band, *Tc-zfh1* is expressed at the ventral midline. Upon knockdown of *TC011114* severe defects occur already in early germ band stage embryos. Often, first defects can be observed at the posterior part of the embryo (E). Later these defects become more severe and different structures of the embryos are affected (F). G-I) The early *Tc-twist* expression is not affected by the knockdown of *Tc-zfh1*(G) while, *Tc-twist* expression is missing in most of the thorax and abdominal segments (H) compared to *Tc-twist* wildtype expression (I).

In summary, the expression analysis of genes differentially expressed in *Tc-dpp* and *Tc-sog* kd embryos, as well as genes downregulated after knockdown of *Tc-Toll* and *Tc-twist* confirmed two aspects. First, the reliability of the experimental approach and the RNA-sequencing data and second, expression patterns of genes could be identified which clearly differ from the already investigated expression domains of their *Drosophila* homologs. Finally, first functional studies for *Tc-uif*, *Tc-tartan*, *Tc-htl* and *Tc-dof*, *LanB1* and *zfh1* indicate a function of these genes in early but also in later development of *Tribolium* embryos.

3 Discussion

3.1 Verification of the RNA-sequencing data

The identification of the single nodes in a GRN is a requirement for uncovering evolutionary changes in the respective network. As comparative studies by a candidate gene approach are only helpful to investigate changes in the regulation of already known homologs, we used differential transcriptome analyses by RNA-sequencing after pRNAi. This approach enables the genome wide identification of new potential components of the *Tribolium* DV-GRN. In fact, we uncovered a broad range of interesting candidates. 796 genes showed up as differentially expressed in knockdown embryos lacking Toll or BMP signaling components. Determination of the knockdown penetrance for each sample as well as testing the knockdown efficiency by qRT-PCR and the quality control of the isolated RNA of the respective samples, helped to select the best possible starting material for a comparative transcriptome analysis. During the bioinformatics analysis, two different programs were used to compare the dependence of the resulting data on the used algorithms. As more than 85% of the differentially expressed genes identified by edgeR overlapped with those identified by DESeq2 we considered only the genes which showed up in both programs for further analysis. In a next step we tried to identify some of the already known DV-GRN components in the different knockdown backgrounds compared to the control. *Tc-twist*, *Tc-Toll* as well as *Tc-sog* were found to be significantly downregulated in the respective knockdown samples. However, *Tc-dpp* did not appear as downregulated upon knockdown of *Tc-dpp*. It could be, that this was due to the poorly annotated *Tc-dpp* sequence in the official gene set the RNA-sequencing reads were mapped to (OGS 2/Tcas 3.0). The new official genome (OGS 3/Tcas 5.2) shows a sequence of almost twice the size. Nevertheless, other marker genes expressed in the serosa like *Tc-zerknüllt 1 (zen) 1*, *Tc-zen2* or *Tc-dorsocross (doc)* or on the dorsal side like *Tc-iroquois (Tc-iro)* showed the expected downregulation in *Tc-dpp* knockdown samples (Nunes da Fonseca et al., 2008; van der Zee et al., 2005; van der Zee et al., 2006). Both, *Tc-Toll* as well as *Tc-twist* kd showed a downregulation of the mesodermal expressed genes *Tc-twist*, *Tc-snail* and *Tc-cactus*. These first results suggest a successful generation of RNA from different knockdown backgrounds as well as an accurate bioinformatics analysis of the RNA-sequencing data. Next, I tried to reproduce and thus verify the differential regulation of some candidate genes by ISH. Due to the fate shift of the serosa, a lot of genes upregulated in *Tc-Toll* kd embryos compared to the control showed expression in the serosa. Screening the expression patterns of some of those genes in wildtype and *Tc-Toll* knockdown embryos, showed the expected expansion of the serosa and thus of the expression domains of these genes (Fig. 2.1). Proving the biological authenticity of the RNA-sequencing data legitimates further studies on expression patterns of genes potentially involved in the DV-GRN of *Tribolium castaneum*.

3.2 Expression patterns of some candidates suggest an involvement in DV patterning

Among 796 differentially expressed genes we found 222 to be differentially expressed in more than one knockdown condition with a FDR of 1% (Fig. 1.6). The majority of the identified genes differentially expressed between *Tc-sog* and *Tc-dpp* knockdown showed strong expression in the extraembryonic serosa (Fig. 2.5 A-E) and only 3 out of 14 genes showed expression within the embryo proper (Fig. 2.5 F-H). In addition, these genes are all strongly expressed in the head anlagen of differentiated blastoderm embryos. In fact, the analysis of the expression domains of this group reflects the strong interaction of the anterior-posterior (AP) and dorsoventral (DV) patterning system during early embryogenesis. Loss of some of the most important DV patterning genes like *Tc-Toll*, *Tc-sog* and *Tc-dpp* do not exclusively affect the fate determination along the DV axis, but cause also a contrary shift of the embryo-serosa border, and thus influence the size of the presumptive head and the serosa.

With high chance, the genes downregulated in *Tc-Toll* and *Tc-twist* RNAi embryos are acting in specification of the presumptive mesoderm. Indeed, the ISH screen revealed that 12 genes show high expression levels in the mesoderm or in region directly flanking the mesoderm. By relaxing the FDR to 5%, additional ventrally expressed genes were identified. The identification of already known elements of the early dorsoventral patterning system like *Tc-twi*, *Tc-snail*, *Tc-cactus* served as control to verify the accuracy of the bioinformatic analysis. Furthermore, the results showed a different regulation of the Delta/Notch pathway in *Tribolium* compared to *Drosophila*. In the fly, both *enhancer of split* homologs (*E(spl)1* and *E(spl)3*) as well as mRNA of the Notch ligand Delta are expressed in the neurogenic ectoderm, while Notch signaling is inhibited in the mesoderm by the repression of *Delta* (Aranda et al., 2008; De Renzis et al., 2006; Vassin et al., 1987). In contrast, all three *Tc-Delta*, *Tc-E(spl)1* and *Tc-E(spl)3* seem to be active in the mesoderm. During late differentiated blastoderm, the *enhancers of split* expression domains slowly clear from the mesoderm and get enhanced at its borders. Those findings suggest that the pathway has a different region of activity and might thus influence also other downstream components. The FGF signaling pathway is represented by the receptor *Tc-heartless* and a more downstream component *Tc-dof*. Both are also mesodermally expressed in *Drosophila* (Beermann and Schroder, 2008; Sharma et al., 2015). Furthermore, important genes involved in cell adhesion (*integrins*, *laminin B1* and *dystroglycan*) could be identified as targets of *Tc-Toll* and *Tc-Twist*. However, *zinc finger homeodomain 1 (zfh1)* was the only transcription factor showing a distinct mesodermal expression pattern and a function in DV patterning.

3.2.1 *Tc-uninflatable* knockdown affects the formation of abdominal segments

Two genes differentially expressed upon *Tc-sog* and *Tc-dpp* kd showed neuroectodermal mRNA expression domains in the ISH screen. In *Drosophila*, *uninflatable* (*uif*) is localized in the apical plasma membrane of all ectodermal derived epithelia and is mainly involved in tracheal inflation (Zhang and Ward, 2009) and in antagonizing Notch signaling during imaginal wing disc development (Xie et al., 2012). The co-expression with the Delta/Notch components *E(spl)1* and *E(spl)3* (Fig. 2.3 A and B), could indicate an earlier involvement of *uninflatable* in *Tribolium* embryogenesis, although loss of *Tc-uif* only affects late embryogenesis (Fig. 2.6 D and E). The embryos show thinner abdominal segments which suggest defects in the segment addition zone. However, none of the marker genes showed an altered expression pattern (Appendix D). Also *Drosophila* embryos show no early alterations in embryonic development due to loss of *uninflatable*, although also *Dm-uif* is expressed in the early embryo before gastrulation (Zhang and Ward, 2009). So far, no linkage of the early expression pattern of *Tc-uif* and the rather late effect on the development of the abdominal segments could be identified. To further investigate the role of *Tc-uif* in dorsoventral patterning of *Tribolium*, a more detailed analysis of the phenotype would be necessary.

3.2.2 *Tc-tartan* is an early regulator in neurogenesis

Tartan is a transmembrane protein containing an extracellular leucine-rich repeat (LRR) domain (Milan et al., 2001). Early *Drosophila tartan* expression arises in transversal segmental stripes and two additional longitudinal ventral stripes before the expression is restricted in sensory mother cells and proneural clusters in later development. However, *Dm-tartan* deficient embryos show defects in the formation of the central and peripheral nervous system. But as the neurons are not completely absent, it is likely that *Dm-tartan* does not act alone, but that the pathway is at least partially redundant (Chang et al., 1993). Interestingly, a second closely related gene with LRRs, *Dm-capricious* (Lorenzen and Capko, 2003), was identified in the *Drosophila* genome. Unlike *Dm-tartan*, *Dm-cap* does not show an early expression before gastrulation but is expressed in motorneurons and muscles in later stages (Milan et al., 2001), supporting the redundancy in neuron development. *Tc-tartan* is exclusively expressed in the neuroectoderm of blastoderm embryos with enhanced expression in the head anlagen (Fig. 2.7 G and 2.3 A). Later, strong expression levels are visible in segmental clusters in the neuroectoderm (Fig. 2.7 B and C). Former studies (Chang et al., 1993) showed that *Dm-tartan* expression is probably negatively regulated by Single-minded (Sim) on the ventral side and by Decapentaplegic (Dpp) on the dorsal side of the embryo. Expansion of the *Tc-tartan* expression domain towards the ventral side after loss of *Tc-twist* (Fig. 2.7 D) suggests, that *Tc-tartan* is negatively regulated either by Twist itself or like *Dm-tartan*, by a Twist target (e.g. Sim). Unlike in *Drosophila*, loss of *Tc-*

tartan results in complete loss of proneural clusters in thorax and abdominal segments as indicated by the absence of *Tc-ash* expression (neural marker) (Fig. 2.7 E compared to F). The significantly stronger defects are in line with the fact, that I identified only a single gene in *Tribolium* that shows more similarities to *Dm-tartan*. Thus, it seems that *Tc-tartan* is absolutely required for development of the nervous system in *Tribolium* embryos.

3.2.3 Involvement of the FGF pathway in formation of mesodermal derived tissue

Fibroblast growth factors (FGFs) as well as their corresponding receptors (FGFRs) play key roles in early embryonic development and cell migration in both, invertebrates and vertebrates (Bottcher and Niehrs, 2005; Muha and Muller, 2013). Previous studies revealed that while two different FGF receptors (Heartless and Branchless) are responsible for heart formation and development of the tracheal system in *Drosophila*, only a single FGFR ortholog exists in *Tribolium*. *Tc-heartless* acts in both processes (Beermann and Schroder, 2008; Beiman et al., 1996; Klambt et al., 1992; Sharma et al., 2015). The analysis of *Tc-heartless* (*Tc-htl*) knockdown embryos show that the *Tribolium* FGF receptor is not only essential for the development of the cardioblasts (Fig. 2.8 C''), but that *Tc-htl* kd embryos show the same malformation of the hind gut (proctodeum) and the malpighian tubules like *Tc-twist* kd embryos (Fig. 2.8 B' and C'). These defects indicate a general involvement of *Tc-htl* in the development of all mesodermally derived tissues, including the somatic muscles. In fact, knockdown of *Tc-htl* in the pBA-19 line with muscle-specific expression of GFP results in complete loss of the body wall muscles (Fig. 2.8 C''') similar to loss of *Tc-twist*. Thus, also the single FGF receptor Heartless seems to have a prominent role in formation of the somatic muscles. Previous studies in *Drosophila* underline the importance of *heartless* in the dorsal-directed migration of mesodermal cells including the dorsal somatic muscles (Gisselbrecht et al., 1996). These findings could be also verified by other studies (Sharma et al., 2015). Furthermore, it was shown that *Tc-Heartless* also acts in the development of the tracheal network, thereby combining the function of two separate FGF receptors in *Drosophila*. Another component of the FGF pathway could be identified as being upregulated in *Tc-Toll* and *Tc-twist* knockdown embryos. The mRNA of the adaptor protein Downstream of FGFR (*Dof*), also known as *Stumps*, is co-expressed with both FGF receptors in *Drosophila*. It is thought to promote the migration of both, mesodermal as well as tracheal cells (Imam et al., 1999; Vincent et al., 1998). The involvement in FGFR-dependent cell migration could also be demonstrated by the knockdown of *dof* in *Tribolium*, which is like *Dm-dof* co-expressed with its receptor Heartless (Fig. 2.8 D). Although the effect was weaker compared to knockdown of *Tc-heartless*, *Tc-dof* kd embryos showed at least partial loss of the cardioblast cell row (Fig. 2.8 C'' and D'') and somatic muscles (Fig. 2.8 C''' and D'''). In summary, my results indicate a similar role of FGF signaling in the DV-GRN of *Tribolium castaneum* compared to *Drosophila*.

3.2.4 Extracellular matrix components (ECMs) and their role in mesoderm formation

Basement membranes (BM) provide mechanical stability and are physical barriers between different cell types. They are essential for tissue morphogenesis like differentiation, shape, adhesion, survival and migration of cells. BMs consist of Laminins, Collagen IV and other extracellular matrix (ECM) components like Nidogen. Laminins bind to cell surface receptors to mediate cellular responses (Kusche-Gullberg et al., 1992; Montell and Goodman, 1989; Urbano et al., 2011). The transcripts of *Tc-Laminin B1* (FDR1%) as well as two of its receptors: *Tc-Integrin α PS2/Inflated* (FDR1%) and *Tc-Dystroglycan* (FDR5%) were identified as upregulated in *Tc-Toll* and *Tc-twist* kd embryos. In *Drosophila* only *LanB1* is expressed in the presumptive mesoderm (Bogaert et al., 1987; Dekkers et al., 2004; Montell and Goodman, 1989; Schneider and Baumgartner, 2008; Urbano et al., 2011; Wehrli et al., 1993). In contrast, all three of them showed mesodermal expression in *Tribolium* blastoderm embryos (Fig. 2.4 I and N; data not shown for *dystroglycan*). The most obvious defect upon knockdown of *Tc-LanB1* is an irregular shape of the posterior segments (Fig. 2.9 D'). In addition, I could show the loss of the mesodermally derived cardioblasts (Fig. 2.9 E') and an irregular shape and uneven distribution of the somatic muscles (Fig. 2.9 F'). Compared to loss of *LanB1* in *Drosophila*, which only results in mild muscle defects (Urbano et al., 2009), the knockdown of *Tc-LanB1* seems to cause stronger defects. Furthermore, the early co-expression of the three ECM components in *Tribolium* could indicate an ancestral feature of ventral furrow formation which might have been partially lost in *Drosophila*. It was shown that the interaction of Laminin, Integrins and Dystroglycan plays an important role in gastrulation of many animals, especially in vertebrates (Ettensohn and Winkelbauer, 2004). However, we did not find evidence for an involvement in ventral furrow formation of the ECM components in *Tribolium*. Analyzing defects in mesoderm invagination requires more complex and time-intensive methods like preparation and staining of cross-sections. A more careful analysis of embryos lacking ECM components might confirm a more ancestral role of Laminin B1, Integrin α PS2 and Dystroglycan in mesoderm invagination during the gastrulation of *Tribolium* embryos.

3.2.5 Zfh1 - A new essential regulator maintaining late *Tc-twist* expression

Zinc finger homeodomain 1 (Zfh1) is a promising candidate for being an essential component of the DV-GRN of *Tribolium*. It is upregulated after knockdown of *Tc-Toll* and *Tc-twist*. Fitting the transcriptomic data, *Tc-zfh1* is, similar to its *Drosophila* homolog (Casal and Leptin, 1996; Lai et al., 1991), exclusively expressed in the mesoderm (Fig. 2.10 A-D). This gene was also isolated by screening a cDNA expression library derived from *Drosophila* embryos in which all cells show mesodermal characteristics (Casal and Leptin, 1996). As both, homeodomain and zinc-finger proteins possess the most common DNA-binding motifs, they are involved in a wide range of developmental processes in *D. melanogaster* (Fortini et al., 1991). Zfh1 belongs to a rare class of transcription factors containing both, homeodomains as well as zinc finger domains. Loss of Zfh1 function in *Drosophila* embryos results in various degrees of spatially restricted defects in cell fate or positioning and the lack the caudal visceral mesoderm (CVM) (Broihier et al., 1998; Kusch and Reuter, 1999). Thus, it is unlikely that *Dm-Zfh1* is required for the initial mesoderm formation or for the differentiation of mesodermally derived tissues (Lai et al., 1993). Knockdown of *Tc-zfh1* by RNAi leads to multiple severe morphogenetic defects during germ band formation (Fig. 2.10 E and F). Loss of the *Tc-zfh1* expression domain after *Tc-twist* knockdown indicates that at least early *Tc-zfh1* expression is dependent on Twist or one of its targets. However, late *Tc-zfh1* expression is similarly to *Drosophila*, independent of Twist (data not shown). In contrast, late *Tc-twist* expression is deleted in all abdominal segments upon knockdown of *Tc-zfh1* (Fig. 2.10 G-I). These findings indicate that *Tc-zfh1* is not only a target of Twist, but that it also involved in maintaining *Tc-twist* expression in the elongating germ band. Little is known about the re-initialization of *twist* expression in the growth zone of *Tribolium*. The strong effect on *Tc-twist* expression suggests, that compared to its role in *Drosophila*, *Tc-zfh1* is an essential component for mesoderm development in *Tribolium*. In summary, the identification of *Tc-zfh1* could be a first step in uncovering the pathways acting in the segment addition zone of short germ insects like *Tribolium*.

Part of the *Tribolium* phenotype after loss of *zfh1* is a strong sterility effect. Pupal as well as adult injections with a standard concentration of 1µg/µl dsRNA resulted in complete sterility and high mortality of the female beetles. This effect could be avoided by lowering the concentration of the injected dsRNA. It was already shown that Zfh1 loss of function leads to defects in the gonadal mesoderm in *Drosophila* (Broihier et al., 1998; Kusch and Reuter, 1999). Thus, the observed sterility of *Tc-zfh1* dsRNA injected beetles implies a similar role in development of the gonads in *Tribolium*.

3.3 Possibilities and limitations of comparative analysis by RNA-sequencing

Since the *Tribolium* DV-GRN differs from the well-studied dorsoventral patterning system of *Drosophila*, the main goal of this study was to identify new genes functioning in the establishment of the DV axis of *Tribolium*. In addition, differences in the position, regulation and function of already known elements within the network should be uncovered. Thus, we performed a differential transcriptome analysis after knockdown by pRNAi as a global and unbiased approach.

3.3.1 Stronger influence of *Tribolium* homologs on early embryonic development

Some genes or even whole pathways seem to play comparable roles in *Drosophila* and *Tribolium*, like the components of the FGF pathway (*heartless* and *dof*). Other *Tribolium* DV patterning homologs show a tendency to have a stronger influence on the early development compared to *Drosophila*. While two genes regulate the determination and differentiation of proneural clusters in *Drosophila* (*tartan* and *capricious*), the single *Tribolium* homolog (*Tc-tartan*) is showing comparatively stronger defects after knockdown by pRNAi. The same is true for different components of the extracellular matrix (ECM). The mRNA of Integrin, Laminin B1 and Dystroglycan is co-localized in the mesoderm of *Tribolium*. In contrast, they have complementary expression domains in *Drosophila*. Moreover, the strong defects after knockdown of *Tc-laminin B1* suggest a relevant and maybe more ancestral role of ECM components in mesoderm development. Another gene with an only minor role in the DV-GRN of *Drosophila* is *zfh1*. However, my results show that *Tc-zfh1* is essential for the maintenance of mRNA expression of the mesodermal key regulator *Tc-twist* during germ band formation and extension. This new role of Zfh1 which was not shown so far might be an adaption to the more ancestral developmental mode of short-germ embryogenesis. The stronger influence of *LanB1*, *heartless* and *tartan* on *Tribolium* DV patterning can be explained by the fact that only single homologs were identified in *Tribolium*. In contrast, the *Drosophila* genome contains a second homolog for each of these genes. In *Tribolium* these genes are absolutely required for functions which are distributed between two genes in the fly. If a duplication and a subsequent sub-functionalization occurred during evolution in drosophilids or if one of these genes was secondarily lost in the beetle, remains unclear.

3.3.2 Comparative analysis for *de novo* identification of DV-GRN components

In total we could identify 796 genes (Fig. 1.6 A, table) which were differentially expressed in the knockdown embryos compared to the control with a false discovery rate (FDR) of 1%. More than 300 differentially expressed genes could be identified upon knockdown of each, *Tc-Toll*, *Tc-twist* and *Tc-dpp* knockdown. 18 genes showed differential expression levels in *Tc-sog* knockdown embryos compared to the control. A more thorough analysis on two subgroups: *Tc-Toll* kd versus *Tc-twist* kd and *Tc-sog* kd versus *Tc-dpp* kd revealed numerous genes showing typical dorsoventral expression patterns. First functional studies on some of the genes showing promising expression patterns resulted in interesting new insights in the *Tribolium* DV-GRN.

The identified genes and their function in DV patterning of *Tribolium* revealed some of the differences in the DV-GRN of *Drosophila* and *Tribolium*. However, only one gene has a profound new role in *Tribolium* embryogenesis. One explanation could be that the *Tribolium* DV-GRN does not drastically differ in the genes that are involved but rather in the interplay of those genes. This theory fits the findings suggesting that evolutionary changes in GRN occur most likely on the level of transcriptional regulation instead of changes in protein structure. Thus, comparative transcriptome analysis after RNAi can only suggest a list of genes that are potentially influenced. It remains open if the genes showed up due to a simple fate shift (e.g. shift of the embryo-serosa border) or if the regulation of their expression was directly influenced by the loss of their regulator. For this purpose, a ChIP sequencing approach can be used. ChIP sequencing detects only genes that are bound by a specific gene (e.g. Dorsal). In consequence, the identified genes are most likely direct target genes. The most promising approach might thus be a combination of both, transcriptome analysis and ChIP sequencing. However, the data set provide a great basis for several new questions on early development of *Tribolium castaneum*.

3.3.3 Reasons for the detection of false positives

Although genome wide comparative analysis after RNAi is a great achievement for the field of evolution & development, one should not disregard technical difficulties. So far no “gold standard” bioinformatic pipeline for analysis of RNA-seq data is available. Different programs are provided for the intermediate steps like trimming, mapping of the reads, generation of count tables and identification of differential expression. In addition, improved versions of used programs as well as new developed tools for bioinformatic analyses are constantly released. Thus, it is challenging to find the best method to analyze these data and to ensure the accuracy of the generated lists of potential candidate genes. Choosing stringent settings like low false discovery rates (FDR) should ensure the breakdown of the data set to a manageable number of genes. However, this procedure poses a danger of missing potential interesting candidates. On the other hand, false positive candidates should be avoided. Nevertheless, the appearance of false positives during comparative analyses is a constant problem in analyzing RNA-sequencing data (Conesa et al., 2016).

The generation of lists containing differentially expressed genes in more than one knockdown condition also resulted in a list of genes which are allegedly differentially expressed in both, *Tc-Twist* and *Tc-dpp* knockdown embryos. A closer look on the fate shift caused by the respective knockdowns revealed that there is almost no overlap in the regions affected by both knockdowns (Fig. 2.12). Indeed, an ISH screen resulted in the identification of only one distinct expression pattern (*fushi tarazu*). In addition, examining the genomic region revealed that most of the genes showed a hit in a poorly annotated region with low RNA seq support. Thus, most of those genes can be considered as false positives (Dassen, Bachelor Thesis 2016).

One reason for false positives is a low cutoff. Genes with low fold-changes can be wrongly detected as positive hit (Sims et al., 2014). In addition, genes with very low expression levels and thus low raw read counts can show false high fold-changes in comparative analysis. For example, a gene with a read count of 2 in wildtype samples could show a read count of 8 in a knockdown sample and thus produce a high fold change. Such low read counts are problematic as they might only reflect background signal and have to be removed by normalization. Since these genes are measured with higher noise, measuring a large fraction of the genes with low read counts can produce a dataset that is biased towards identifying differentially expressed genes with low read counts. (Busby et al., 2013). The choice of analysis tool (programs) is also connected to the detection rate of false positives (Soneson and Delorenzi, 2013). The algorithms of both DESeq2 and edgeR, show inflated false positives rates compared to other programs (Rocke et al., 2015). Another possible source for false positive results is the mapping of the reads to a genome. The genome used for this work in 2013 was the official genome OGS2 (Tcas 3.0). Although, many gene models were already quite accurate some had to be annotated

and changed dramatically in the new official genome OGS3 (Tcas 5.2) published in 2016. Thus, some of the false positive can be explained by mismapping of the reads. However, it could be interesting to map our RNA sequencing data to the reannotated genome and compare the resulting lists of differentially expressed genes. It might be also worth to run some of the analyses on improved versions of the used programs or even by newly developed tools. In summary, the bioinformatic analysis of RNA sequencing data is a critical step in global comparative analyses. The pipeline for the analysis should be chosen carefully according to the number of groups compared and the general biological question of the study.

3.4 Conclusion

In summary, we achieved the aim of a global and unbiased identification of *Tribolium* DV-GRN components in *Tribolium castaneum*. In total 116 potential candidate genes from different comparisons were investigated by an ISH screen. The identified localized expression patterns and first functional studies indicate a potential involvement of some of the discovered genes in dorsoventral patterning. The analysis of the 28 genes differentially regulated upon *Tc-sog* and *Tc-dpp* knockdown (14 with FDR of 1%, 14 with a FDR of 5%) revealed that the neuroectodermal expressed genes *Tc-uniflatable* and *Tc-tartan* are both involved in the development of *Tribolium* embryos. Especially the investigation of the 58 genes which showed up as differentially regulated after knockdown *Tc-Toll* and *Tc-twi* (38 with FDR of 1%, 20 with a FDR of 5%) led to the discovery of new expression patterns, such as the mesodermal expression of the *Tc-E(spl)* genes, as well as new early phenotypes caused by the knockdown of genes known to have later and often less important roles in *Drosophila*. In particular, *Tc-zfh1* is likely to be an essential component of the *Tribolium* DV-GRN that is required to maintain the expression of *Tc-twi* during germ band elongation. Compared to expensive and time-consuming RNAi or mutant screening projects, differential expression analysis by RNA sequencing provides faster results of equal accuracy and biological relevance.

3.5 Outlook

Also, the analysis of 30 genes (FDR of 1%) differentially expressed in *Tc-Toll* kd embryos resulted in potentially interesting candidates (Dassen, Bachelor Thesis 2016). One of the most interesting genes is *TC011067*. Its expression domain in late uniform blastoderm stages spans the ventral most region along the whole AP axis and strongly resembles the expression domain of *Tc-cactus*. Due to a partial inside-out phenotype and missing head structures after pRNAi, *TC011067* was also identified as potential DV patterning gene by the iBeetle⁴ screen. *TC011067* is annotated as Serine Protease P125 and is currently investigated in our lab. First results by Salim Din Muhammad suggest that *TC011067* is not only a Toll target but that it is also a positive feedback element, which is likely to act upstream of Toll. Thus, this gene might help to gain important insights in the early establishment and stabilization of the nuclear Dorsal gradient and the spatial and temporal influence of the nuclear Dorsal gradient on the transcriptional regulation of its target genes. This finding proves that the enormous amount of data can be used for a broad range of questions on early embryonic DV patterning and morphogenesis. Another important step could be the improvement of the data set by BLASTing the RNA-seq reads to the new official gene set (OGS 3). Results of a colleague already showed that the accuracy of the new genome does not only reduce the detection of false positives, but that it also results in gain of some new potential candidates.

⁴ The iBeetle projects is a large-scale RNAi screening project in the red flour beetle *Tribolium castaneum*. Using the RNA interference method, genes are silenced in the pupal and larval developmental stages. The observed phenotypes are annotated in the public iBeetle-Base. The here described results are based on personal communication with Muhammad Salim Din Muhammad.

CHAPTER II

Fog signaling and its role in epithelial morphogenesis in *Tribolium castaneum*

4 Introduction

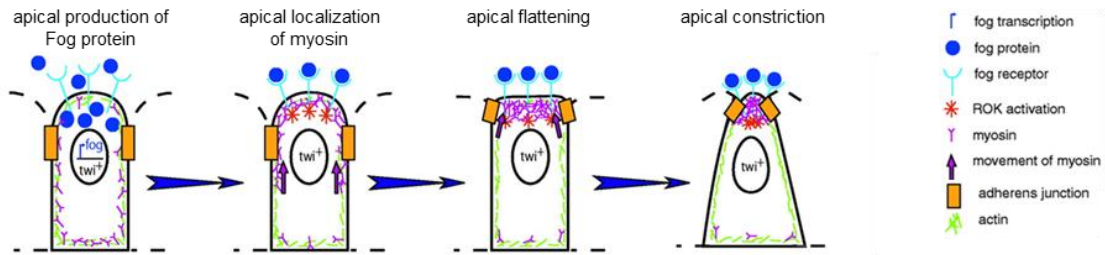
4.1 The role of cell shape changes in embryonic development

The determination of cell fates by antero-posterior and dorsoventral patterning during early embryogenesis is crucial for the development of complex structures like organs. However, another mechanism should not be ignored. Cell migration and morphogenetic movements of epithelial sheets are essential for correct formation and folding of tissues. Morphogenesis, the reorganization of cells and tissues into new forms, is an essential part of animal development (Sawyer et al., 2010). These movements ensure the internalization of cells from the outer surface to the interior by ingression of single cells or the invagination of cell sheets. Spatial and temporal changes in the cytoarchitecture and the resulting cell shape changes are the underlying processes for morphogenetic movements (Suzuki et al., 2012). To study morphogenesis in the context of development it is necessary to understand the molecular mechanisms of how patterning genes interfere with cytoskeleton components in order to change cell shapes (Dawes-Hoang et al., 2005; Leptin, 1994).

The invagination of epithelial cell sheets during gastrulation is shared in many organisms (Leptin, 1999). The Fog signaling pathway is one of the best studied processes in initiating early morphogenetic movements by cell shape changes and plays a major role during gastrulation of *Drosophila melanogaster* (Manning and Rogers, 2014).

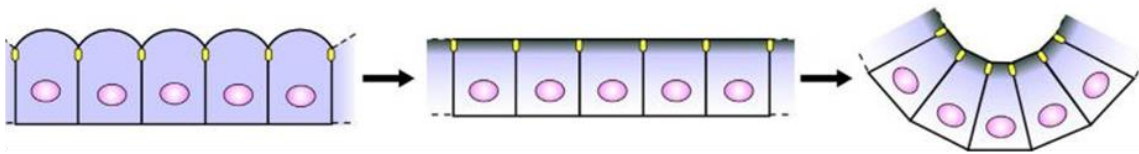
The process of cell shape changes is taking place in different steps (Fig. 1.1 A). First, the apical surface of cells is domed. Subsequently, Fog signaling activates ROK which leads to rearrangements of the actomyosin network. The actomyosin network is connected to adherens junctions, which are facilitating its localization to the apical side of the cells. The force generated by apically localized contraction of the actin-myosin cytoskeleton results in flattening of the apical cell surface. At the same time, the cells start to elongate along the apical-basal axis, leading to a columnar shape of the previous cuboidal cells. The continued constriction of apical actin-myosin pulls the adherens junctions close together, resulting in the apical constriction of the cells (Dawes-Hoang et al., 2005). The reduction of the apical surface diameter is also affecting the cell shape of the neighboring cells and hence triggering bending of the whole tissue sheet (Fig. 1.1 B). These cell shape changes are especially important to drive the internalization of the presumptive mesoderm and the posterior midgut primordium during fly gastrulation (Fig. 1.1 C) (Manning and Rogers, 2014; Parks and Wieschaus, 1991).

A Apical constriction by rearrangement of the actin-myosin network



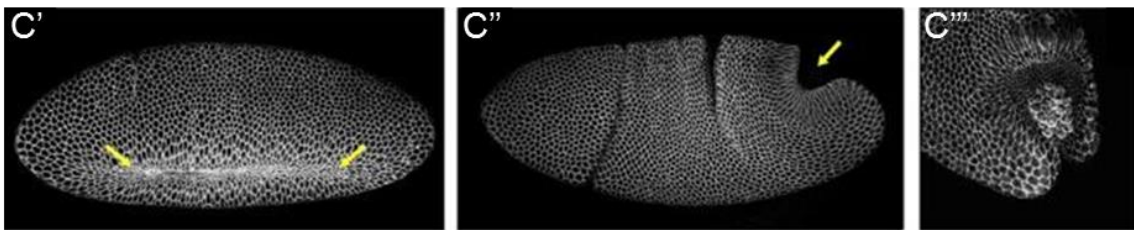
Wieschaus et al., 2005

B Folding/bending of epithelial sheets



Manning and Roger, 2014

C Internalization of mesoderm and posterior midgut



Manning and Rogers, 2014

Figure 1.1: Morphogenetic events induced by Fog signaling

Model of Fog function in controlling cell shape changes in the mesoderm of *Drosophila embryos*. (A) Fog signaling at the apical side of the cell (blue dots) results in localized activation of ROK (red asterisk) and leads to a rearrangement of the actin-myosin network. Thus, myosin (pink) is relocated to the apical side of the cell (arrows). In consequence, by contraction of the actin-myosin cytoskeleton the domed apical cell surface gets pulled down and flattens. In addition, the adherens junctions (Baumert et al.), connected to the actin-myosin network, move to the apical edge of the cell (arrows). The result of these movements and contractions is the apical constriction of the cells. (B) This process is essential for the bending and folding of epithelial cell sheets during embryonic gastrulation. (C'-C''') A *Drosophila* embryo undergoing gastrulation. Embryos were stained for Neurotactin to outline cells. The yellow arrows indicate cell groups undergoing Fog pathway induced apical constriction. (C') Ventral furrow formation. (C'') Posterior midgut invagination. (C''') Closer view of posterior midgut cells undergoing apical constriction. Germ cells are carried in with this invagination. (modified from Dawes-Hoang et al., 2005 and Manning and Rogers, 2014)

4.2 The Fog signaling pathway

Formation of the ventral furrow and invagination of the posterior midgut are the first morphogenetic movements in *Drosophila* embryogenesis and were extensively studied (Leptin, 1994). One of the best understood pathways regulating these processes is the Folded gastrulation (Fog) pathway, which induces apical constriction of cells and thus folding of epithelial sheets (Manning and Rogers, 2014).

4.2.1 The Pathway components and their interaction

Folded gastrulation (Fog) is a secreted protein localized in cells of the presumptive mesoderm and posterior ectoderm (Costa et al., 1994; Manning and Rogers, 2014; Morize et al., 1998). Fog is expressed in a ventral stripe in the presumptive mesoderm and a smaller posterior domain, precisely mimicking the pattern of constriction initiations (Costa et al., 1994). Experiments showed that a depletion of Fog in some cells does not affect a wide area of cells. Thus, it is likely that Fog diffusion to the neighboring cells is rather limited. Loss of Fog in *Drosophila* embryos prevents apical constrictions in both, the posterior midgut and the ventral furrow (Costa et al., 1994). In addition, problems in germband extension (convergent extension) occur which leads, as a secondary effect, to wrinkled or twisted embryos (Parks and Wieschaus, 1991) (Fig. 1.2).

Apical constriction is initiated when Folded Gastrulation (Fog) binds to the G-protein coupled receptor (GPCR) Mist (Mesoderm Invagination Signaling Transducer), which was first identified as Methuselah-like 1 by a GPCR targeted RNAi screen in 2013 (Adams and Celniker, 2000; Brody and Cravchik, 2000; Manning et al., 2013). GPCRs are a large group of receptors for classical neurotransmitters and neuromodulators that are present in vertebrates and invertebrates (Brody and Cravchik, 2000; Venter et al., 1988), although only few are involved in regulating morphogenesis. Mist possesses an extracellular domain enabling the interaction with large ligands like Fog. In *Drosophila* the *mist* expression domain largely overlaps with *fog* expression and includes the ventral presumptive mesoderm as well as the posterior-dorsal region of posterior midgut primordium (Dawes-Hoang et al., 2005; Manning et al., 2013). Similar to *fog* the loss of *mist* affects correct ventral furrow and posterior midgut formation during gastrulation (Manning et al., 2013; Parks and Wieschaus, 1991).

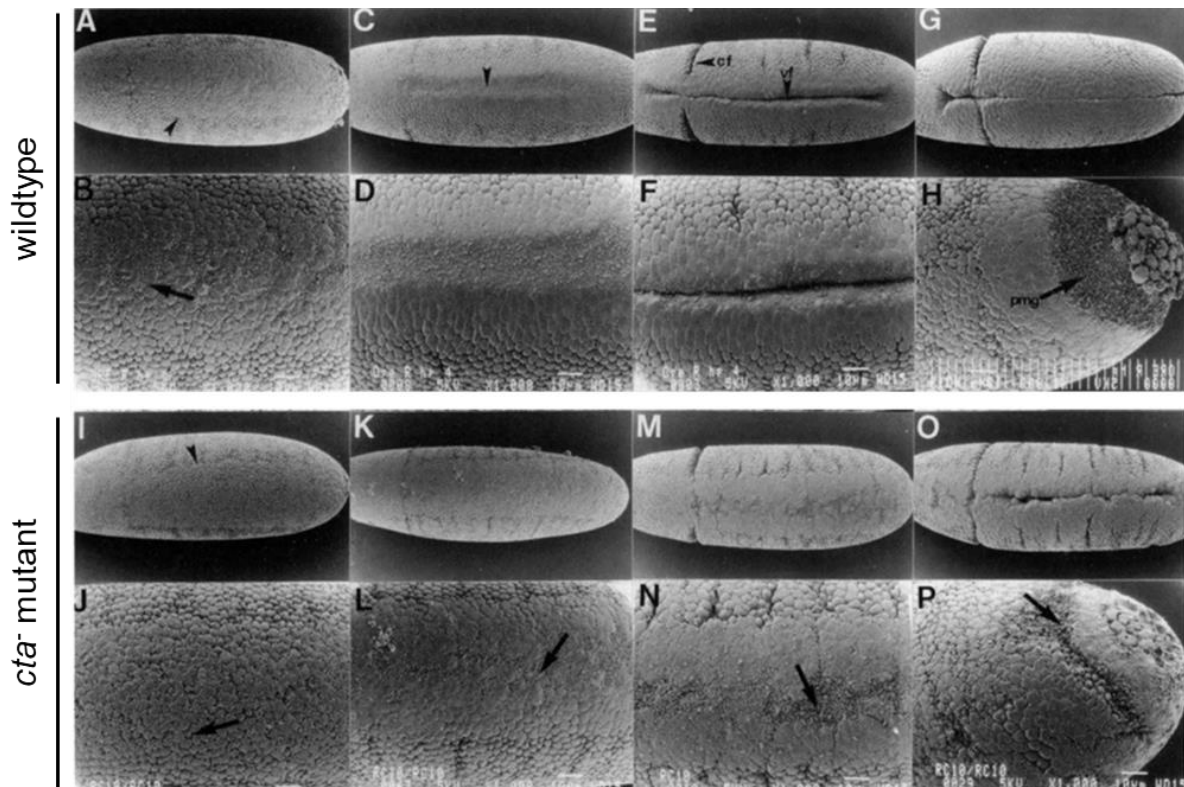


Figure 1.2: *Cta*⁻ mutant embryos show several defects during gastrulation

Scanning Electron Microscopy (Misof et al.) of wildtype and *cta*⁻ mutant embryos. All are ventral views. H and P show dorsolateral views. (A, C, E, G, I, K, M, O) and (B, D, F, H, J, L, N, P) show the embryos depicted in (A, C, E, G, I, K, M, O). (A and B) Wildtype embryo at the onset of ventral furrow formation. The arrow in (A) indicates the edge of the flattened zone. The arrow in (B) points to a midcentral cell beginning apical constriction. (I and J) Beginning ventral furrow formation in a *cta*⁻ mutant embryo. As in wildtype, a flattened zone of cells is visible (arrow in I). Some midcentral cells undergo apical constriction (arrow in J). (C and D) Wildtype embryo forming a shallow groove (arrow in C). (K and L) A *cta*⁻ mutant embryo of an analogous stage to the WT embryo in (C and D). The *cta*⁻ mutant embryo has constricted some cells (arrow in L), but has failed to form a shallow groove. (E and F) Wildtype embryo that has deepened and closed over the ventral furrow. The forming cephalic fold is also apparent. (M and N) A *cta*⁻ mutant embryo of similar stage to the embryo in (E) and (F). No ventral groove has formed. Instead, only some of the midcentral cells have constricted (arrow in N). (G) Wildtype embryo that has begun to extend its germband. (O) A *cta*⁻ mutant embryo that has closed over its ventral furrow, even though some midcentral cells have failed to change shape. This embryo failed to extend its germband, instead forming folds on the ventrolateral sides. (H) Wildtype at a stage similar to the embryo in (G). Cell shape changes similar to those forming the ventral furrow form the posterior midgut invagination. The posterior midgut begins as a shallow cup under the pole cells. (P) Because very few cells at the posterior pole of the *cta*⁻ mutant embryo change their shape (arrow), it fails to form a posterior midgut invagination. (modified from Parks and Wieschaus, 1991)

Transmission of the extracellular Fog signal across the plasma membrane by Mist is dependent on a trimeric G-protein interacting with the GPCR. Identified in a screen for female sterile mutations, the G-protein α -subunit Concertina (*Cta*) was the pathway element which was discovered first (Schupbach and Wieschaus, 1989). *Cta* mRNA is uniformly expressed in *Drosophila* embryos and is required to recruit a Rho guanine nucleotide exchange factor (RhoGEF2) and Myosin II to the apical membrane (Kerridge et al., 2016; Parks and Wieschaus, 1991). In detail, the receptor Mist is interacting with a trimer consisting of $G\alpha$, $G\beta$ and $G\gamma$. Upon binding of Fog, *Cta*'s exchange of GTP for GDP enables *Cta* to dissociate from its partners and thus to activate the downstream target RhoGEF2. Activation of RhoGEF2 in turn results in activation of the GTPase Rho1 and Rho Kinase (Rok) (Manning and Rogers,

2014). This signaling cascade finally results in apical-medial accumulation of non-muscular Myosin II (Fig. 1.3) and thus, in pulsatile contraction of the actomyosin network (Dawes-Hoang et al., 2005; Martin et al., 2009). The morphological defects observed in *cta* mutant embryos coincide with the effects of loss of Fog and Mist. Lack of Fog, Mist or Cta results not only in failure of posterior midgut primordium invagination and an abnormal ventral furrow formation, but affects various invagination events during *Drosophila* development, like the internalization of the salivary glands or folding of the wing imaginal discs (Costa et al., 1994; Manning and Rogers, 2014; Nikolaidou and Barrett, 2004).

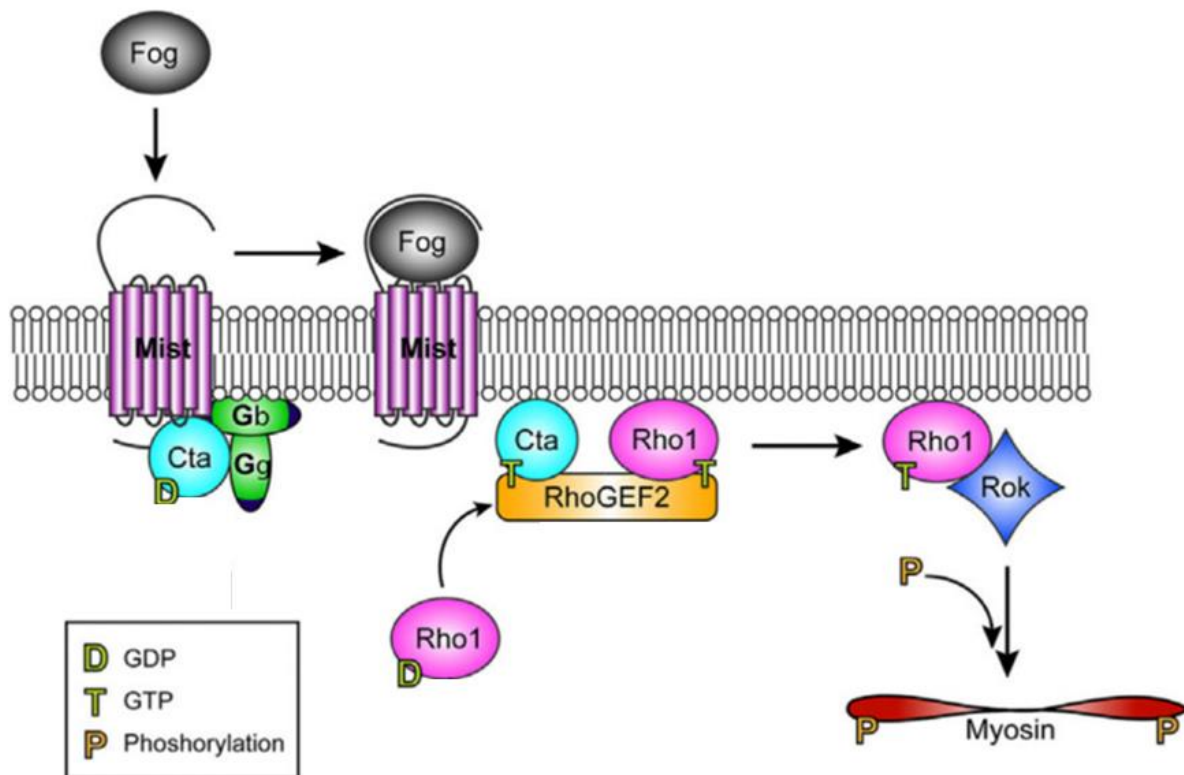


Figure 1.3: The Fog signaling pathway

Scheme depicting the interaction of the Fog signaling components. The G-protein coupled receptor (GPCR) Mist interacts with the inactive, α -subunit of a G-protein (Cta) bound to GDP. When the ligand Fog binds to the receptor, it stimulates the exchange of GTP for GDP, which enables Cta to dissociate from its heterotrimer partners, G β and G γ . The subsequent activation of RhoGEF2 results in activation of Rho1 and Rok. Finally, the phosphorylation of the regulatory light chain of non-muscle myosin II by Rok induces apical actomyosin network contraction in the cells. (modified from Manning and Rogers, 2014).

4.2.2 Regulation of Fog signaling

Fog signaling plays an important role in initiating ventral furrow formation and posterior midgut invagination by apical constriction. *cta* and *RhoGEF2* are expressed ubiquitously in *Drosophila*. The expression domains of *fog* and *mist* largely overlap, but seem to be under independent control (Dawes-Hoang et al., 2005; Manning et al., 2013; Manning and Rogers, 2014).

Twist and Snail function as the master regulators of mesoderm specification and ventral furrow formation (Leptin, 1991; Leptin and Grunewald, 1990). Former experiments could show that *twist* mutant embryos, lack mesodermal *fog* expression, indicating that Fog activity in the ventral furrow is completely dependent on Twist (Costa et al., 1994). However, the posterior expression domain remains unaffected after loss of *twist* or *snail* (Leptin, 1994). Surprisingly, mesodermal localization of *mist* is probably regulated by Snail. *snail* mutant embryos lack ventral *mist* expression, whereas its expression is maintained upon loss of *twist*. Similar to *fog*, *mist* expression around the posterior midgut primordium is unaffected even after loss of both, *twist* and *snail* (Manning et al., 2013). In contrast to Twist, which is known as a key activator, Snail mainly functions as a transcriptional repressor (Leptin, 1991). Thus, it might be that *mist* expression is not activated by Snail itself, but rather indirectly by a Snail target (Manning et al., 2013).

4.2.3 Fog and T48 - Two distinct mechanisms of myosin localization

Former results indicate that Fog signaling is not the only pathway regulating the coordination and contraction of the actomyosin network to induce apical constriction (Dawes-Hoang et al., 2005). Although all cells show apical accumulation of myosin after ubiquitous expression of *fog*, basal myosin is only lost in ventral cells. Loss of *RhoGEF2* also results in reduction of the basal myosin, but the cells fail to accumulate myosin to the apical side. In contrast to loss of *fog*, *mist* or *cta*, embryos lacking *RhoGEF2* do neither invaginate the mesoderm nor the posterior midgut (Barrett et al., 1997; Hacker and Perrimon, 1998). Thus, apical myosin localization seems to be not only dependent on Fog signaling, but on an additional factor.

Another target of Twist is the ventrally localized transmembrane protein T48 (Gould et al., 1990; Leptin, 1991). It has been shown that T48 contributes complementary to Fog signaling to the induction of apical constriction via direct binding with RhoGEF2 (Fuse et al., 2013; Kolsch et al., 2007). Similar to *twist*, the mRNA of the transmembrane anchor T48 is expressed in a broad ventral stripe in the presumptive mesoderm. The protein is localized to the apical cell membrane recruiting RhoGEF2. Unlike *fog* or *mist*, *T48* is not expressed at the posterior midgut primordium (Fig. 1.4 B-F). This is in line with observations that *T48* mutant embryos show no defects in posterior midgut invagination.

Nevertheless, loss of *T48* results in disorganized and delayed formation of the ventral furrow. These results indicate that neither Fog signaling nor *T48* is absolutely required for mesoderm internalization (Kolsch et al., 2007). The fact that *cta+T48* double mutants completely fail to form a ventral furrow and to invaginate the posterior midgut rather suggest, that they might act in parallel to induce apical constriction (Kolsch et al., 2007; Manning and Rogers, 2014). While Fog signaling causes via activation of *Cta* the release of RhoGEF2 from microtubules, *T48* concentrates RhoGEF2 to the apical membrane (Manning and Rogers, 2014). Thus, Twist regulates two targets acting in separate pathways to modify and activate the actomyosin network during *Drosophila* gastrulation (Fig. 1.4 A).

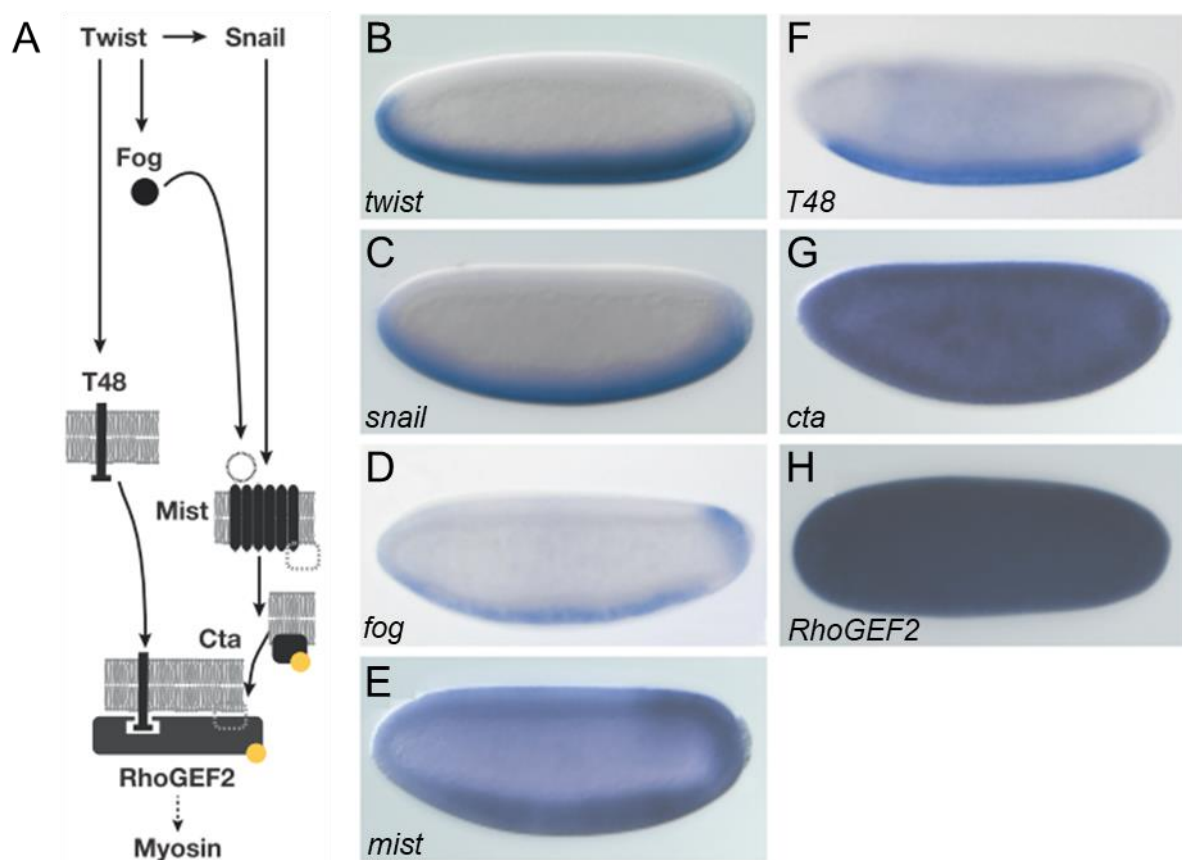


Figure 1.4: Regulation of apical constriction by Twist and Snail

(A) Scheme of regulatory inputs on Fog signaling. Two pathways act complementary to induce apical constriction. (B-H) mRNA expression patterns of *twist*, *snail*, *fog*, *mist*, *T48*, *cta* and *RhoGEF2* at the onset of *Drosophila* gastrulation. (modified from Urbansky et al., 2016)

4.3 Conservation of Fog signaling in insect morphogenesis

So far it was stated, that Fog signaling is poorly conserved. The ligand Fog was assumed not to be conserved outside of the genus *Drosophila* (Manning and Rogers, 2014), and that its receptor Mist is not conserved outside of insects. In contrast, downstream components like members of the Gα12/13 family, RhoGEFs or RhoA have been proven to be highly conserved regulators of apical constriction in vertebrates (Suzuki et al., 2012). They are involved in different processes like cytoskeletal and cell shape changes, such as neurite outgrowth and retraction, tumor cell invasion, or angiogenesis during human development (Waterhouse et al., 2011; Xiang et al., 2013).

However, recent data from our lab (Rodrigo Nunes da Fonseca and Cornelia von Levetzow, Kai Conrads, Matthias Pechmann) as well as by Urbansky et al., 2016 draw a different picture. It seems that Fog is a fast-evolving protein containing neither conserved domains nor transmembrane regions. The rapid and dramatic sequence changes require a careful phylum based reciprocal BLAST approach to identify *fog* in other insect species (Conrads, Master Thesis 2015). Comparative studies by Urbansky et al., 2016 using *Drosophila melanogaster* and the midge *Chironomus riparius*, a basal member of the Diptera, suggest that Fog signaling is involved in gastrulation in only some highly derived lineages. *Chironomus* possesses a different mode of mesoderm internalization. Instead of forming a deep tube-like ventral furrow, single cells move from the epithelial surface inwards (ingression). Unlike *Drosophila*, mesoderm internalization in *Chironomus* seems to work independently of Fog signaling. Ectopic expression of *fog* mRNA prior to gastrulation was sufficient to induce cell shape changes, resulting in ventral furrow formation similar to *Drosophila* gastrulation. Two different *fogs* were identified in *Chironomus*. While *fog1* was not expressed at all, *fog2* showed a broad domain of expression before onset of gastrulation. Nevertheless, loss of *fog2* did not result in early morphogenetic defects, suggesting a late function of Fog in the midge (Urbansky et al., 2016). Thus, it seems likely that Fog function was recruited from later developmental stages to accelerate the process of gastrulation in some insects with fast developing embryos. The identification of *twist and snail*, *fog*, *mist*, *T48*, *cta* and *RhoGEF2* in the genomes of major families of winged insects indicates a conservation of these genes for more than 400 million years (Misof et al., 2014; Urbansky et al., 2016).

The work by Kai H. Conrads (unpublished) uncovered the function of Fog signaling also in mesoderm and gut invagination in the jewel wasp *Nasonia vitripennis* (Hymenoptera). Furthermore, our group could identify the respective orthologs of *fog*, *mist* and *cta* in the red flour beetle *Tribolium castaneum* (Coleoptera). Both organisms exhibit more ancestral features during embryonic development compared to *Drosophila*.

4.4 Different modes of mesoderm internalization

The highly diverse class of insects possesses various modes of embryonic development. Changes in embryogenesis are often correlated with changes in morphogenesis and thus, with different strategies of mesoderm invagination (Roth, 2004). Three basic modes of internalization can be distinguished (Fig. 1.5).

Type I can be found in many dipterans, coleopterans and neuropterans (Bock, 1939). The cells of the presumptive mesoderm undergo apical constriction and simultaneously apicobasal elongation, which results in formation of a well-defined ventral furrow. At the same time, the lateral neuroectodermal sheets move ventral and fuse at the ventral midline. This results in a tube-like structure of the internalized mesoderm (Leptin and Grunewald, 1990; Sweeton et al., 1991). Type II mesoderm internalization is determined by disruption of the epithelial continuity. The ectodermal cells separate from the future mesoderm, which remains a stiff plate. As the ectodermal tissue moves over the mesoderm and fuses at the ventral side, the mesoderm gets internalized. This more passive mode of mesoderm invagination is often found in hymenopterans and some lepidopterans (Fleig et al., 1988; Roth, 2004). Type III mode strongly differs from the mechanisms mentioned so far and is common for numerous hemimetabolous insects (Anderson, 1972; Jura, 1972). The mesodermal cells build an irregular mass that gets pushed inwards by the ectodermal cells fusing at the ventral midline. During the whole process of internalization, the mesodermal cells stay mitotically active and either no or only a shallow and less distinct ventral furrow can be observed (Roth, 2004). This type shows some similarities with a process called ingression, in which single cells move inwards in a less organized way. However, variations in mesoderm formation can be found within a single insect order (Roth, 2004). Ingression-like mesoderm internalization has also been reported for different more basally branching flies like *Chironomus riparius* (Urbansky et al., 2016) or *Anopheles gambiae* (Goltsev et al., 2007), and seems to be independent of Fog signaling.

While type I mesoderm internalization is common for highly derived flies like *Drosophila*, it seems that hemimetabolous insects mainly internalize their mesoderm via the ingression-like type III mode (Anderson, 1972). The fast embryogenesis of many holometabolous insects require a simple, but highly organized mechanism for mesoderm internalization, indicating that formation of a ventral furrow by apical constriction might be derived from a more ancient mode of cell ingression (Roth, 2004; Urbansky et al., 2016).

Type I: apical constriction



Type II: mesoderm forms a stiff plate



Type III: irregular internalization of mesodermal cells

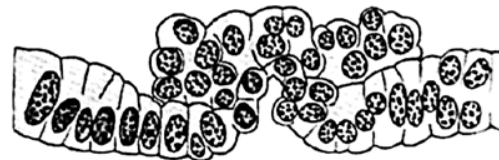


Figure 1.5: Three types of mesoderm internalization

Type I: Cells of the presumptive mesoderm undergo apical constriction, resulting in a deep ventral furrow. Type II: The neuroectoderm separates from the mesodermal cells, which form a stiff plate. The ectodermal epithelium covers the mesoderm and fuses at the ventral midline. Type III: The mesodermal cells stay mitotically active, while they get passively internalized by the ectoderm moving to the ventral side. (modified from Roth, 2004)

4.5 Morphogenetic movements during *Tribolium* gastrulation

Morphogenetic evolution usually originates in changes of gene regulation. In detail, it was shown that differences in gene expression can be correlated to changes in tissue and cell behavior (Urbansky et al., 2016).

Unlike in *Drosophila*, *Tribolium castaneum* gastrulation involves complex morphogenetic movements not only of embryonic tissues, but also of two distinct extraembryonic membranes: amnion and serosa. At the onset of gastrulation, these membranes undergo drastic rearrangements. After cellularization the cells are evenly distributed in the undifferentiated blastoderm. The serosa becomes first visible in the differentiated blastoderm stage after ~8 h after egg lay (30°C). In this stage the serosa cells are wider compared to the cells of the embryo proper. The embryo-serosa border is running from a more anterior position on the ventral side (Fig. 1.6 A'') to a more posterior position on the dorsal side (Fig. 1.6 A and A'). The cells neighboring the serosa border are part of the amnion, which dorsally slightly

extends towards the posterior pole (Fig. 1.6 A)⁵. At around the same time, cells at the posterior pole of the egg start to undergo apical constrictions and form a cup-shaped pit, the so-called primitive pit (Fig. 1.6 A pp and A'). The primitive pit finally becomes a deep fold while the amnion and serosa start to spread to the ventral side, covering the embryo proper (Handel et al., 2000) (Fig. 1.6 B and B'). At the same time, the mesodermal cells undergo apical constriction and form a ventral furrow. The edges of the extraembryonic membranes are not yet closed at that time (serosal window) (Fig. 1.6 B''). After serosal window closure, the mesoderm gets fully internalized. The abdominal segments are successively added from a posterior segment addition zone (Fig 1.6 C-C''). During germ band extension the embryo is completely covered by the serosa and additionally by the amnion on the ventral side (Fig. 1.6 D and D'). The segments are now well-defined and the appendages like legs and mouth parts start to form (Fig. 1.6 D'').

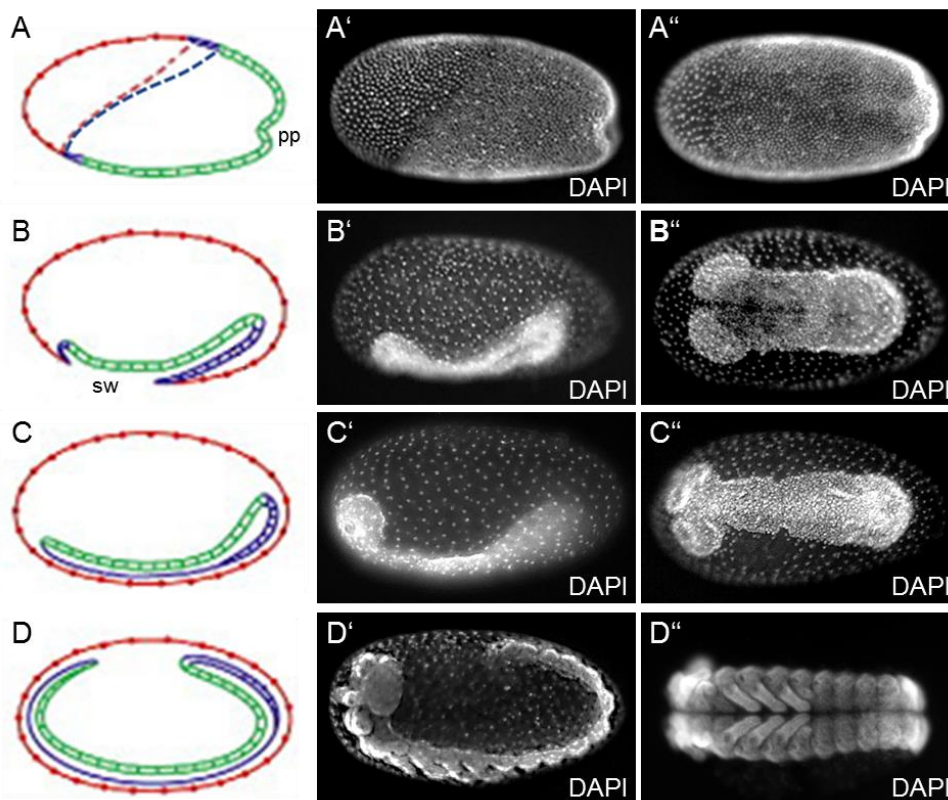


Figure 1.6: Gastrulation of *Tribolium castaneum*

(A–D) Schematic wildtype gastrulation and germ band extension. (A'–D') Lateral and (A''–D'') ventral view of DAPI stained embryos corresponding to the developmental stages depicted in A–D. (A) The formation of the posterior primitive pit (pp) in differentiated blastoderm embryos marks the onset of gastrulation. The anterior extraembryonic serosa (red) with its flattened and stretched-out cells can be easily distinguished from the embryo proper (green) with its columnar and cells in higher density (A' and A''). The cells neighboring the serosa border (purple) will form the amnion. (B) During gastrulation amnion and serosa overgrow the germ rudiment and form a deep posterior and a smaller anterior fold. (B and B'') The edge of the extraembryonic tissue forms the serosal window (Sweeten et al.). (C–C'') After closure of the serosal window, the amnion and the serosa are visible as separate membranes and protect the embryo during germ band extension (D–D''). (modified from van der Zee, 2005)

⁵ In former schemes the amnion comprised the whole dorsal-most side reaching to the primitive pit. Due to unpublished results by Matthew A. Benton, the borders of the amnion were modified in A.

The morphogenetic movements involved in mesoderm internalization in *Tribolium* vary along the antero-posterior (AP) axis (Fig. 1.7). The mesoderm of the most anterior segments (pregnathal) stays relatively flat and forms a stiff plate, while the ectoderm breaks the contact and migrates ventrally until it fuses at the ventral midline (Fig. 1.7 A-A'' and D). This mechanism resembles type II mode which is also observed during the gastrulation of *Nasonia vitripennis* (Hymenoptera). Similar to mesoderm internalization of *Drosophila* (type I), the more posterior parts of the mesoderm in gastrulating *Tribolium* embryos (thorax) form a deep ventral furrow until the ectodermal plates fuse on top of it (Fig. 1.7 B-B'' and D). Interestingly, even a third type of mesoderm internalization can be observed during *Tribolium* gastrulation. The cells of the segment addition zone lack *Tc-twist* expression and form a multilayered mass. These cells clearly differ from the remaining epithelial cells and get pushed inwards by the ectoderm moving to the ventral midline (Fig. 1.7 C-C'' and E) (Handel et al., 2005; Roth, 2004).

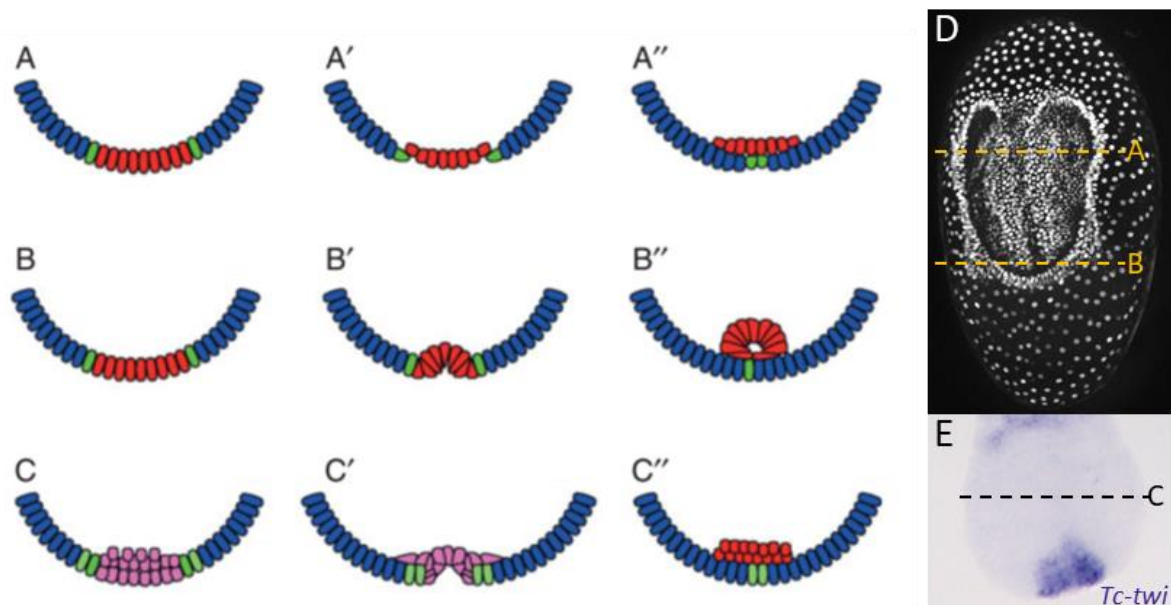


Figure 1.7: Different mechanisms of *Tribolium* mesoderm internalization along the AP axis

Schematic model of different modes of mesoderm internalization. blue = lateral ectoderm, green = mesectoderm, red = mesoderm precursors expressing *twist*, pink = mesoderm precursors not expressing *twist*. (A-A'') The anterior mesoderm forms a stiff plate and gets covered by the ectodermal epithelium. (B-B'') The mesoderm of the thorax segments gets internalized, similar to *Drosophila*, by establishing a deep ventral furrow. (C-C'') In segments deriving from the growth zone (abdominal), a multilayered mass of cells is internalized by the migration of the lateral ectodermal cells. (D) *Tribolium* embryo during gastrulation. The lines correlate to the different mechanisms of mesoderm internalization. (E) Location of mesoderm internalization in the segment addition zone depicted in C. (modified from Lynch et al., 2012)

4.6 Aims of the study

Previous results from our group suggest, that Fog is indeed conserved outside of drosophilids. Orthologs of the fast-evolving Fog protein could be identified not only in *Tribolium*, but also in *Nasonia vitripennis*. Recent studies seem to confirm the theory that apical constrictions in an epidermal sheet might be an adaption to enable a very fast gastrulation (Urbansky et al., 2016). *Tribolium* is a more basally branching member of the insects compared to the fruit fly. Thus, it differs drastically in embryogenesis and early morphogenetic movement. In consequence, the role of Fog signaling might deviate from its role during *Drosophila* gastrulation.

In this work, I carefully analyze the expression patterns of *Tc-fog*, *Tc-mist*, *Tc-cta* as well as *Tc-T48*. As a second potential receptor (Smog), which might have a function redundant or maybe complementary to *mist*, was recently identified in *Drosophila*, I also analyzed the expression and function of *Tc-smog*. Furthermore, we wanted to analyze the influence of Fog signaling on different morphogenetic movements like mesoderm and gut internalization during *Tribolium* gastrulation. Thus, I investigated different defects in the respective knockdown embryos. In addition, the examination of changes in the mRNA expression patterns of the Fog signaling components in different knockdown backgrounds, may give further insights into the regulation of apical constriction by Fog signaling in *Tribolium castaneum*.

5 Results

5.1 Expression patterns of the Fog signaling key components in *Tribolium castaneum*

One homolog for each of the key components of *Drosophila* Fog signaling: *folded gastrulation (fog)*, *mesoderm invagination signal transducer (mist)* and *concertina (cta)* could be identified by BLAST approaches (iBeetle Genome Browser; OGS 3.0). None of these genes shows an mRNA expression in syncytial stages of embryogenesis (data not shown). However, a BLAST search using transcriptomes of different embryonic stages (pre-blastoderm, blastoderm and differentiated blastoderm), indicates at least a maternal supply of the ligand *Tc-fog* and the G-protein α -subunit *Tc-cta* (iBeetle Genome Browser; RNA-Seq data was supplied by Michael Schoppmeier, Ho Chung, Ho Ryun and Uli Loehr). In fact, low expression levels are often hard to detect by *in-situ* hybridization (ISH).

The mRNA expression patterns of the major players (*Tc-fog*, *Tc-mist*) and *Tc-cta* were determined by ISH. A first signal of *Tc-fog* mRNA is detectable in the late blastoderm (Fig. 2.1 A) and becomes enhanced during the differentiated blastoderm stage (Fig. 2.1 B-E). It persists throughout gastrulation and during germ band extension (Fig. 2.1 F-H). Similar to the *Dm-fog* expression, *Tc-fog* is expressed in an additional domain on the ventral side of the embryo proper. In the differentiated blastoderm *fog* can be detected in a small mesodermal domain (Fig. 2.1 B). This expression domain expands to a broad stripe in the posterior mesoderm (Fig. 2.1 C and D) including the ventral part of the gastrulation fold (Fig. 2.1 E). However, *fog* expression only covers the posterior half of the *Tc-twist* domain (unpublished data, Rodrigo Nunes da Fonseca). During late gastrulation, the germ rudiment is covered by the amnion as well as the serosa. The mesodermal *Tc-fog* expression is now located in the posterior part of the extending germ band (Fig. 2.1 F-H).

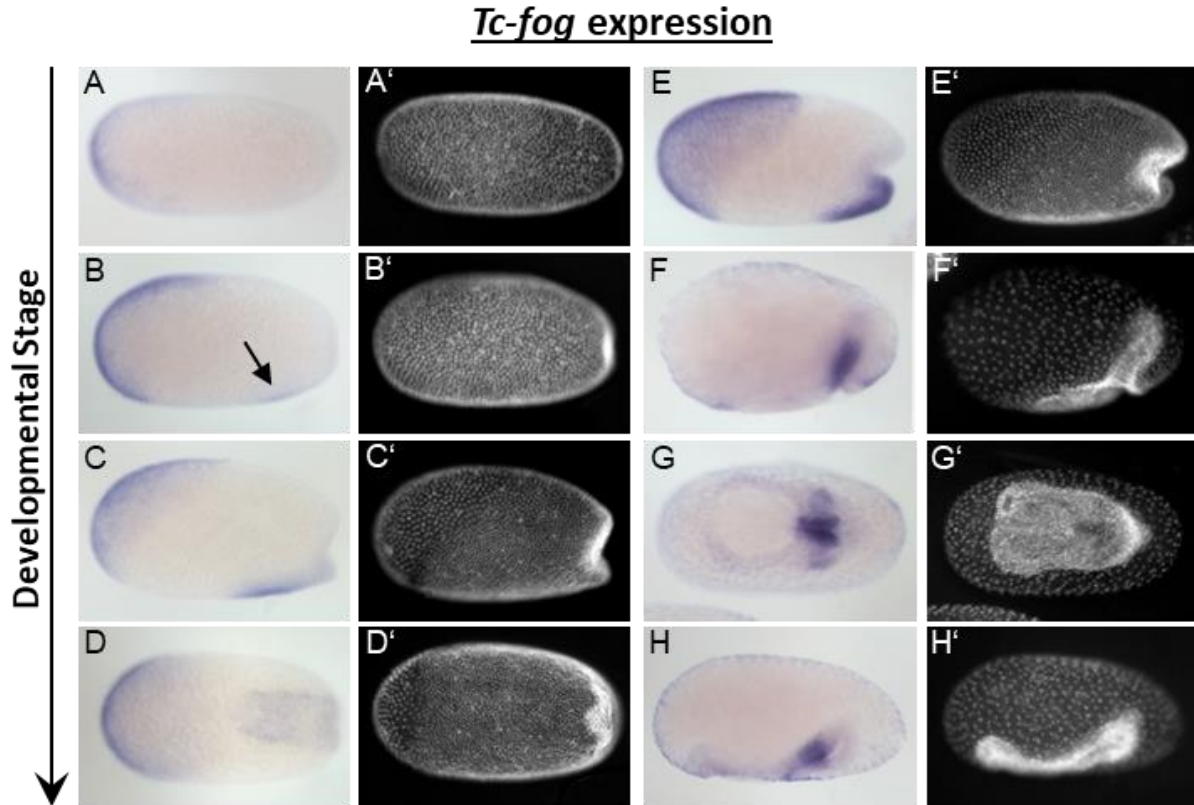


Figure 2.1: Expression patterns of *Tc-folded gastrulation (Tc-fog)* throughout early embryogenesis

(A-H) Whole mount ISH of wildtype embryos from early blastoderm until beginning of germ band extension. (A'-H') DAPI staining of the respective embryos. The anterior is left, all dorsal view, except D and G which are ventral views. (A) Extraembryonic *Tc-fog* expression starts at the anterior pole of the embryo similar to markers of the early serosa (B-E) and persists throughout the serosa until late differentiated blastoderm stage. (B) Embryonic *Tc-fog* starts at a ventral domain most likely in the presumptive mesoderm. (C-E) The expression becomes enhanced at the ventral midline in later stages. (F-H) Both, the serosal as well as the embryonic expression persist throughout gastrulation and beginning germ band extension.

Although Fog signaling components are not expressed in the amnioserosa of *Drosophila* (Costa et al., 1994; Manning et al., 2013), the extraembryonic mRNA expression domain is shared by the ligand and its receptor in *Tribolium*. Also, *Tc-mist* becomes first expressed in the serosa (Fig. 2.2 B). However, around the time the primitive pit starts to form, *Tc-mist* expression in the serosa starts retracting to the ventral side and eventually disappears at the onset of gastrulation (Fig. 2.2 C-F). Similar to *Tc-fog*, *Tc-mist* is expressed in an additional domain in the embryo proper. The expression starts at the differentiated blastoderm stage at the posterior pole of the egg (Fig. 2.2 B). During formation of the primitive pit (Fig. 2.2 C, D and E) and the posterior amniotic fold (Fig. 2.2 F), the posterior expression of *Tc-mist* becomes strongly enhanced. While the germ band extends, *mist* expression is restricted to the posterior segments. A pattern of stripes and spots is forming (Fig. 2.2 G and H).

Tc-mist expression

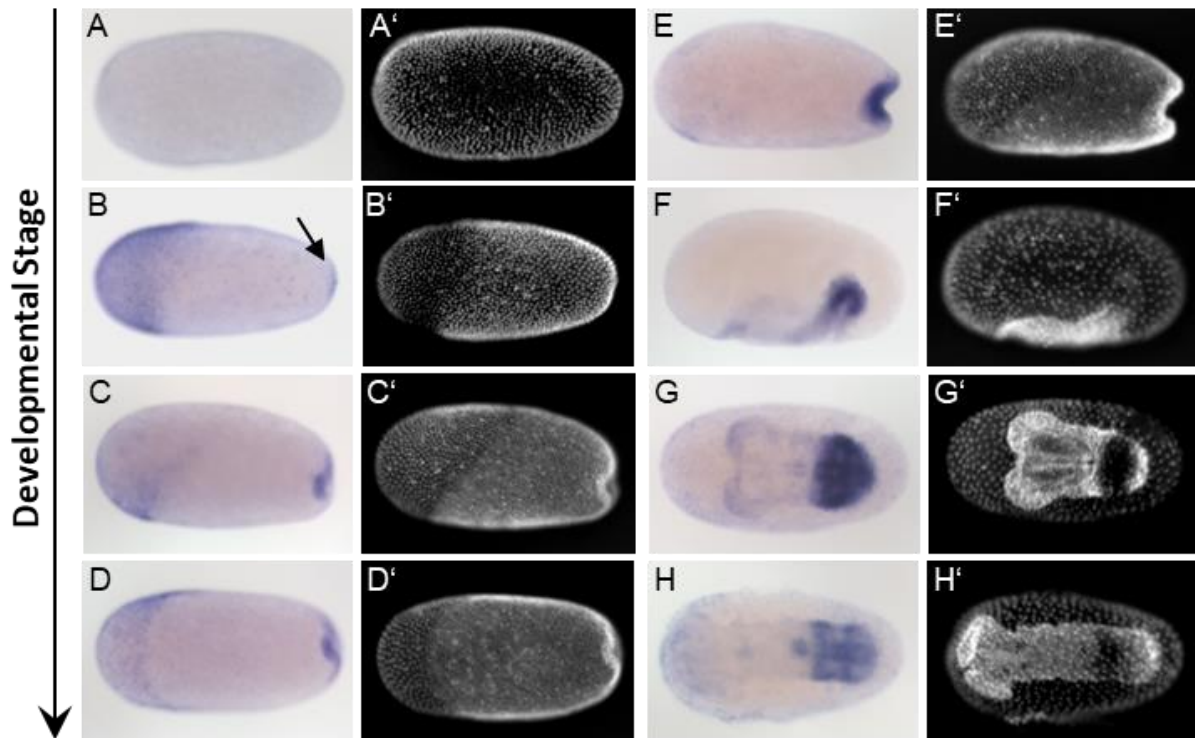


Figure 2.2: Expression patterns of *Tc-mist* throughout early embryogenesis

(A-H) Whole mount ISH of wildtype embryos from early blastoderm until beginning of germ band extension. (A'-H') DAPI staining of the respective embryos. The anterior is left, all dorsal view, except D, G and H which are ventral views. (A-H) Wildtype expression of *Tc-mist*. (B) *Tc-mist* is first detected in the serosa of early differentiated blastoderm embryos. Around the same time *Tc-mist* expression becomes also initiated at the posterior pole. (C-E) The serosal expression of *Tc-mist* starts to vanish starting on the dorsal side until it finally completely disappears right before gastrulation. In contrast, expression becomes enhanced in the posterior region and is eventually visible throughout the posterior amniotic fold (F) which indicates the onset of gastrulation. (G) During germ band extension *Tc-mist* is expressed in the region of the posterior segments. (H) The expression pattern subsequently expands and becomes segmental when germ band extension proceeds.

The mRNA expression of the G-protein α -subunit *Tc-Concertina* (*Cta*) is co-localized with the posterior expression domain of the receptor *Mist*. First signs of *Tc-cta* expression are visible in the early differentiated blastoderm stage (Fig. 2.3 B). As the embryo begins to gastrulate, the posterior expression of *Tc-cta* becomes stronger (Fig. 2.3 C-E). In contrast to *Tc-mist* expression, the borders of the *concertina* expression domain are not sharp but fuzzy (Fig. 2.3 C and D). However, late *cta* expression is rather weak and stays restricted to the most posterior part of the developing embryo (Fig. 2.3 G and H).

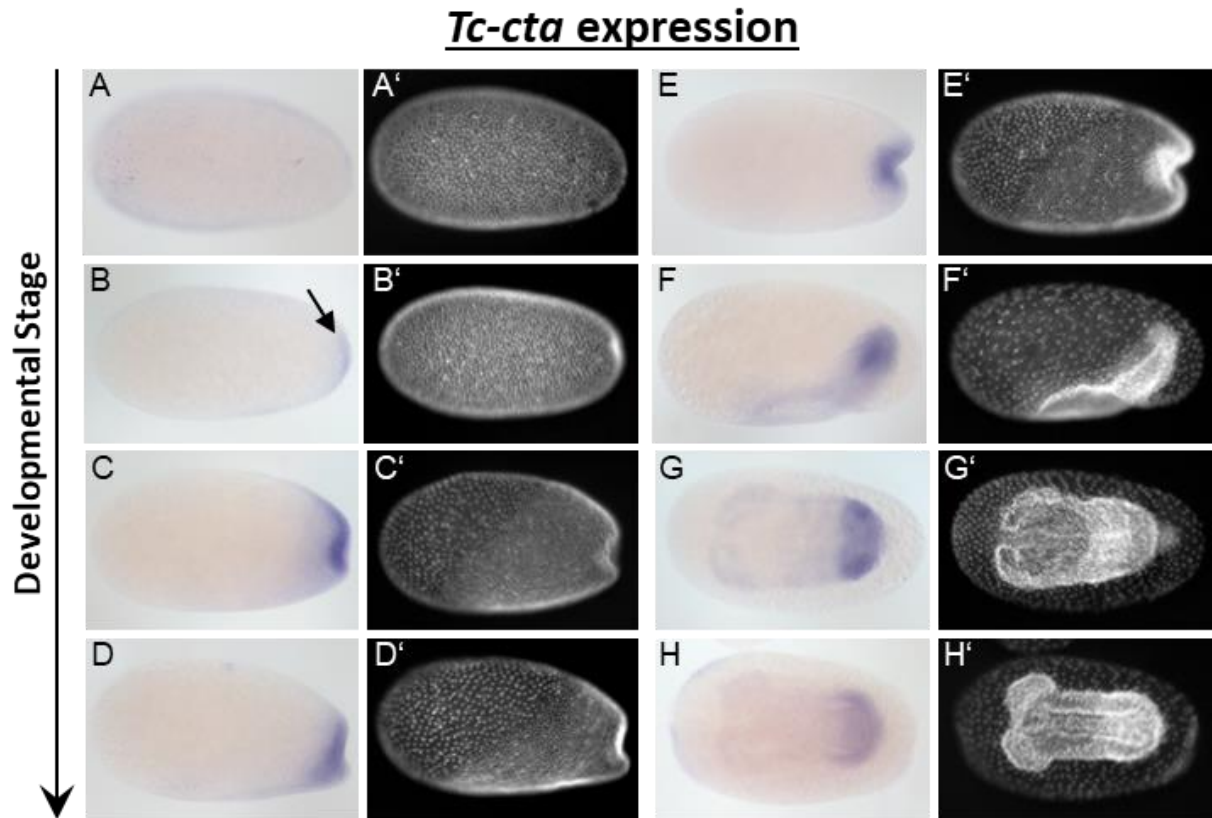


Figure 2.3: Expression pattern of *Tc-concertina* (*Tc-cta*) throughout early embryogenesis

(A-H) Whole mount ISH of wildtype embryos from early blastoderm until beginning of germ band extension. (A'-H') DAPI staining of the respective embryos. The anterior is left, all dorsal view, except G and H which are ventral views. (A-H) Wildtype expression of the G-protein α -subunit *Tc-cta*. Similar to *Tc-fog*, *Tc-cta* becomes first time visible shortly before primitive pit formation at the posterior pole of the embryo (B) and gets stronger during posterior amniotic fold formation (C-F). (G and H) During gastrulation and early germ band elongation *Tc-cta* is expressed in the segment addition zone of the embryo.

In *D. melanogaster*, the mRNA expression domains of the ligand *Fog* and its receptor *Mist* largely overlap (Manning et al., 2013). In contrast, in *Tribolium* *Tc-fog* and *Tc-mist* only share their extraembryonic expression domain in the serosa, whereas they do not overlap in the embryo proper. Only *Tc-fog* is expressed in the mesoderm, which later gets invaginated by the formation of the ventral furrow. Instead, they share their expression domain in the extraembryonic serosa. Moreover, *mist* and the downstream component *concertina* are both expressed at the primitive pit, which develops into a deep fold during *Tribolium* gastrulation. Later they are expressed in the segment addition zone (Fig. 2.4).

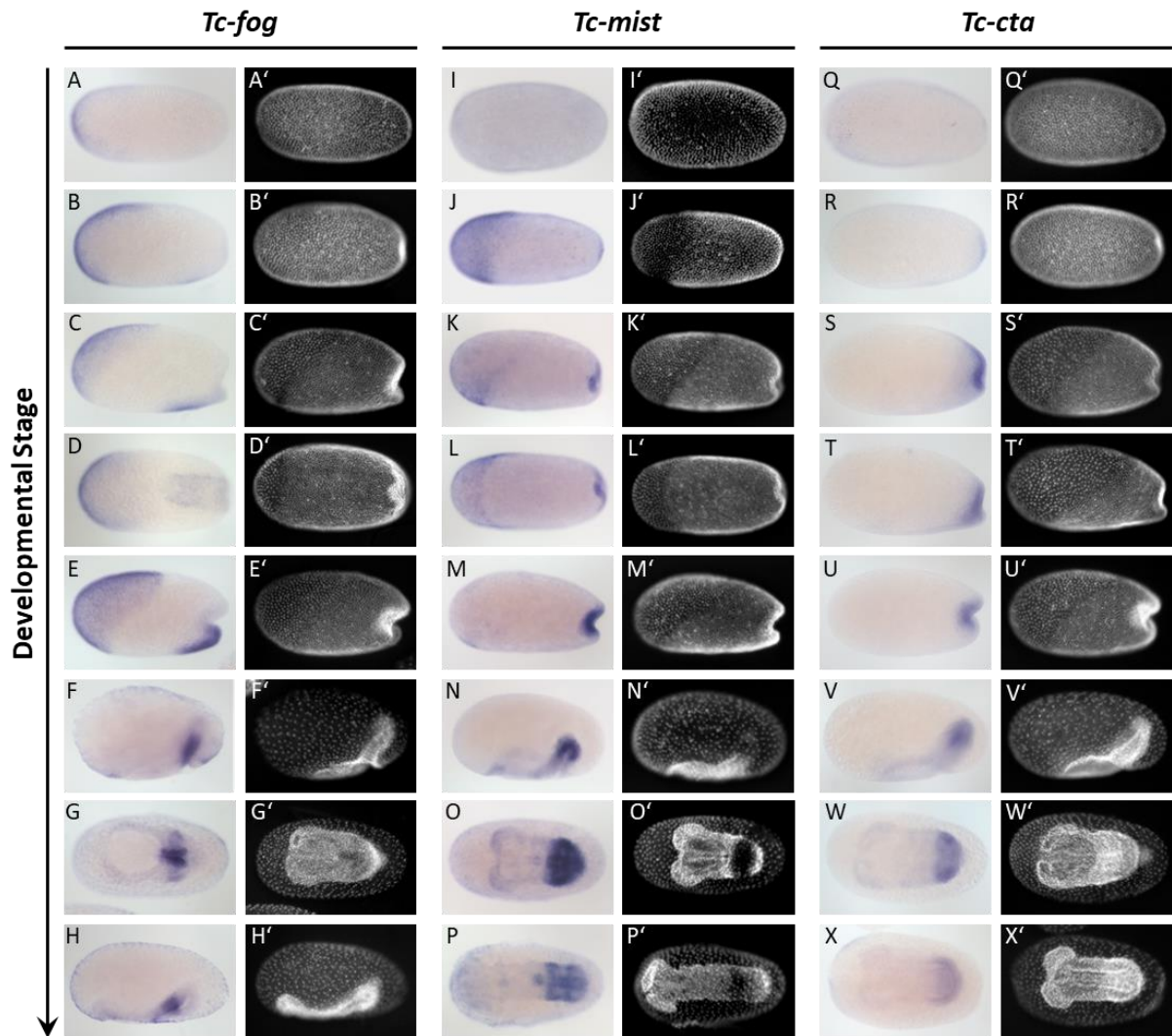


Figure 2.4: Comparison of the Fog signaling mRNA components expression domains

(A-X) Whole mount ISH of wildtype embryos from early blastoderm until beginning of germ band extension. (A'-X') DAPI staining of the respective embryos. The anterior is left, all dorsal view, except G and H which are ventral views., except for (D, G, L, O, P, W and X) which show ventral surface views. (A-H) Wildtype expression of *Tc-fog*. (I-P) Wildtype expression of *Tc-mist*. (Q-X) Wildtype expression of G-protein α -subunit *Tc-cta*. The receptor Mist and its ligand Fog show both an overlap in their extraembryonic mRNA expression domains. Furthermore, the posterior mRNA expression around the primitive pit is shared by *Tc-mist* and *Tc-cta*.

5.2 Knockdown of Fog signaling components in *Tribolium* results in a variety of defects

In *Drosophila*, Fog signaling plays an essential role in cell shape changes and thus the internalization of epithelial sheets. Fog deficient embryos show disorganized apical constriction of presumptive mesodermal cells, the posterior midgut does not invaginate and the germ band fails to extend (Costa et al., 1994).

To analyze the functional relevance of the Fog pathway in *Tribolium* embryogenesis, I produced not only *Tc-cta* knockdown (kd) but also *Tc-fog* kd and *Tc-mist* kd embryos by parental RNAi (pRNAi). Unfortunately, the *Tc-cta* kd leads to lethality and sterility of the injected beetles. Interestingly, the mutations in the *cta* gene were first isolated in a screen for female sterile mutations (Schupbach and Wieschaus, 1989). Females homozygous for these mutations survive but are sterile (Parks and Wieschaus, 1991). Even injection of adult beetles instead of pupae did not result in a sufficient amount of eggs for statistical analyses. Similarly, the injection of *Tc-mist* dsRNA leads to a sterility effect although much milder compared to *Tc-cta* kd. The best results were accomplished by injection of *Tc-fog* dsRNA. Nevertheless, it was necessary to characterize the phenotype of *mist* and *concertina* knockdown embryos. DAPI stainings, as well as live-imaging movies revealed that the knockdown of all three key components of the pathway results in similar defects (Fig. 2.5).

Extending *Tc-fog* kd germ band embryos show a variety of morphological defects (Fig. 2.5 A). The serosa fails to migrate over the posterior pole and leaves the embryo uncovered at the ventral and posterior side. Thus, the embryo looks broader at the posterior end. However, the anterior head lobes are covered by the serosa. Similar defects are observed in *Tc-mist* and *Tc-cta* knockdown embryos of the same developmental stage (Fig. 2.5 B and C). In summary, the loss of *Tc-fog*, *Tc-mist* and *Tc-cta* affects the embryos in the same way. Furthermore, the phenotypic penetrance was for all three knockdowns around 75-95% (*Tc-fog* kd: N=163; *Tc-mist* kd: N=57; *Tc-cta* kd: N=83).

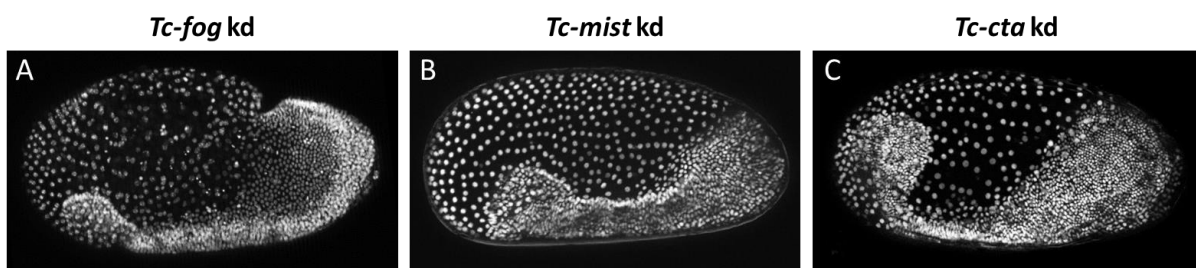


Figure 2.5: Knockdown of *Tc-fog*, *Tc-mist* and *Tc-cta* by RNAi results in the same phenotype.

(A-C) DAPI staining of *Tc-fog*, *Tc-mist* and *Tc-cta* knockdown embryos. The anterior is left, all lateral view, the dorsal side is upwards. All pictures show lateral views of embryos during early germ band extension. In all three knockdown embryos the serosa is only covering part of the future head lobes while the posterior of the embryo is broader and not covered by serosa.

5.3 Fog signaling is required for primitive pit formation

Live-imaging is an excellent method to get a more detailed impression of the early morphogenetic movements during *Tribolium* embryogenesis and its disturbance after RNAi. Compared to looking at fixed samples, live-imaging enables real-time analysis of morphogenetic changes. To image enough embryos for proper statistics, the development of more than only one embryo was tracked at the same time. As control, embryos from mock (H₂O) injected mothers were simultaneously imaged.

To further characterize the embryonic and extraembryonic development of knockdown embryos compared to the wildtype, we used a “Life-Actin” line (created by Tania Vazquez Faci; Van der Zee lab; unpublished). In this transgenic line, the cell outlines are labeled by GFP fused to actin. The pictures in Figure 2.6 show stills from movies of wildtype and *cta* knockdown embryos and are used for an accurate description of the various defects. Due to the strong sterility effect after injection of dsRNA for *Tc-cta*, the statistics are based on embryos upon *Tc-fog* kd. More than 180 embryos of mothers injected with *Tc-fog* dsRNA were analyzed by live-imaging (Fig. 2.7, movies in Appendix H). Around 76% (N=139) of the embryos showed a strong phenotype (Fig. 2.7 A). A limiting factor for the evaluation of the different defects is the orientation of the respective embryos. Thus, the number of the analyzed embryos (N) varies between the subgroups of defects (see Fig. 2.7 B, and Table C).

In a wildtype undifferentiated blastoderm embryo, the cells are evenly distributed and shaped. The posterior pole does not show a sign of invagination yet (Fig. 2.6 A and A'). Around 8h AEL the extraembryonic serosa is specified in the anterior part of the egg. As the serosa cells are bigger they can be easily distinguished from the embryo proper (Fig. 2.6 B, dashed line marks the embryo-serosa border). Around the same time, the most-posterior cells start to flatten (Fig. 2.6 B'). These cells subsequently bend inwards and the primitive pit is formed (Fig. 2.6 C and C'), which finally becomes a deep amniotic fold (Fig. 2.6 D and D') when the embryo gastrulates. The extraembryonic tissue (amnion and serosa) starts to cover the germ band on the ventral side which can be easily seen by the still open serosal window (Fig. 2.6 E, arrow). After around 14h AEL the serosal window finally closes (Fig. 2.6 F, arrow) and the germ band elongates.

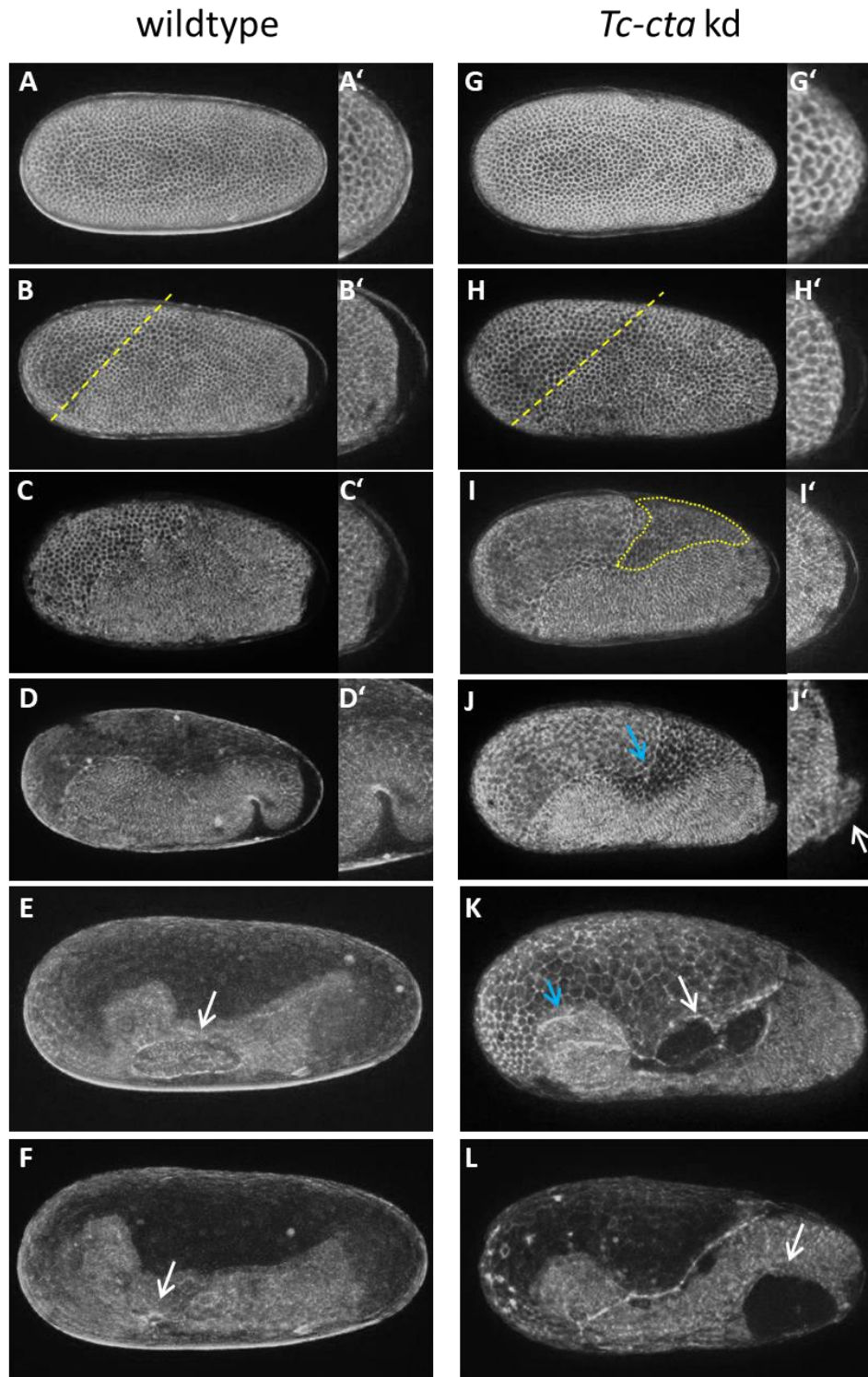


Figure 2.6: Description of the *Tc-cta* knockdown phenotype throughout early *Tribolium* embryogenesis

Stills from movies of a Life-Actin line. The anterior is left, the dorsal side is upwards. (A-F) Development of a WT embryo. (A) Undifferentiated blastoderm wildtype embryo. (B) In the differentiated blastoderm the serosa is specified. (B') The most posterior cells of the embryo start to flatten. (C and C') The primitive pit is formed. (D and D') During gastrulation, the primitive pit develops to a deep fold. (E) Amnion and serosa envelop the embryo. (F) The serosal window closes during germ band extension. (G-L) Development after *Tc-cta* knockdown. (G and G') No defects are visible in an undifferentiated blastoderm embryo. (H/H' and I/I') The posterior cells flatten but no primitive pit is formed. (I/I') The amnion cells become visible at the posterior-dorsal side of the egg (I; yellow outline). (J/J') The actin-myosin cable at the border of the serosa-amnion border becomes visible (blue arrow). Aggregation of cells at the posterior pole of a *Tc-cta* kd embryo (white arrow). (K; blue arrow) The serosa only covers part of the head lobes but not the remaining embryo. (K; white arrow) The serosa rips off from the amnion. (L) Sometimes holes open during germ band extension.

Compared to the wildtype, *cta* and *fog*-RNAi embryos show several defects in embryonic development, especially in morphogenesis. Although the most-posterior cells move slightly away from the vitelline membrane surrounding the egg (compare Fig. 2.6 G/G' and H/H'), they do not undergo apical constriction. In 95% (Fig. 2.7 B) of differentiated blastoderm stage embryos no formation of a primitive pit can be observed (Fig. 2.6 compare C/C' and I/I'). Instead, the extraembryonic amnion cells become visible at the posterior-dorsal side of the egg (Fig. 2.6 I; white outline), as they become broader. However, in *cta*-RNAi as well as *fog*-RNAi embryos, they look more similar to the flat and broad serosa cells, from which they are separated by an actin-myosin cable (Fig. 2.6 J, blue arrow). In 96% (Fig. 2.7 B) of the knockdown embryos, the serosa and the amnion remain on the dorsal side of the egg. Furthermore, embryos lacking Fog signaling components do not form a deep posterior amniotic fold during gastrulation (compare Fig. 2.6 D and J). The embryo starts to develop without getting covered by amnion and serosa. In addition, one can observe an aggregation of cells at the posterior pole (Fig. 2.6 J/J' arrow) in ~85% (Fig. 2.7 B) of the kd embryos. Probably, the serosa cells do not manage to flatten and are thus not able to surround the embryo. In consequence, they rip off from the amnion cells when the lateral sides of the embryo start to condensate (Fig. 2.6 K; white arrow, 96% see Fig. 2.7 B). Interestingly, the serosa is still able to cover at least part of the head lobes in around 90% (Fig. 2.7 B) of the embryos (Fig. 2.6 K; orange arrow). In some embryos, holes open up in the abdominal segments of the elongating germ band (Fig. 2.6 L). These holes become wider as the germ band elongation proceeds. However, only about 29% of the *Tc-fog* knockdown embryos show this dramatic defect. Thus, it is likely that this effect represents the strongest phenotypic defect.

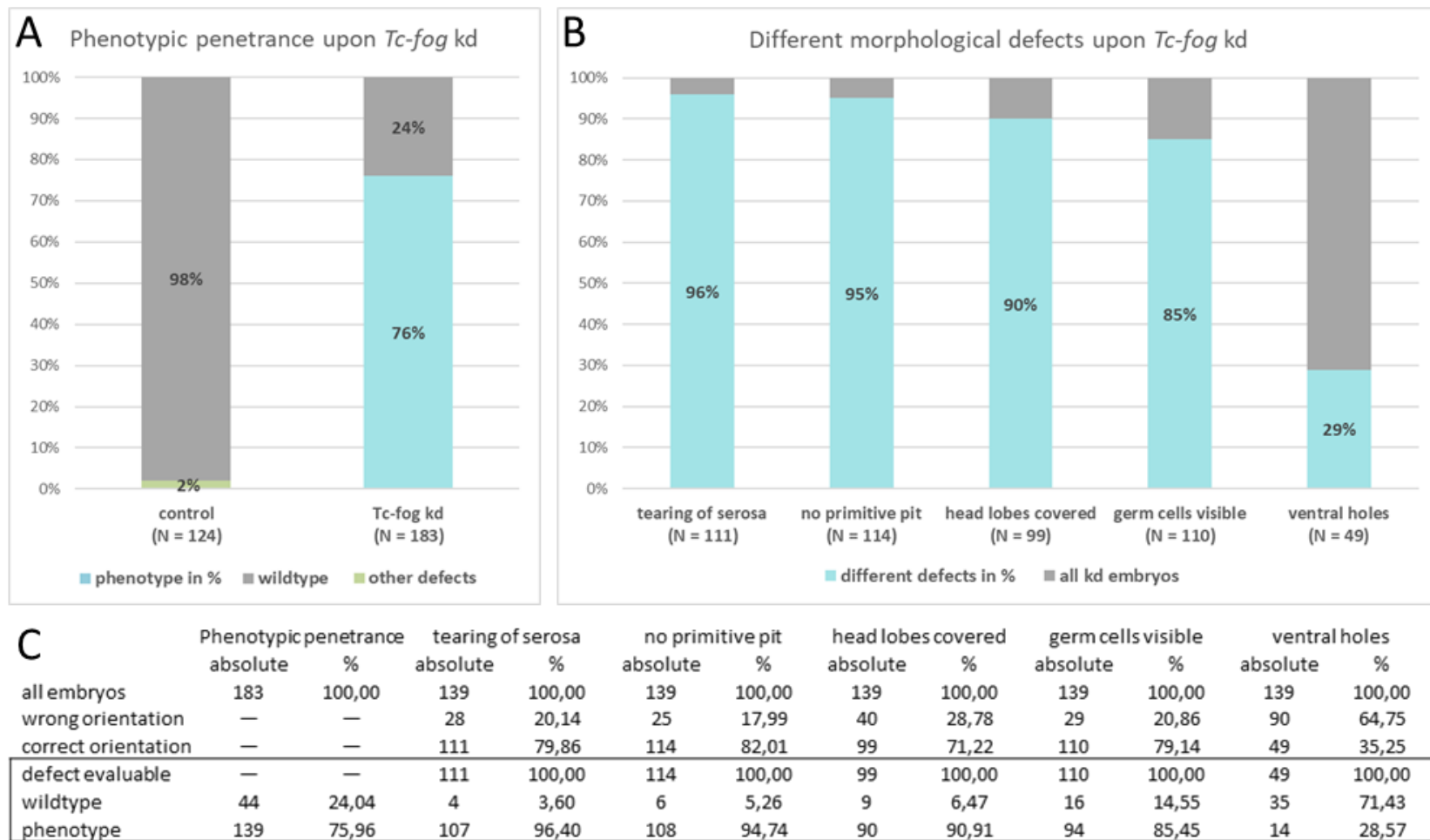


Figure 2.7: Statistical characterization of the *Tc-fog* kd phenotype

(A) 98% of the offspring of beetles injected with H₂O show a normal development (N=124). In comparison, the relative phenotypic penetrance upon *Tc-fog* RNAi is 76% (N=183). (B) Knockdown of *Tc-fog* results in several morphological defects. In 96% of all knockdown embryos the serosa does not expand towards the ventral side of the egg and ruptures from the embryo proper around beginning of germ band extension. Nevertheless, the anterior head lobes of almost all knockdown embryos (90%) are covered by the serosa. In addition, the majority of *Tc-fog* kd embryos (95%) fail to form a primitive pit. Instead, in around 85% of the offspring the presumptive primordial germ cells become visible at the posterior end. Less often (29%) the formation of holes along the midline of the embryos could be observed. (C) The table shows the absolute numbers as well as the percentage of the control as well as the *fog* kd embryos and their different defects.

5.4 Mesoderm invagination is delayed upon *Tc-fog* knockdown

Another essential step during *Tribolium* gastrulation is the invagination of the ventrally located mesoderm. A deep ventral gastrulation furrow forms in wildtype embryos. However, compared to *Drosophila*, the depth of this furrow varies along the antero-posterior axis (Handel et al., 2005). After disruption of Fog signaling, *Drosophila* embryos show an incomplete invagination of the mesoderm during gastrulation (Kolsch et al., 2007; Sweeton et al., 1991). To test for a potential conserved function of Fog signaling in mesoderm internalization, I used *Tc-fog* knockdown embryos. As the invagination of the mesoderm and especially the closure of the overlying ectoderm is difficult to track via live imaging, fixed embryos were investigated. In order to ensure proper staging, the embryos were primarily staged using a two-hour time window. Second, the process of segmentation was determined by an *in-situ* hybridization using the segmentally expressed pair-rule gene *Tc-gooseberry* (*Tc-gsb*) (Davis et al., 2001). Simultaneously, the mesoderm was stained with an mRNA probe for *Tc-twist*. To visualize and compare the mesoderm invagination along the entire antero-posterior axis, wildtype as well as *fog* knockdown embryos were sectioned in 30 μ m slices.

In horseshoe stage embryos (~16-18h AEL) the anterior part of the ventral furrow is quite shallow (Fig. 2.8 A₁), whereas the furrow becomes more prominent in middle and posterior regions of the gastrulating embryo (Fig. 2.8 A₂ and A₃). Nevertheless, the mesoderm is not yet internalized and the ectoderm is still widely open. In comparison, slightly older wildtype embryos around serosal window closure (~19-21h AEL) show a complete internalization of the *Tc-twist* expressing mesodermal cells along the entire AP-axis (Fig. 2.8 B₁-B₃). At that time point, the embryo proper got completely covered by amnion and serosa (Fig. 2.8 B) and the neighboring ectodermal plates have fused on top of the mesoderm. The gastrulation of embryos upon *Tc-fog* knockdown differs from the wildtype situation. Due to the missing primitive pit and amniotic fold formation, the Fog-deficient embryos around 19-21h AEL did not get covered by amnion and serosa (Fig. 2.8 C). Although the overall morphology looks very different from wildtype embryos of the same age, the number of *Tc-gooseberry* stripes indicate a similar developmental stage (Fig. 2.8 compare B and C). Nevertheless, the mesoderm internalization is clearly delayed. The location of the *Tc-twist* expressing cells in the cryo-section resembles the situation of younger wildtype embryos. The ventral furrow is less curved in *Tc-fog* knockdown embryos compared to the control, especially in posterior regions (Fig. 2.8 compare A₃ and C₃). Furthermore, the borders of the ectodermal plates did not yet fuse along the ventral midline (Fig. 2.8 C₁-C₃).

To investigate ventral furrow formation on a cellular level, embryos of the respective stages were stained with a nuclear marker (Sytox green) and the cell outlines were visualized by an F-actin labeling with Phalloidin (magenta). Wildtype embryos after serosal window closure have a completely internalized mesoderm which has already differentiated to a mesenchymal mass and is covered by the ectoderm (Fig. 2.8 E-E''). The progress of mesoderm internalization in embryos of the same developmental age lacking *Tc-fog* mRNA, resembles more a younger wildtype situation (Fig. 2.8 compare D-D'' and F-F''). The depth of the ventral furrow as well as the progress of ectoderm closure is similar between *Tc-fog* knockdown embryos 19-21h AEL and wildtype embryos around the horseshoe stage.

Although *Tc-fog* knockdown embryos form a ventral furrow for mesoderm internalization the depth of the furrow and the timing differ from the wildtype situation. The mesoderm internalization upon loss of Fog signaling is delayed compared to the wildtype control.

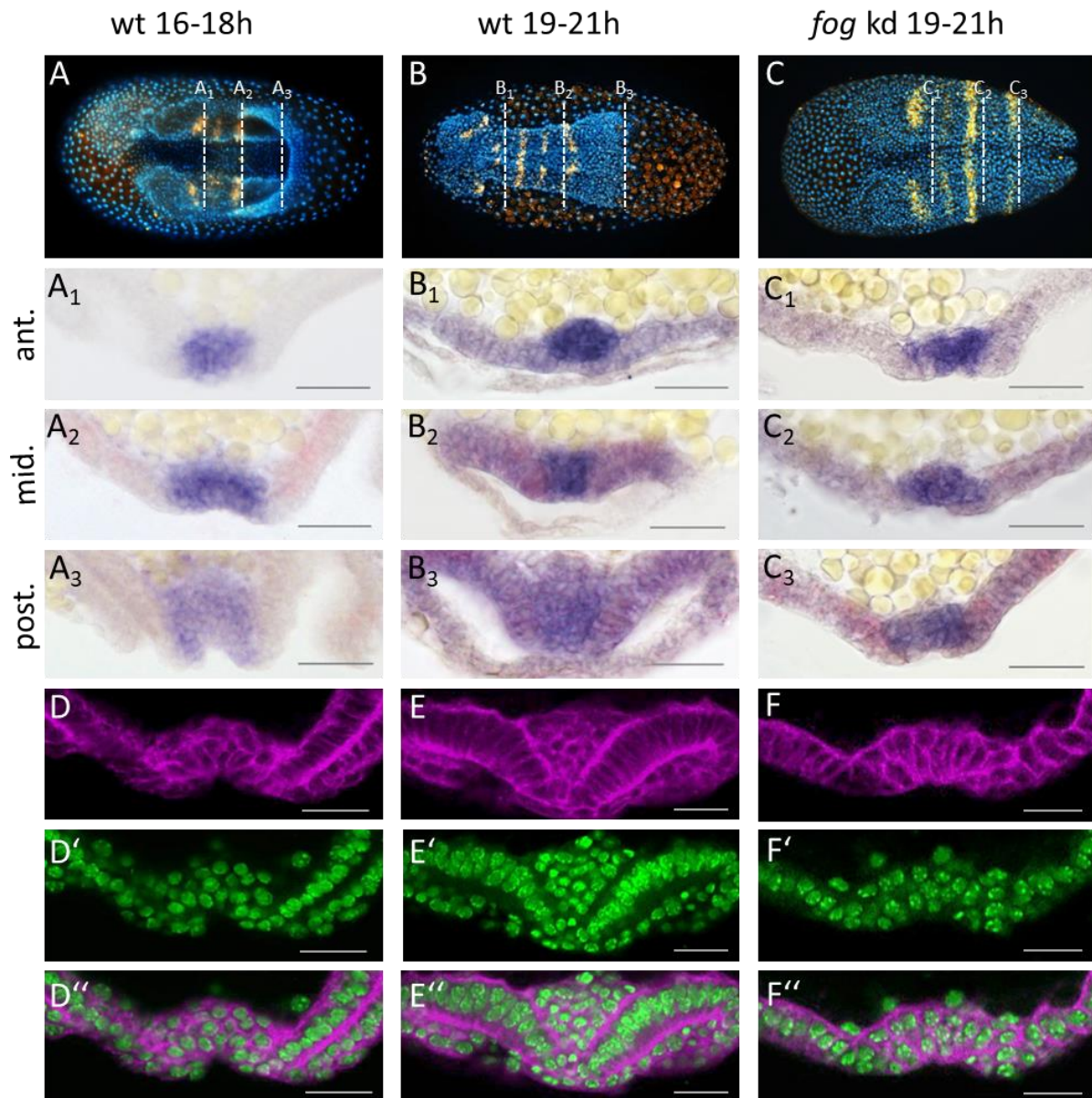


Figure 2.8: Mesoderm internalization is delayed in *Tc-fog* RNAi embryos

(A-C) Whole mount ISH of embryos from early horseshoe wildtype embryos (16-18h AEL, 25°C) and slightly older (19-21h AEL, 25°C) wildtype and *fog* kd embryos. DAPI staining in blue. *Tc-gooseberry* (orange in A-C; red in A₁-C₃) was used as segmental marker to determine the developmental stage and as orientation along the antero-posterior axis. The fourth stripe between C₂ and C₃ is very weak, but visible in lateral views. The anterior pole points to the left. (A₁-C₃) Cryosections of the respective embryos seen in A-C. *Tc-gooseberry* expression was detected by Fast Red (magenta) and the mesodermal marker *Tc-twist* was stained by NBT/BCIP (blue). The figure shows three different sections of each embryo along the antero-posterior axis. (A₁-A₃) Wildtype embryos at the horseshoe stage show already the formation of a ventral furrow in order to internalize the mesoderm. Whereas the furrow is very deep in posterior regions (A₃), it is flatter in the anterior part of the embryo. (B₁-B₃) When the germ band starts to elongate, the mesoderm is already fully internalized along the whole antero-posterior axis. (C₁-C₃) In comparison, the ectoderm is not yet closed on top of the mesoderm in *Tc-fog* kd embryos of the same age. (D-F'') Phalloidin (magenta) and Sytox (green) staining of a posterior area of embryos of an equivalent age as the embryos in A-C. Although wildtype embryos around 19-21h AEL have an internalized mesoderm which already starts to differentiate, *fog* kd embryos show the formation of a ventral furrow (F-F'') comparable to younger wildtype embryos (D-D'').

As the first results suggested that at least the depth and speed of ventral furrow formation is affected but probably not the mesoderm internalization itself, further experiments were done. During germ band extension, the internalized mesoderm becomes segmented. These segmental cluster of *Tc-twist* expressing cells can be visualized in longitudinal sections (Figure 2.9). In wildtype embryos the mesoderm is on the ventral side covered by the ectoderm. Furthermore, the sections clearly show the organization of the differentiating mesoderm in the respective thorax and abdominal segments of the elongating embryo (Fig. 2.9 A-B'). The whole embryo proper is protected by the amnion, from which it is separated by a liquid filled space, the amniotic cavity (Fig. 2.9 C). *Tc-fog* knockdown embryos show a general developmental delay (Fig. 2.9 D). Although the *Tc-twist* positive cells are at this stage completely covered by the ectoderm, the organization of the mesoderm seems to be affected. Some of the mesodermal cells are not as deeply internalized as in control embryos (Fig. 2.9 D-E'). Furthermore, the development of the segments is defective after *Tc-fog* knockdown. The segmental mesoderm looks misshaped and less organized (Fig. 2.9 compare B and E). The morphogenetic defects are most severe at the posterior end of the developing embryo. Instead of covering the ectoderm on the ventral side, the amnion is located posterior-dorsally to the embryo proper. Neighboring the amnion, the serosa is covering the yolk on the dorsal side of the egg (Fig. 2.9 F). These results suggest that the mesoderm gets indeed internalized even after loss of Fog signaling. However, the internalization is not as organized as in wildtype embryos.

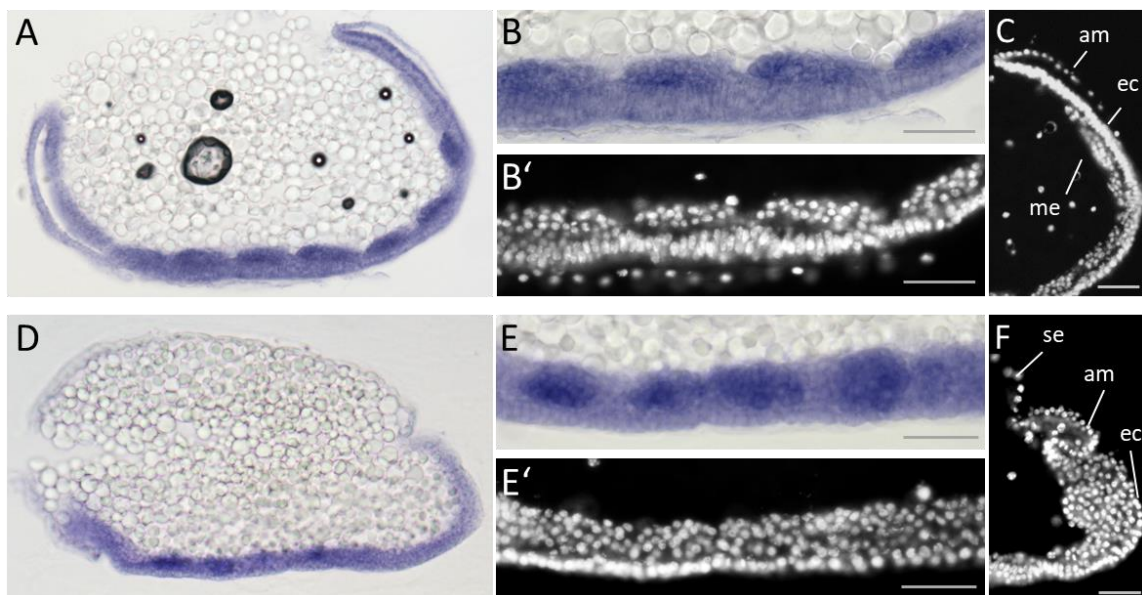


Figure 2.9: Internalization of the mesoderm in extending germ band embryos

(A, B, D, E) Whole mount ISH of elongating germ band embryos. (B', C, E' and F). DAPI staining of the respective embryos. Anterior points towards the right, dorsal side is up. (A) The mesoderm of almost fully extended wildtype embryos is visualized by the expression of *Tc-twist*. (B) The mesoderm is internalized and covered by a layer of ectodermal cells. (C) In the posterior segment addition zone, the mesoderm (me) is facing the yolk. The amnion (am) covers the ectoderm (ec) on the ventral side. (D and E) Also *Tc-fog* RNAi embryos of the same age show internalization of the mesoderm. (E' and F) However, the segmental mesodermal packs seem to be less defined, especially in posterior regions of the embryo.

As the mesoderm internalization is clearly affected by loss of Fog signaling, it is interesting to further investigate the formation of different mesodermally derived tissues. Two different transgenic lines were used in order to visualize the development and organization of somatic muscles and cardioblasts. Uninjected control embryos of the pBA-19 line (Lorenzen et al., 2003) express EGFP in all somatic muscle cells shortly before hatching of the larva (Fig. 2.10 A). Although the muscles are clearly visible in *Tc-fog* knockdown embryos, they seem to be less organized compared to the very structured somatic muscle pattern in control embryos (Fig. 2.10 B).

A second mesodermally derived tissue is the dorsally located heart. The enhancer trap line G04609 (or heart-GFP line; Trauner et al., 2009; Koelzer et al., 2014) expresses EGFP in the cardioblast cell row (Fig. 2.10 C, white arrows). In control embryos, the cardioblast cell rows move to the dorsal side of the embryo, where they fuse during dorsal closure. However, in *Tc-fog* knockdown embryos, the number of cardioblasts is strongly reduced (Fig. 2.10 D, white arrow). In addition, there is a second EGFP signal in the heart-GFP line, which is presumably a subgroup of cells located next to tendons (Koelzer et al., 2014). Also this group of cells is affected by loss of Fog signaling. Although most of these cells seem to be present, they are unevenly distributed and form misshaped groups (Fig. 2.10 compare C and D). In summary, the results indicate a delay in mesoderm invagination upon loss of *Tc-fog*. However, similar to *Drosophila*, the vast majority of the mesoderm gets internalized. Compared to wildtype embryos, the internalization process is less organized. In consequence, the differentiation of cardioblasts as well as the accurate positioning of the somatic muscles is affected.

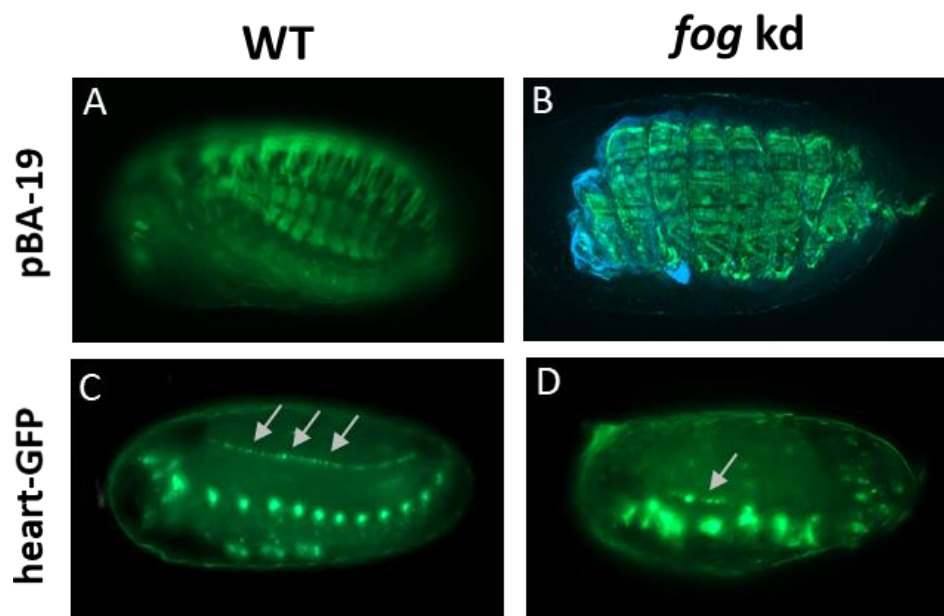


Figure 2.10: Defects of the mesodermal derived tissue in late embryonic development

(A and B) Embryos of the pBA19 enhancer trap line embryo (Lorenzen et al., 2003). The body wall muscles marked by EGFP in the pBA19 line (A) are formed after *Tc-fog* kd (B) although they show a more disorganized distribution compared to wildtype. (C and D) embryos of the enhancer trap line G04609. The cardioblast cell row (the presumptive heart) of this enhancer trap line expresses EGFP (green) (Trauner et al., 2009; Koelzer et al., 2014). (C) In wildtype embryos the cardioblast cells can be easily observed (arrows), while there is only a small bunch of GFP positive cardioblasts formed in *Tc-fog* RNAi embryos.

5.5 Positioning of the primordial germ cells is controlled by Fog signaling

One of the most important roles of Fog signaling in *Drosophila* is the posterior midgut invagination. During gastrulation, a group of cells at the posterior pole undergoes apical constriction and thus start to invaginate. In *Tribolium*, the process of primitive pit and amniotic fold formation seems to correlate with the invagination of the posterior midgut in *Drosophila*. As shown before, *Tc-mist* as well as *Tc-cta* are both expressed at the posterior pole (Fig. 2.4). Furthermore, in 95% of the analyzed embryos (Fig. 2.7 B), loss of one of the main Fog signaling components results in absence of the primitive pit (Fig. 2.6 H-J). In wildtype embryos, the cells at the posterior pole give rise to the posterior midgut and hindgut (Berns et al., 2008). Unlike in *Drosophila*, *Tribolium* embryos do not develop pole cells. However, the cells forming the primitive pit are positive for the putative primordial germ cell marker *Tc-tapas* (Fig. 2.11 A and E) (unpublished data Jeremy Lynch, University of Illinois Chicago). During gastrulation these cells move to the inside, although the exact mechanisms of primordial germ cell internalization in *Tribolium castaneum* are yet unknown. When the germ band starts to elongate, the primordial germ cells form a cluster of cells located at the posterior tip of the segment addition zone (Fig. 2.11 B and F).

Analyzing live-imaging movies *Tc-fog* knockdown embryos revealed that 85% of the gastrulating knockdown embryos show the formation of an external cluster of cells at the posterior end (Fig. 2.6 J and 2.7 B). Further experiments show that this cell cluster expresses *Tc-tapas* (Fig. 2.11 C and G). The cells remain at the posterior pole associated with presumptive endoderm even during germ band extension (Fig. 2.11 D and H). It seems that Fog signaling is required for the correct positioning of the primordial germ cells during *Tribolium* gastrulation.

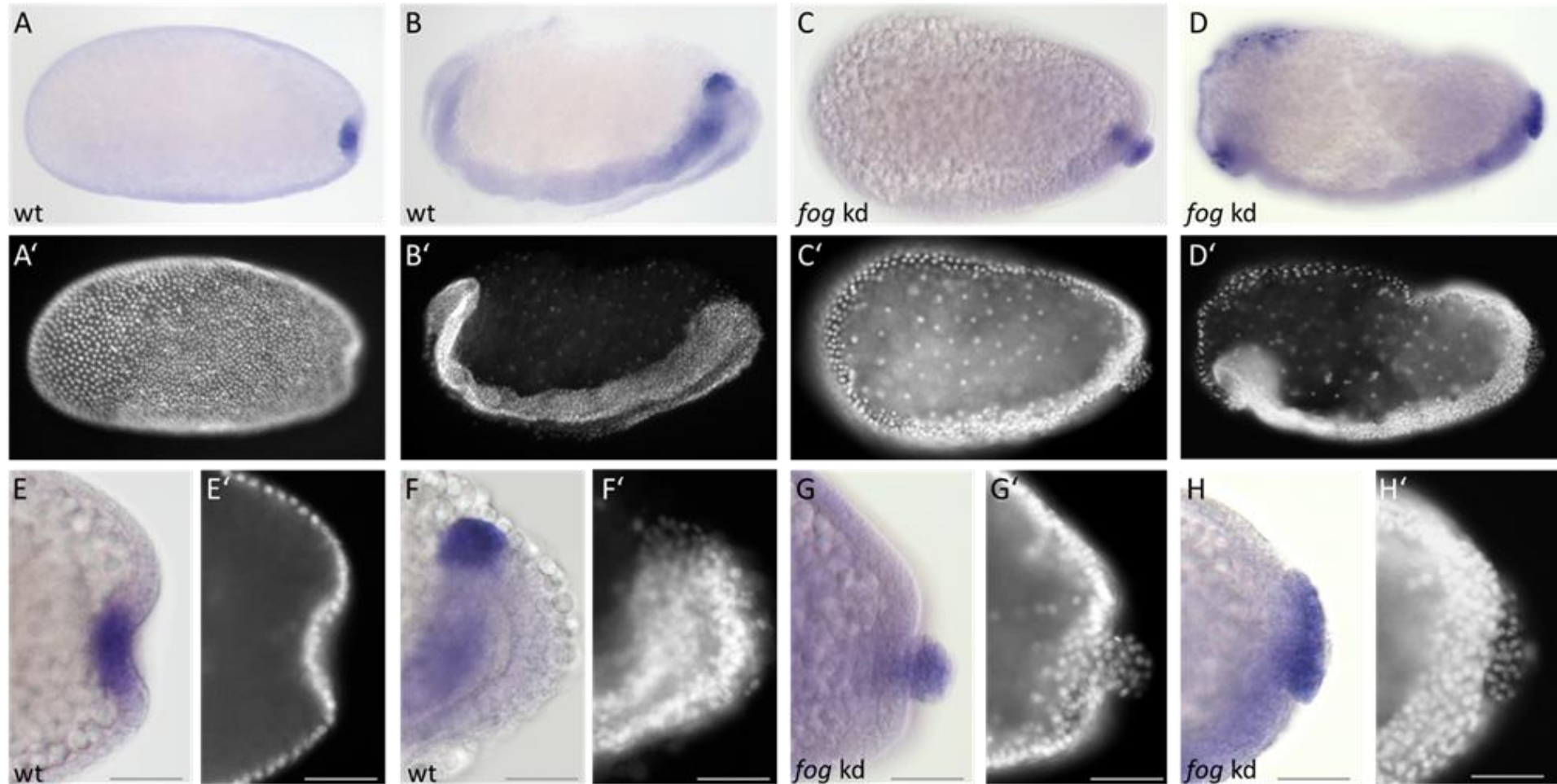


Figure 2.11: Germ cells upon *Tc-fog* knockdown visualized by *Tc-tapas*

(A-H) Whole mount ISH for the potential germ cell marker *Tc-tapas* of embryos at primitive pit stage (A, C, E and G) and germ band extension (B, D, F and H). (A'-H') DAPI staining of the respective embryos. The anterior to the left. All embryos shown in lateral views. (A and E) *Tc-tapas* was used to visualize the future germ cells, which are located in the primitive pit region of wildtype embryos. (B and F) Later during germ band elongation the germ cells got already invaginated and are visible at the posterior end of the embryo. In comparison, *Tc-fog* knockdown embryos (C and G) do not develop a primitive pit and the *Tc-tapas* expressing cells are separated from the embryo proper. (D and H) Also during gastrulation the germ cells do not get internalized and are visible at the posterior pole of the egg, sitting on top of the extending germ band.

5.6 Regulation of Fog signaling in *Tribolium*

In *Drosophila melanogaster*, the ventrally expressed transcription factors *twist* and *snail* are required for both, specification of the mesoderm and activation of ventral *fog* expression (Manning and Rogers, 2014). Loss of *Dm-twist* and *Dm-snail* cause depletion of the mesodermal *fog* domain (Leptin, 1994). However, the dorsoventral gene regulatory network (DV-GRN) of *Tribolium* differs from the *Drosophila* dorsoventral patterning system. To identify the regulatory mechanisms of Fog signaling in *Tribolium*, it was necessary to analyze the expression domains of *Tc-fog* and *Tc-mist* in different RNAi backgrounds.

Like in *Drosophila*, *Tribolium twist* shows expression in a ventral stripe (Sommer and Tautz, 1994). As *Tc-fog* expression is co-localized in a mesodermal domain (Fig. 2.12 A), it seemed likely that its mesodermal expression is regulated by Twist in *Tribolium*, too. Interestingly, neither *Tc-fog* nor *Tc-mist* showed changes in their mRNA expression pattern after knockdown of *Tc-twist* (Fig. 2.12 B and F). Prior experiments in *Tc-snail* embryos showed the same result for *Tc-fog* (unpublished data from Cornelia von Levetzow). Thus, it seems that unlike in *Drosophila*, mesodermal Fog signaling is not regulated by Twist or Snail but by another dorsoventral patterning gene.

Similar to *Drosophila*, Toll is the key regulator of the DV-GRN in *Tribolium* (Lynch and Roth, 2011). The dynamic nuclear Dorsal gradient, with peak level at the ventral side then activates different target genes in a concentration-dependent manner (Chen et al., 2000; Nunes da Fonseca et al., 2008). The loss of Toll results in dorsalization of the embryo (Fonseca et al., 2009). The mesoderm as well as parts of the neuroectoderm are missing. Furthermore, the embryo-serosa border becomes straight and is shifted towards the posterior pole, which causes also a reduction of the presumptive head region. As expected, the embryonic ventral expression domain of *Tc-fog* is depleted in *Tc-Toll* knockdown embryos (Fig. 2.12 C). Due to a reduction of the ventral serosa, *Tc-mist* shows a weak uniform expression. The posterior mRNA expression of *Tc-mist* however, remains unaffected (Fig. 2.12 G).

Another gene which was chosen to analyze the regulation of Fog signaling in *Tribolium* was *Tc-caudal* (*Tc-cad*). *Tc-caudal* is expressed in a posterior-to-anterior gradient and is thus an essential part of the posterior system (Schroder et al., 2000; Wolff et al., 1998). Similar to *Tc-Toll* knockdown embryos, *Tc-caudal* deficient embryos still form a primitive pit, although the formation of the posterior amniotic fold is less distinct. In addition, the dorsal serosa is expanded towards the posterior pole. Analysis of the *Tc-fog* expression domain upon *Tc-caudal* knockdown revealed on the one hand a loss of the mesodermal expression and on the other hand the *de novo* appearance of a posterior *Tc-fog* domain (Fig. 2.12 D). Thus, it is likely that Caudal regulates *Tc-fog* expression in opposing ways. It activates *Tc-*

fog expression in the mesoderm and simultaneously inhibits *fog* at the primitive pit. However, loss of *Tc-caudal* did not influence the expression of *Tc-mist* (Fig. 2.12 H).

The results of the careful analyses of Fog signaling components in different genetic backgrounds suggest, that Fog signaling in *Tribolium* might be regulated not only by dorsoventral patterning. Rather also parts of the antero-posterior gene regulatory network are involved.

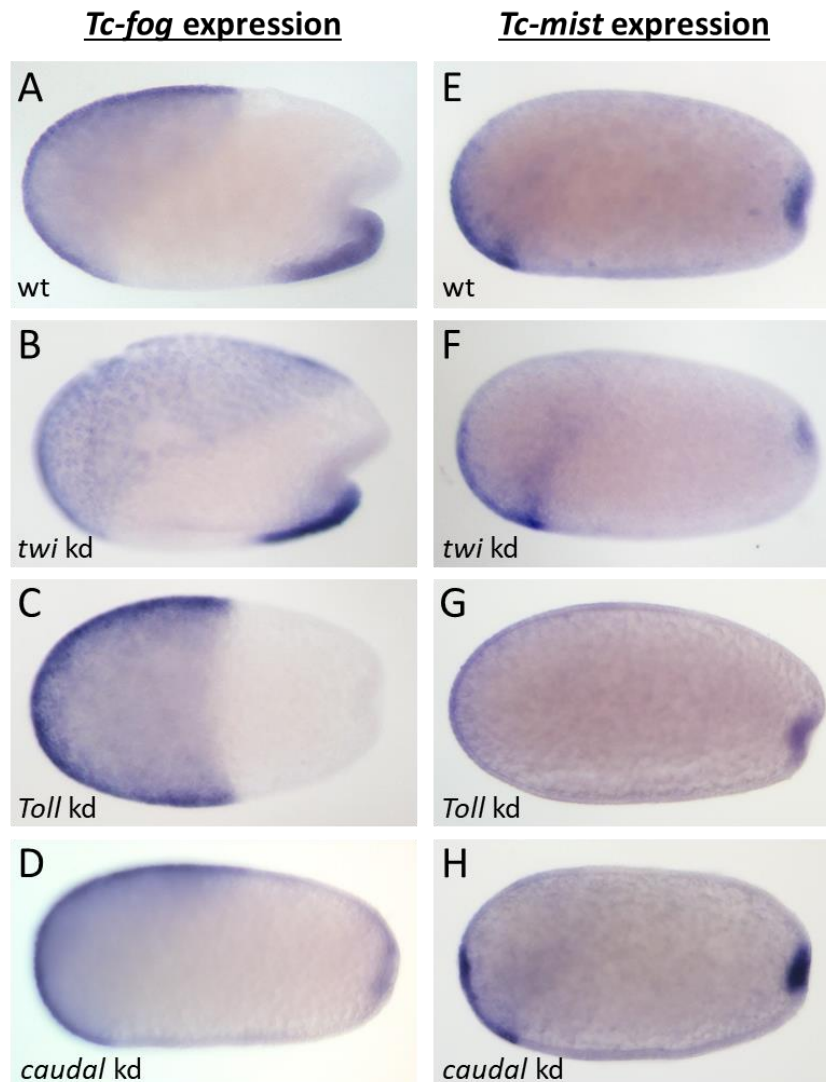


Figure 2.12: Expression of *Tc-fog* and *Tc-mist* in different RNAi backgrounds

(A-H) Whole mount ISH of wildtype and knockdown embryos around primitive pit stage. The anterior is left, the dorsal side is upwards. (A) In wildtype embryos of the primitive pit stage, *Tc-fog* is expressed in the serosa and the posterior part of the future mesoderm. (E) Similarly, also *Tc-mist* shows in addition to a posterior expression domain at the primitive pit, serosal expression. However, the expression starts to faint from the dorsal side of the serosa. (B and F) Knockdown of *Tc-twist* does not influence the expression domains of *fog* and *mist*. (C) Although the ventral posterior expression domain is abolished in *Tc-Toll* kd embryos, they are still able to form a primitive pit. (G) *Tc-Toll* RNAi embryos are still expressing *mist* around the primitive pit. (D) *Tc-caudal* knockdown causes loss of the ventral *Tc-fog* expression, whereas a new expression domain appears at the posterior pole. (H) However, both *Tc-mist* expression domains remain unaffected by loss of *Tc-caudal*.

As afore mentioned, unlike *Tc-fog* knockdown embryos, embryos after *Tc-Toll* knockdown are still able to form a posterior fold comparable to the amniotic fold. However, this fold looks more radial-symmetric than in wildtype embryos (Fig. 2.13 A). Due to loss of the mesoderm in *Toll* knockdown embryos, the ventral *Tc-fog* expression domain gets lost, whereas *Tc-mist* expression is still detectable (Fig. 2.13 C and G). To analyze the effect of the posterior mRNA expression of the receptor without the embryonic mRNA expression of its ligand Fog on the formation of the amniotic fold, embryos deficient for both, *Tc-Toll* and *Tc-fog* were generated. dsRNA for both genes was co-injected in a transgenic line expressing nuclear EGFP (each 1 μ g/ μ l) (Sarrazin et al., 2012). The development of the double knockdown embryos and a wildtype control were documented by live-imaging.

94% of the offspring derived from mothers injected with dsRNA for *Tc-Toll* and *Tc-fog* showed a phenotype (Fig. 2.13 B). Nevertheless, not all of the defective embryos showed the expected defects for a double knockdown. Around 7% of the embryos showed the typical phenotype of a *Tc-fog* knockdown (Fig. 2.13 B). Interestingly, none of the 76 investigated embryos showed only the defects of a *Tc-Toll* single knockdown. However, 99% of the double knockdown embryos showed no sign of primitive pit formation and embryo invagination (Fig. 2.13 A and B). Furthermore, the germ cells were also visible in some of the double knockdown embryos. Statistics on the occurrence of germ cells were not possible as the germ cells are not easy to detect in nGFP embryos.

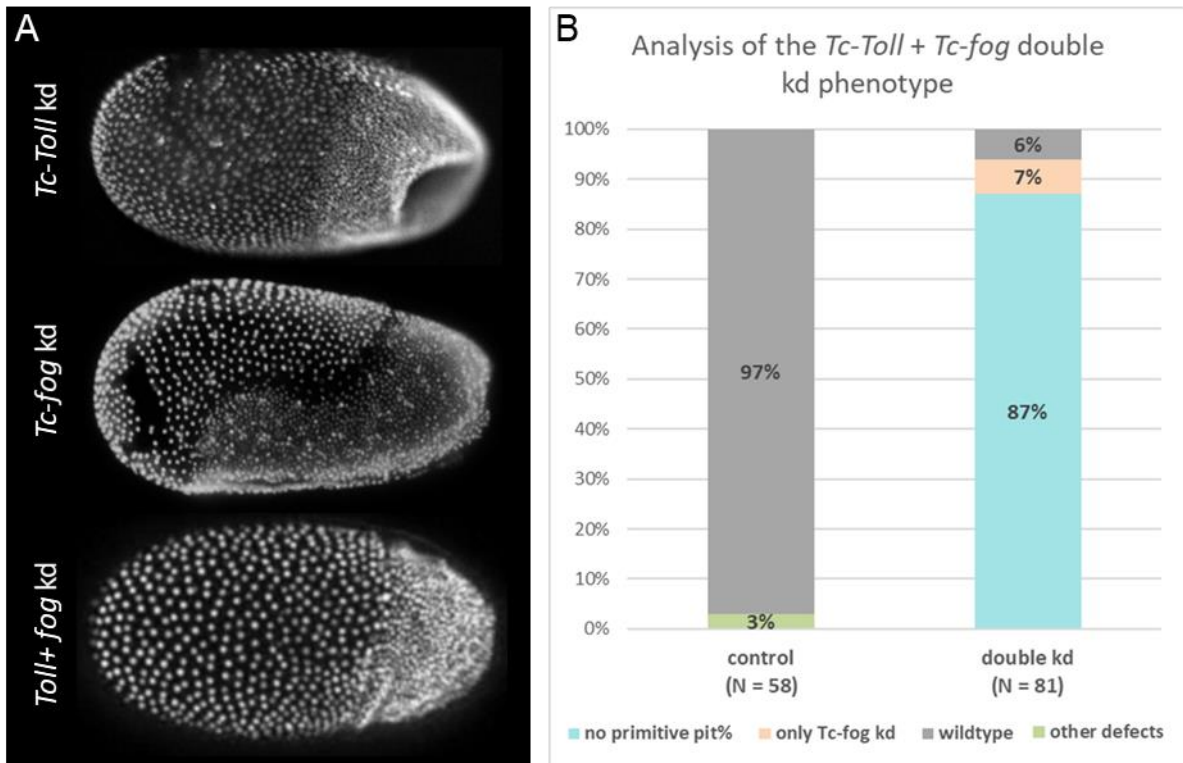


Figure 2.13: Double knockdown of *Tc-Toll* and *Tc-fog* results in loss of the posterior amniotic fold

(A) DAPI staining of *Tc-Toll*, *Tc-fog* and *Tc-Toll* + *Tc-fog* knockdown embryos. The anterior pole points to the left, the dorsal side points upwards. All pictures show lateral views of embryos during formation of the posterior amniotic fold. Although, the posterior fold is forming upon knockdown of *Tc-Toll*, it is missing in *Tc-fog* knockdown embryos and after double knockdown of *Tc-Toll* + *Tc-fog*, respectively. (B) The statics shows that 97% of the mock embryos (H_2O injected mothers) develop a normal primitive pit. 3% of the control embryos show a natural occurrence of random defects. 87% of the embryos derived from mothers injected with *Tc-Toll* + *Tc-fog* dsRNA do not form a primitive pit. 7% of the knockdown embryos show only the defects typical for a *Tc-fog* single knockdown and 6% of the embryos were wildtypes.

These results indicate that the formation of a posterior fold in *Tc-Toll* knockdown embryos depends on Fog signaling. Although the ventral *Tc-fog* mRNA expression neighboring the posterior pole is missing upon *Tc-Toll* knockdown, the formation of an amniotic fold suggests that the posterior localized receptor still gets activated. One explanation could be a long-range signaling by diffusion of the Fog protein diffusing from the serosa. Another possibility is, that Fog signaling might have a distinct function in serosa spreading and that this spreading, which is absent in *Tc-Toll* + *Tc-fog* double knockdown embryos, might be required for primitive pit formation.

5.7 Serosa spreading - A novel function of Fog signaling

So far, it was believed that Fog signaling is especially important for apical constrictions during insect gastrulation. However, both the ligand *Tc-fog* as well as its receptor *Tc-mist* are expressed in the extraembryonic serosa during the differentiated blastoderm stage (Fig. 2.14 A and B). Although the serosal *Tc-mist* expression disappears during gastrulation (Fig. 2.2 E), *Tc-fog* expression persists (Fig. 2.14 F-H). The membrane marker GAP43-YFP (Benton et al., 2013) enables the visualization of the cell outlines during embryonic development. During gastrulation of wildtype embryos, the serosal cells flatten and thus become wider (Fig. 2.14 C). The change of the cell shape is important as the serosa cells do not undergo further cell divisions, but have to surround the whole embryo proper during germ band extension (Fig. 2.14 E). At the stage of serosal window closure, the serosal cells have reached the highest level of cell flattening, seem to have the same size and are evenly distributed in the entire egg (Fig. 2.14 E and E', blue marked cells).

The single knockdown of *Tc-fog* leads usually to a weaker phenotype when the dsRNA is not injected into adults but embryos (injections performed by Matt A. Benton). As *fog* is maternally supplied (iBeetle Genome Browser; RNA-Seq data was supplied by Michael Schoppmeier, Ho Chung, Ho Ryun and Uli Loehr), the already existing protein weakens the RNAi effect. Although, the loss of *Tc-fog* is still strong enough to cause defects in internalization of the germ cells (Fig. 2.14 D), the serosa manages to cover the embryo during germ band elongation (Fig. 2.14 F). This circumstance enables a more accurate comparison of the serosa spreading in wildtype and *Tc-fog* knockdown embryos. Compared to the evenly enlarged serosa cells in wildtype embryos, the serosa of weak *Tc-fog* kd looks less organized. The anterior serosa cells are still very small and not as flat as more posterior cells. Furthermore, the more posterior serosa cells are extremely large and stretched (Fig. 2.14 F and F', red marked cells). This effect is probably caused by the condensation of the embryo proper which pulls the neighboring serosa cells ventrally.

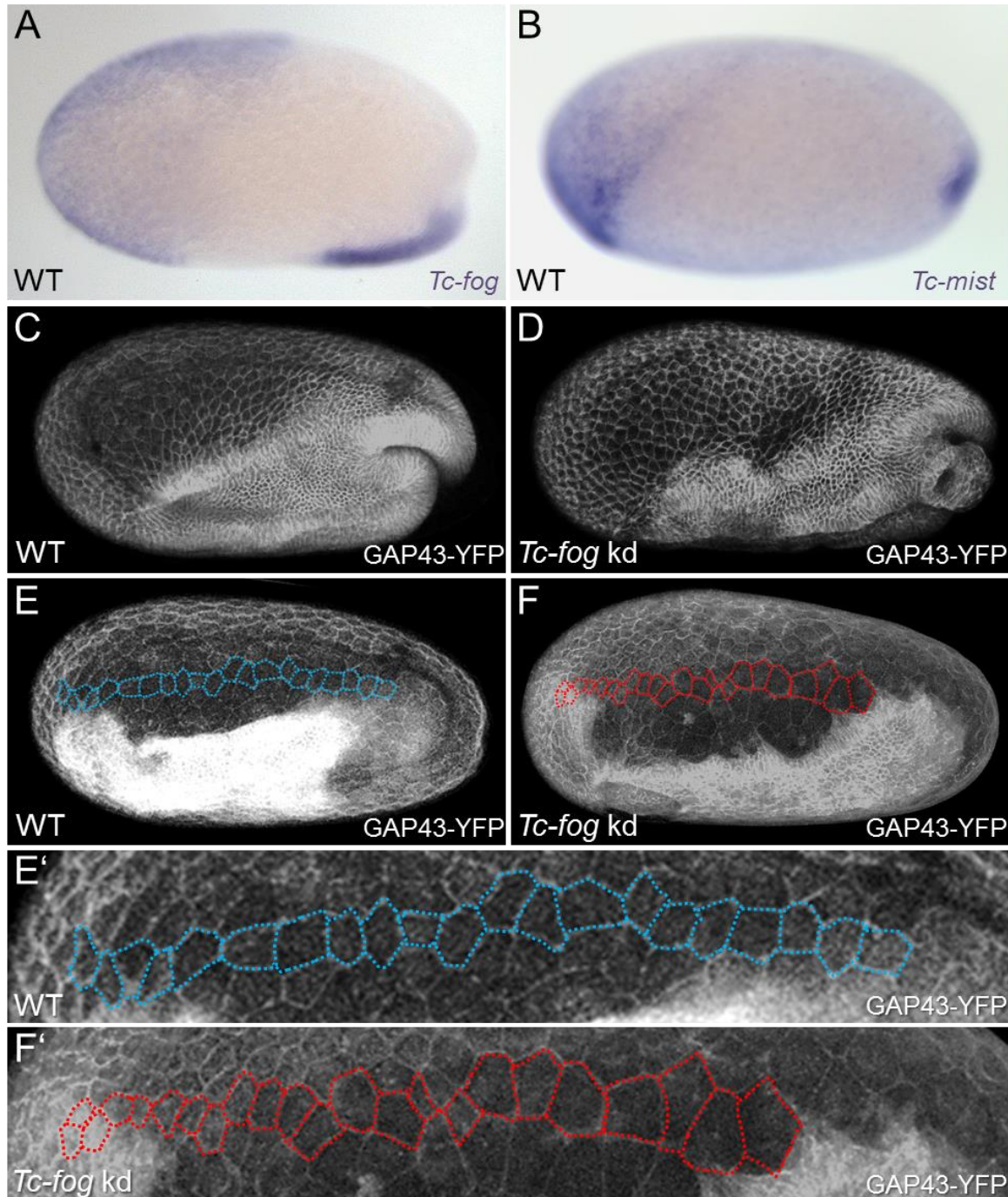


Fig. 2.14: Loss of *Tc-fog* affects serosal expansion

(A and B) Expression of *Tc-fog* and *Tc-mist* in differentiated blastoderm wildtype embryos. Both genes are expressed in the extraembryonic serosa. (C, E) Wildtype embryos injected with H₂O and the membrane marker GAP43-YFP. (D and F) Embryo injected with *Tc-fog* RNAi and GAP43-YFP. (E' and F') Higher magnification of embryos depicted in E and F. The anterior is left, the dorsal side is upwards. (A) Wildtype expression of *Tc-fog*. (B) Wildtype expression of *Tc-mist*. (C) A wildtype embryo at the beginning of gastrulation. Amnion and serosa starts to fold over the embryo proper. (E) The same embryo depicted in C shortly after serosal window closure. The serosa cells (blue) are evenly sized and distributed (also see E'). (D) A *Tc-fog* knockdown embryo showing a mild phenotype. Although the germ cells are visible during gastrulation, serosa and amnion manage to over grow the embryo. (F) Shortly before serosal window closure, a weak *Tc-fog* kd shows an uneven pattern of the serosa cells (red). (F') The anterior serosa cells are very small, whereas the more posterior serosa cells look wider and plane. (pictures C-F provided by Matthew A. Benton)

The co-expression of *Tc-fog* and *Tc-mist* already suggested a potential function of Fog signaling in the serosa of *Tribolium* embryos. In addition, the formation of an amniotic fold after *Tc-Toll* knockdown (Fig. 2.6 C and G) supposes, that the Fog protein might diffuse from the serosa to the posterior pole and acts via long range signaling. Our recent results in weak *Tc-fog* knockdowns indicate that the serosa might not only be a second source for posterior Fog signaling, but that it might have a novel function in coordinated cell flattening and spreading of the serosa cells during gastrulation.

5.8 Knockdown of *smog* does not result in morphogenetic defects

Recent studies (Kerridge et al., 2016), revealed that a second G-protein coupled receptor (GPCR) called Smog, is required for cell shape changes associated with both mesoderm invagination and ectoderm elongation. This additional receptor of Fog signaling is ubiquitously expressed in *Drosophila*. To analyze if Smog is also involved in early *Tribolium* morphogenesis, it was first identified by a BLAST approach (iBeetle Genome Browser; OGS 3.0).

In a second step, the expression pattern of *Tc-smog* was determined. Different embryonic stages, including the yet uncellularized pre-blastoderm (syncytium) (Fig. 2.15 A'), the blastoderm (Fig. 2.15 B'), the differentiated blastoderm (Fig. 2.15 C'), different gastrulation stages (Fig. 2.15 D'-F') and the early elongating germ band (Fig. 2.15 G' and H') were analyzed. None of the stages showed a definite staining result. The weak color reaction seen in all embryonic stages (Fig. 2.15 A-H) could indicate a weak uniform expression of *Tc-smog*. However, also the sense probe showed a very weak signal. Such weak stainings can also be interpreted as unspecific background staining. According to transcriptomic data (iBeetle Genome Browser; RNA-Seq data was supplied by Michael Schoppmeier, Ho Chung, Ho Ryun and Uli Loehr), *smog* is weakly expressed in the ovaries but not in the blastoderm. However, other transcriptome data suggest a general expression of *Tc-smog* in a not further defined stage (RNA-Seq data was supplied by the iBeetle consortium and 9 external contributors). Functional studies on knockdown embryos generated by both, parental⁶ (N=11) as well as embryonic (N=20) dsRNA injection did not indicate a function of *Tc-smog* on early morphogenetic movements or cell shape changes in *Tribolium catsaneum* (data not shown).

⁶ The injection of *Tc-smog* dsRNA in pupae as well as in adults results in sterility of the females. Thus, the knockdown experiment was repeated by embryonic injections.

Tc-smog expression

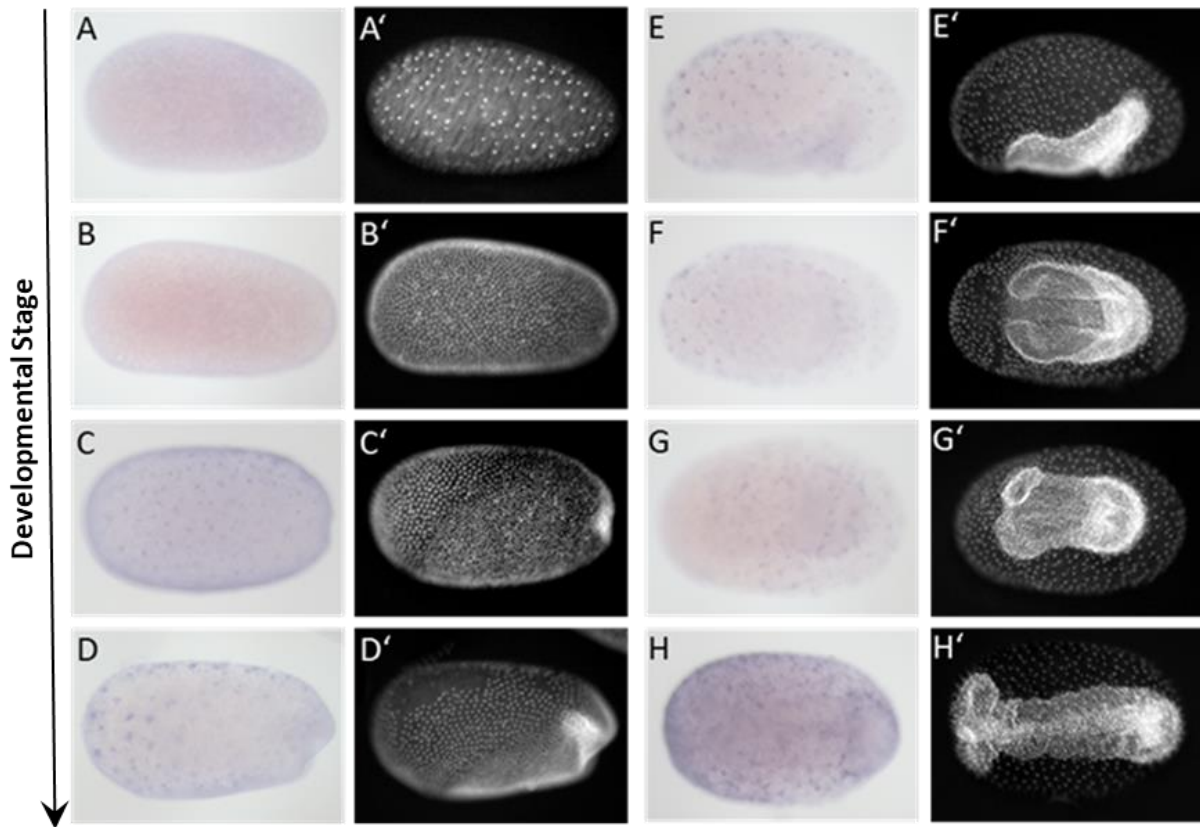


Figure 2.15: Expression patterns of *Tc-smog*

(A-H) Whole mount ISH of wildtype embryos from early blastoderm until beginning of germ band extension. (A'-H') DAPI staining of the respective embryos. The anterior pole to the left, the dorsal side upwards, except for F, G and H which show ventral surface views. In *Tribolium castaneum smog* is either not expressed or shows a very weak uniform expression throughout early embryonic development. The blue dots in C-H are unspecific background staining.

5.9 T48 does not contribute to mesoderm internalization in *Tribolium castaneum*

Another gene which contributes to cell shape changes in *Drosophila melanogaster* is *T48*. It encodes for a transmembrane protein that helps to recruit RhoGEF2 to apical membranes. Under control of *Dm-Twist*, it is expressed in a ventral stripe (Gould et al., 1990; Leptin, 1991). Like loss of *Fog* or *Cta* alone, the depletion of *T48* affects mesoderm internalization but does not block it completely. Thus, a strong effect on mesoderm internalization could only be detected by abolishing both *T48* and *Fog* signaling (Kolsch et al., 2007). Most likely, *T48* and *Fog* signaling act in parallel to concentrate RhoGEF2 apically and they redundantly contribute to mesoderm invagination in *D. melanogaster* (Manning and Rogers, 2014).

Tc-T48 has been identified and cloned in our lab previously, but no expression or functional data could be obtained using ISH and RNAi (unpublished data, Rodrigo Nunes da Fonseca and Cornelia von Levetzow). As the quality of the *Tribolium* genome increased over the last years, and transcriptomic data of different developmental stages became available, we wanted to review the previous results. I could verify the old sequencing data by BLAST to the new official genome (iBeetle Genome Browser; Tcas 5.2/OGS 3.0). An *in-situ* hybridization using an additional probe, which does not overlap with the previously used one, did result in uniformly stained embryos of different developmental stages (data not shown), consistent with transcriptomic data of blastoderm and differentiated blastoderm embryos (iBeetle Genome Browser; RNA-Seq data supplied by Michael Schoppmeier, Ho Chung, Ho Ryun and Uli Loehr). However, parental (N=296 embryos) as well as embryonic RNAi (N=30 embryos) experiments could not demonstrate a role of *T48* in mesoderm internalization of *Tribolium castaneum*. Thus, a double knockdown of both *Tc-fog* and *Tc-T48* by co-injecting the dsRNA into pre-blastoderm embryos was created (injections by Matthew A. Benton). Unlike in *Drosophila*, *Tribolium* double knockdown embryos did not show visible defects in ventral furrow formation (data not shown). However, compared to the embryos injected only with *Tc-fog* dsRNA, the general phenotype seemed to be stronger in the *Tc-fog* and *Tc-T48* double knockdown embryos. Only 8 out of 20 (40%) *Tc-fog* kd embryos showed a strong phenotype, whereas 16 out of 20 (80%) double kd embryos showed the typical morphological defects, like the serosa remaining on the dorsal side, no primitive pit formation and visible germ cells (data not shown). Regarding uniform *T48* expression and the influence on all aspects of the phenotype, it is likely that *T48* in *Tribolium castaneum* does not exclusively enhance mesoderm internalization but instead is a more global factor contributing to cell shape changes in the whole embryo.

6 Discussion

6.1 Fog and its conserved role in tissue internalization during gastrulation

As a member of the coleopterans *Tribolium* possesses several more ancestral features of embryonic development, compared to the highly derived fruit fly *D. melanogaster*. *Drosophila* is a typical long germ insect in which all segments develop simultaneously before gastrulation. In contrast, only the head and thorax segments of *Tribolium* are specified prior to gastrulation. The abdominal segments are formed consecutively from a posterior segment addition zone after gastrulation (short germ embryogenesis) (Tautz and Sommer, 1995). The different modes of early tissue specification are not the only differences between the two model systems. While *Drosophila* embryos possess a single rudimentary extraembryonic membrane (amnioserosa), which remains on the dorsal side of the egg throughout embryogenesis, two separate extraembryonic membranes (amnion and serosa) protect the developing *Tribolium* embryos (Tautz and Sommer, 1995). These membranes are an essential part of the first morphogenetic movements taking place during *Tribolium* gastrulation, including the formation of the posterior amniotic fold (Handel et al., 2000).

Fog signaling is affecting the development of various tissues, throughout embryogenesis but especially during gastrulation. Thus, the loss of the Fog signaling components *Tc-fog*, *Tc-mist* and *Tc-cta* results in a highly complex phenotype, including defects in cell shape changes at the posterior pole (amniotic fold formation) and invagination of the mesoderm (Fig. 3.1). In addition, late defects occur in hindgut formation and dorsal closure. Furthermore, the data presented in this work suggest a so far unknown, but more general function of Fog signaling in coordinating tissue-wide cell shape changes like flattening and spreading of the serosa. In the following chapters, the different defects and their dependence on Fog signaling are discussed in detail.

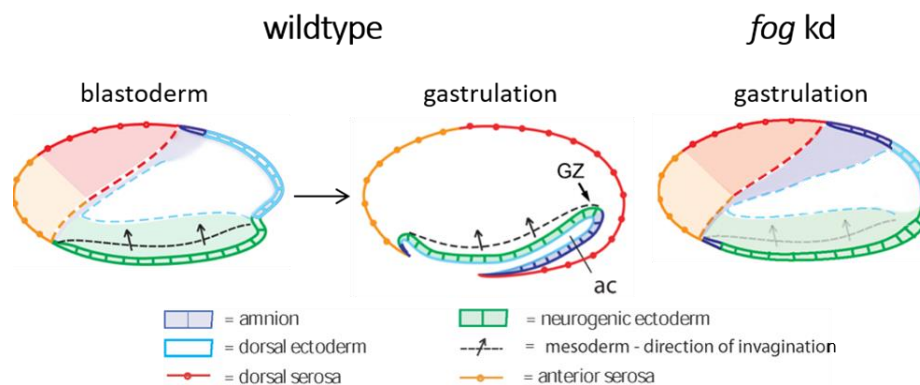


Figure 3.1: Gastrulation after fog knockdown

During gastrulation of wildtype embryos, the ventral mesoderm starts to be internalized (arrows). Around the same time, the serosa (orange/red) and the amnion (purple) start to overgrow the germ rudiment. In contrast, upon *Tc-fog* kd both extraembryonic tissues stay at the dorsal side of embryo. Especially the amnion is strongly pulled towards the posterior-ventral side by the condensation of the embryo proper. However, the primitive pit and the later deep posterior gastrulation fold are completely missing. In addition, knockdown of *fog* results in a delay in mesoderm invagination. modified from (Rodrigo Nunes da Fonseca; unpublished)

The co-expression of *fog*, *mist* and *T48* in the mesoderm of *Drosophila* embryos already indicate a role of Fog signaling in mesoderm development (Kolsch et al., 2007; Leptin, 1991; Manning et al., 2013). Different studies provide accurate information about the role of Fog signaling in inducing apical constriction for successful internalization of the mesoderm. Although the mesoderm gets internalized, the mesodermal cells in loss of function mutant *Drosophila* embryos (*fog*, *mist*, *cta* and *T48*) show an unorganized pattern of apical constriction and a delay in mesoderm invagination (Costa et al., 1994; Dawes-Hoang et al., 2005; Kolsch et al., 2007; Manning and Rogers, 2014).

In contrast to *Drosophila*, the only pathway component showing enhanced expression in the *Tribolium* mesoderm prior to gastrulation is *Tc-fog* (Fig. 1.1 A-E). Nevertheless, *Tc-fog*, *Tc-mist* and *Tc-cta* knockdown embryos show the same defects in mesoderm internalization that have been described in *Drosophila*. In *Tribolium*, the position of *Tc-twist* positive segmental cell clusters covered by the ectoderm (longitudinal sections) of control and *Tc-fog* knockdown embryos, proves the successful internalization of the mesoderm (Fig. 2.9 B and E). However, an analysis of *Tc-twist* expressing cells in cross-sections of carefully staged *Tribolium* wildtype and knockdown embryos revealed a reduction in the depth of the ventral furrow. Especially posterior regions were affected. Loss of *Tc-fog* results in a delay of around 3h in mesoderm invagination (Fig. 2.8).

The effect of Fog signaling on mesoderm internalization in *Tribolium* strongly resembles the situation in *Drosophila*, proving that Fog signaling has indeed a conserved role in regulating morphogenetic movements during gastrulation. Although Fog signaling is essential for timing and coordination of ventral furrow formation, the fact that loss of *Tc-fog* is not sufficient to prevent mesoderm internalization suggests, that Fog signaling is not the only pathway regulating mesoderm morphogenesis.

6.2 Genes with less influence on apical constrictions in *Tribolium* compared to *Drosophila*

In *Drosophila* the transmembrane anchor protein T48 contributes to bending of epithelial sheets by apical constrictions. Complementary to Fog signaling, which activates RhoGEF2 release from microtubules, T48 concentrates RhoGEF2 to the apical membrane (Kolsch et al., 2007; Manning and Rogers, 2014). These parallel pathways explain the incomplete progression of apical constriction in the absence of one of those pathways, as seen in *fog*⁻ mutant embryos (Costa et al., 1994; Kolsch et al., 2007; Sweeton et al., 1991). Embryos deficient for *T48* fail in formation of ventral furrow although invagination of the posterior midgut primordium is unaffected. However, cells lacking T48, only show a less organized and delayed invagination but are still able to undergo apical constriction, although it might be slightly weaker. Recent studies could show that the combined loss of *fog* and *T48* in *Drosophila*, abolishes ventral furrow formation and results in an ingression-like mesoderm cell behavior, reminiscent of mesoderm invagination observed in *Chironomus riparius*. Thus, mesoderm ingression does not require Fog or T48 function (Urbansky et al., 2016). An opposing effect was observed for the early ubiquitous expression of *fog* and *T48* in *C. riparius* embryos. Both genes were sufficient to invoke a *Drosophila*-like invagination of the mesoderm *Chironomus* embryos. *Dm-T48* shows an early mRNA localization in a ventral *twist*-like stripe in the presumptive mesoderm, whereas it is absent from the posterior area of midgut invagination. In *Tribolium*, transcriptomic data suggest a weak *T48* expression prior to gastrulation (although no localized mRNA expression domain could be identified by ISH). In contrast, it seems not to be expressed at all in *Chironomus* (Urbansky et al., 2016). Furthermore, *Tc-T48* knockdown embryos did not show defects in primitive pit or ventral furrow formation. It also did not affect spreading of the serosa. In fact, double knockdown experiments using *Tc-T48* and *Tc-fog* dsRNA resulted in embryos with typical features of strong *Tc-fog* knockdowns, including visible primordial germ cells and lack of posterior amniotic fold formation. This suggests a more general function of T48 for enhancing Fog signaling in all tissues. In summary, the results indicate that an evolutionary gain of early *fog* and *T48* activity in the mesoderm may constitute a genetic switch to increase the speed of fly gastrulation (see results 2.9).

Another Fog signaling component, the GPCR *Smog* which was recently discovered, could be identified in *Tribolium*. *smog* is uniformly expressed in both, *Drosophila* and *Tribolium* embryos. An involvement of *smog* in cell shape changes during mesoderm internalization, PMG invagination and especially ectoderm extension has been reported in *Drosophila* (Kerridge et al., 2016). However, the results by analysis of *Tc-smog* kd by parental as well as embryonic RNAi suggest, that *Tc-smog* has no role during *Tribolium* gastrulation, neither for amniotic fold or ventral furrow formation, nor for serosa spreading or ectoderm morphogenesis.

6.3 The importance of posterior amniotic fold formation by Fog signaling

One of the early morphogenetic movements during *Tribolium* embryogenesis is the formation of a posterior amniotic fold. At the onset of gastrulation, Fog signaling induces apical constrictions of the cells at the posterior pole. In turn, these cells form a cup-like structure which finally converts to a deep fold when the amnion, part of the dorsal ectoderm and the serosa start to move ventrally and thus fold over (posterior amniotic fold) to finally cover the embryo proper (Handel et al., 2000). Embryos lacking one of the Fog signaling components fail to form a primitive pit (Fig. 2.6). In consequence, amnion and serosa remain on the dorsal side and the embryo proper gets not covered.

One theory suggests, that the spreading of the serosa to the ventral side at the onset of gastrulation, might indirectly be required for primitive pit formation. It was proposed that germband condensation drives initiation of amnion folding. Expansion of the amniotic fold and closure of the amniotic cavity are likely driven by contraction of an actomyosin cable at the boundary between the amnion and serosa (Benton et al., 2013). Not only loss of *Tc-fog* but also the double knockdown of *Tc-Toll* and *Tc-fog* embryos results in immobility of the serosa. Similarly, double knockdown embryos do not form a primitive pit, whereas it is still formed upon *Tc-Toll* single kd (Fig. 2.13 A). Thus, it seems possible that the spreading of the serosa influences posterior amniotic fold formation.

During later development, defects in hindgut formation occur in *Tc-fog* knockdown embryos. Although the hindgut fate seems to be unaffected, the invagination tube is located outside of the embryos (von Levetzow, PhD Thesis 2008). The defects in *Drosophila fog* mutant embryos are more severe. It seems that the defective invagination of the PMG primordium during gastrulation results in absence of a tube-like hindgut or posterior midgut in later stages (Lengyel and Iwaki, 2002). However, also in *Drosophila* Fog signaling does not affect the cell fate. The strong defects can be explained by the initial failure of tissue invagination.

Besides the missing pole cells, the posterior amniotic fold in *Tribolium* resembles the posterior midgut (PMG) invagination of *Drosophila* (Handel et al., 2000). The process of PMG invagination in *Drosophila* is well-studied. After the first apical constrictions appear at the dorsal side of the posterior midgut primordium, shrinking of the remaining cell apices results in formation of a cup-like indentation (Sweeton et al., 1991; Turner and Mahowald, 1976). During germ band extension this cup moves dorsally before it becomes deeper by further invagination of the cells, forming a structure referred to as amnioproctodeal tube (Rickoll and Counce, 1980; Sonnenblick, 1941). Only the center cells belong to the PMG primordium. The remaining invaginated cells give rise to the hindgut and the malpighian tubules, as indicated by the expression of the hindgut (proctodeum) marker *brachyenteron* (Berns et al., 2008; Kispert et al., 1994; Singer et al., 1996; Wu and Lengyel, 1998).

Although the hindgut in *Tribolium* is formed much later during germ band retraction, *Tc-brachyenteron* is already expressed at the tip of the posterior amniotic fold during late gastrulation and throughout germ band extension (Berns et al., 2008). Hence it is likely, that the formation of the amniotic fold in *Tribolium* is homologous to the formation of the amnioproctodeal tube in *Drosophila*. Supporting this theory, it has been shown that the midgut epithelium of *Tribolium confusum* probably derives from cells associated with the proctodeal invagination (Handel et al., 2000; Stanley, 1970).

6.4 Positioning of the primordial germ cells is influenced by Fog signaling

One of the most obvious morphological defects after loss of Fog signaling is the failure to internalize the primordial germ cells at the posterior pole (Fig. 2.11). Primordial germ cells (PGCs) are the progenitor cells that give rise to the gametes (Marlow, 2015). Different mechanisms of germ cell formation evolved during insect evolution. While specification of the primordial germ cells in some insects is induced by maternal supply of several gene products (germ plasm), they are specified by zygotically activated transcription factors in others (Lynch et al., 2012).

In many holometabolous insects including *Drosophila* and *Nasonia*, the PGCs emerge from so-called pole cells at the posterior pole of the egg prior to cellularization. Maternally supplied germ plasm induces the formation of the pole cells which get internalized during posterior midgut invagination later in embryogenesis (Fig. 2.3). Another feature that is shared by both species is the localization of *oskar* mRNA in the pole plasm (Ephrussi and Lehmann, 1992; Lynch et al., 2012; Lynch et al., 2011). After crossing the endoderm, the cells migrate to their final position in the gonadal mesoderm (Coffman, 2003; Sonnenblick, 1941). The pole cell-based mode of PGC formation seems to be derived from a more ancestral mechanism, which has been described for hemipterans and some holometabolous lineages, e.g. members of the coleopterans (e.g. *Tribolium*) (Lynch et al., 2012). This second type of primordial germ cell formation is not dependent on maternally supplied pole plasm. The germline fate is specified by zygotic gene expression, often later in embryonic development (Extavour and Akam, 2003). Similar to the system observed in *Drosophila*, PGCs separate from blastoderm after cellularization, get internalized (Fig. 2.3 C1-C4) and translocate to the gonads. *Tribolium* embryos lack a localized *oskar* expression. Instead, ubiquitous mRNA of *Tc-vasa* gets selectively degraded, so that it is only found at the posterior pole at the onset of gastrulation. Later it marks the primordial germ cells (Lynch et al., 2012; Schroder, 2006). Oskar localization is probably secondarily lost in *Tribolium*, as it was also found in *Gryllus bimaculatus* (Ewen-Campen et al., 2012). In contrast to the so far mentioned mechanisms, the PGCs in *Gryllus* form in later embryonic stages

from a subgroup of mesodermal cells which give rise to the future gonads. This probably most ancestral mode of germline specification is usually found in basally branching insects.

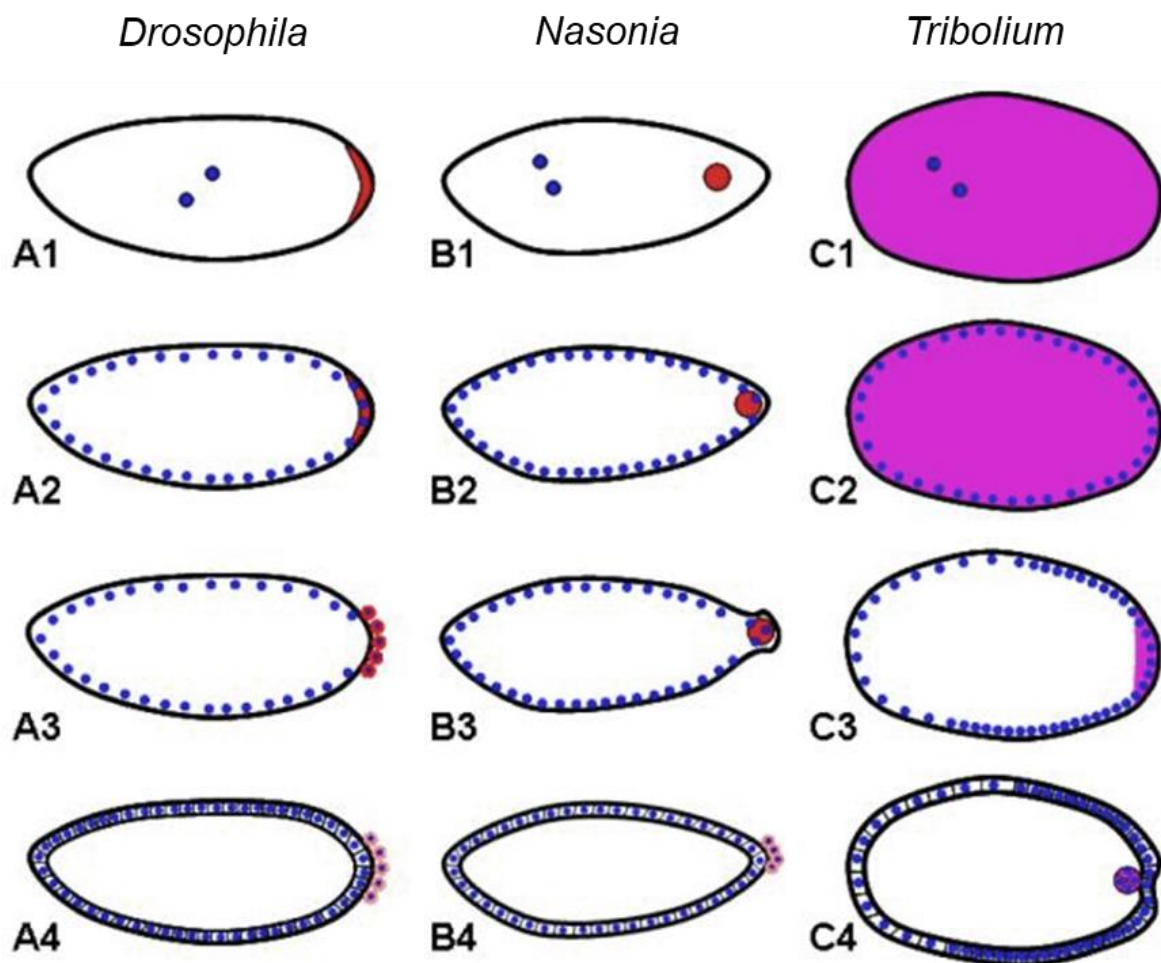


Figure 3.2: Germ cell formation in *Drosophila*, *Nasonia*, and *Tribolium*

Red = *oskar* (*osk*) mRNA, magenta = *Tc-vasa* mRNA, blue = nuclei. (A1-C1) In the early stages of embryogenesis, *osk* mRNA is localized in the posterior pole plasm of *Drosophila* (A1) and oosome of *Nasonia* (B1), while *Tc-vasa* is ubiquitously expressed in *Tribolium* (C1). (A2-C2) In *Drosophila* and *Nasonia* the posterior cells of the syncytial blastoderm interact with the pole plasm (A2), or the oosome (B2), respectively. In the *Tribolium*, the nuclei are surrounded by a homogenous environment (C2). (A3-C3) In the fly the pole cells are formed by single nuclei that entered the pole plasm (A3). In *Nasonia*, the oosome along with multiple nuclei bud simultaneously from the posterior (B3). *Tc-vasa* becomes localized at the posterior pole of late blastoderm *Tribolium* embryos (B4). (A4-C4) After formation of the pole cells and completed cellularization of the blastoderm, *Dm-osk* (A4) and *Nv-osk* (B4) get degraded. (C4) *Tc-vasa* positive cells delaminate from the blastoderm into the interior of the embryo in order to form the primordial germ cells. (Lynch et al., 2012)

Although the different modes of germline specification seem to correlate in general to more derived and more ancestral lineages, the formation of pole cells in coleopterans occurs several times, even within closely related species. Although the PGCs of *Callosobruchus*, a seed beetle, are derived from pole cells, *Atrachya* embryos do not possess these specific cells (Benton et al., 2016; Quan and Lynch, 2016). Thus, it is likely that minor changes in gene regulation act as a switch between the different ways of PGC formation.

I observed a cluster of cells at the posterior pole of *Tc-fog* knockdown embryos which were positive for the putative germ cell marker *Tc-tapas* (Patil et al., 2014). Furthermore, the timing of their occurrence and their location indicate their germline fate.

Fog signaling might influence the direction of PGC positioning in *Tribolium castaneum*. It is possible that the physical circumstances, generated by apical constriction of the most posterior cells, trigger the PGCs to leave the epithelium to the interior of the embryo. As *Tc-fog* knockdown embryos lack apical constrictions in this area, the cells move to the outer surface. Hence, Fog signaling is probably only indirectly required for PGC internalization. The influence of Fog signaling on positioning of the PGCs has shed some more light on the evolutionary history of germline determination in insects. Together with the dependency on maternally supplied gene products, early morphogenetic movements induced by Fog, might explain the transition from a later zygotic germline specification. This also includes extensive cell migration to an early and pole cell based PGC specification in derived species like *Drosophila*.

6.5 The regulatory network underlying Fog signaling

Similar to *Drosophila* dorsoventral patterning, Toll signaling initiates the early fate determination in *Tribolium castaneum* (Lynch and Roth, 2011; Nunes da Fonseca et al., 2008). In both organisms, the two transcription factors *twist* and *snail* are expressed in a ventral stripe and control specification of the mesoderm (Leptin, 1991, 1994; Sommer and Tautz, 1994). In *Drosophila*, ventral Fog signaling is activated by both of them, leading to ventral furrow formation (Manning and Rogers, 2014). The co-localization of *Tc-fog* and *Tc-twist* strongly indicates a regulation of the ventral Fog signaling by *Tc-Twist* similar to *Drosophila*. However, the observation that neither *Tc-fog* nor *Tc-mist* showed changes in their expression domains (Fig. 2.12 B and F) in *Tc-twist* knockdown embryos, is contradictory to this hypothesis. In addition, former results suggest that *Tc-snail* is not required for *Tc-fog* expression (Rodrigo Nunes da Fonseca, unpublished). These data rather suggest that the mesodermal activation of *Tc-fog* depends on other factors.

DV and AP patterning are connected to a certain degree. Thus, the expression pattern analysis of *Tc-fog* and *Tc-mist* in *caudal* knockdown embryos should reveal a possible influence of the AP patterning system on Fog signaling. The knockdown of *Tc-caudal* results in defects in convergent extension and thus, in a broader and shorter germ rudiment. Furthermore, the dorsal serosa is slightly expanded towards the posterior pole (Schroder et al., 2000; Wolff et al., 1998). *Tc-mist* expression remains unaffected upon knockdown of *caudal* (Fig. 2.12 H). The fact that the mesodermal *Tc-fog* expression domain is lost after *Tc-caudal* kd, whereas a new expression domain appears in the region of the

primitive pit (Fig. 2.12 D) suggest, that *Tc-caudal* has two divergent roles in Fog regulation. It activates *Tc-fog* expression in the mesoderm and simultaneously inhibits its expression at the primitive pit. Although *Tc-caudal* deficient embryos form a primitive pit, the amniotic fold is less distinct.

In summary, *Tc-mist* expression seems to be independent of both, the DV patterning system and *Tc-caudal*. However, *Tc-caudal* regulates *Tc-fog* expression in the mesoderm as well as in the primitive pit. Besides changes in the DV-GRN of *Tribolium* (Stappert et al., 2016), also the regulatory network underlying Fog signaling differs from *Drosophila*.

6.6 Serosa spreading and cellularization - A novel function of Fog signaling

6.6.1 Fog signaling regulates flattening of the serosa cells

The serosa is a monolayered epithelium that protects the embryo from desiccation and against pathogens (Jacobs et al., 2013; Panfilio, 2008). To form a differentiated blastoderm, the embryonic cells start to contract and become columnar. In contrast, the serosa cells start to spread and become squamous to finally envelop the embryo and the yolk. Squamous epithelia are often associated with developmental or tissue remodeling processes (Pope and Harris, 2008).

Although, germ band extension seems to be unaffected, *Tc-fog* knockdown embryos are deformed in late stages (von Levetzow, PhD Thesis 2008). These morphological defects can be explained by the late influence of serosa and amnion on dorsal closure of the embryo. At the end of embryogenesis, the extraembryonic membranes rupture (~ 52h AEL) and retract to the dorsal side (Hilbrant et al., 2016; Panfilio et al., 2013). In consequence, the lateral parts of the embryo start to move dorsally and finally fuse at the dorsal midline (Koelzer et al., 2014). This process is disrupted by loss of Fog signaling and the dorsal side of the embryo remains open, similar to *Tc-zen2* knockdown embryos (van der Zee et al., 2005). As the extraembryonic tissue has a great influence on embryonic morphogenesis, different questions raised facing the serosal co-expression of *Tc-fog* and *Tc-mist*. Is the immobility of the serosa after loss of Fog signaling a primary or secondary effect? Could Fog signaling influence cell shape changes in the serosa? If not, why are ligand and receptor co-expressed?

Knockdown of *Tc-Toll* results in dorsalized embryos which lack the mesoderm as well as the ventral ectoderm. The embryo-serosa border becomes straight and is shifted towards the posterior pole, deleting part of the head anlagen. In *Tc-Toll* kd embryos *Tc-fog* is strongly expressed in the symmetric serosa, while *Tc-mist* shows a weaker but uniform expression instead of ventrally enhanced serosal expression in wildtype embryos. Furthermore, the mesodermal expression domain of *Tc-fog* is lost, indicating that it is activated by dorsoventral patterning genes, whereas the posterior *Tc-mist*

expression remains unaffected (Fig. 2.12 C and G). Interestingly, *Tc-Toll* knockdown embryos are still capable to form a primitive pit. This implies that the posterior localized receptor still gets activated.

Two theories might explain the unaffected formation of the posterior amniotic fold. The first explanation could be that the serosa serves as a source for long-range signaling. Diffusion of the Fog protein from the serosa to the posterior pole could be still sufficient to induce apical constrictions and hence primitive pit indentation. *Drosophila* Fog is thought to act as an autocrine factor which only diffuses a couple of cell widths (Costa et al., 1994). However, the *Tribolium* Fog protein is less than half the size of *Dm-Fog*, making long-range signaling more likely (Fig. 3.3).

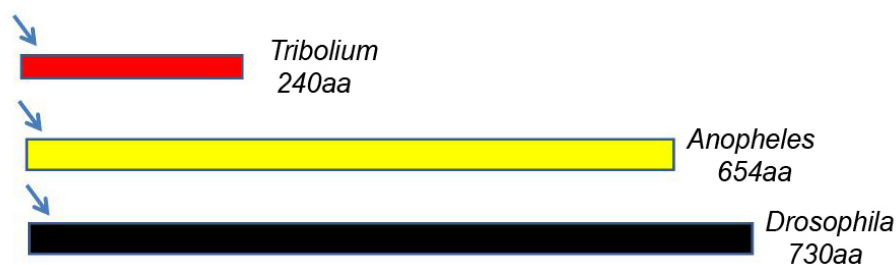


Figure 3.3: Fog is a fast-evolving protein

The Fog protein evolved very fast in both, nucleotide as well as amino acid sequence. Furthermore, the *Tribolium* Fog is much smaller than its *Drosophila* and *Anopheles* orthologs. (Rodrigo Nunes da Fonseca, unpublished)

Nevertheless, the simultaneous expression of *Tc-fog* and *Tc-mist* in the serosa might give hints for another explanation. Fog signaling could have a distinct function in cell shape changes in the serosa, influencing its spreading. Cell flattening requires extensive remodeling of adherens junctions (Szuperak et al., 2011) and changes in the actin-myosin network. The transformation from a cuboidal to a squamous epithelium involves shrinking the lateral membrane and extending the basal and apical membranes (Brigaud et al., 2015). Studies on the amnioserosa cells in *Drosophila* revealed, that its cell shape changes are dependent on a rotation of the microtubule cytoskeleton. The authors suggested that similar mechanisms may underlie the development of other squamous epithelial monolayers (Pope and Harris, 2008).

Injecting *Tc-fog* dsRNA (1 μ g/ μ l) into embryos resulted in weaker phenotypes in which the primordial germ cells did not get invaginated, but amnion and serosa managed to cover the embryo during gastrulation (Fig. 2.14 D and F). Those weak phenotypes enabled a proper comparison of the cell shape changes within the serosa. In wildtype embryos, all serosa cells start to flatten at the same time and are of equal size when they reach their peak levels of flattening at serosal window closure (Fig. 2.14 C and E). Interestingly, the anterior serosa cells did not undergo cell flattening after loss of *Tc-fog*. In contrast, the posterior serosa cells were abnormally enlarged around the stage of serosal window

closure (Fig. 2.14 E' and F'). One feature of a strong *Tc-fog* knockdown phenotype is, that the serosa rips off from the amnion and the embryo proper during germ band condensation (Fig. 2.6 K). If the serosa cells do not undergo cell flattening, they remain on the dorsal side. The embryonic cells move to the ventral side exerting physical force, especially on the lateral serosa cells. As the connection between the serosa and the amnion might be a structural weak point, the cells lose contact and the serosa moves back to the dorsal side.

The results presented in this work indicate that Fog signaling in *Tribolium* is not only required for tissue internalization via apical constrictions, but that it is rather involved in cell shape changes in general, especially for coordinated cell flattening of the serosa cells. This function was never observed before. However, so far Fog signaling was mainly studied in *Drosophila* in which the amnioserosa remains on the dorsal side.

6.6.2 A role of Fog signaling in the blastoderm

The generation of *Tc-fog* knockdowns by embryonic injection revealed another interesting part of the phenotype, which was never observed in knockdown embryos after pRNAi. The injection of higher dsRNA concentrations ($>3 \mu\text{g}/\mu\text{l}$) led to the formation of big holes in the uniform blastoderm. Holes seem to occur naturally also in wildtype embryos but usually close very fast. The holes which form in the early blastoderm of *Tc-cta*, *Tc-fog* and *Tc-mist* knockdown embryos remain open (unpublished data by Matthew A. Benton). As Fog signaling induces pulsatile contraction of the actomyosin network (Dawes-Hoang et al., 2005; Martin et al., 2009), it might also influence the coordination of the cytoskeleton during cellularization and in the early blastoderm.

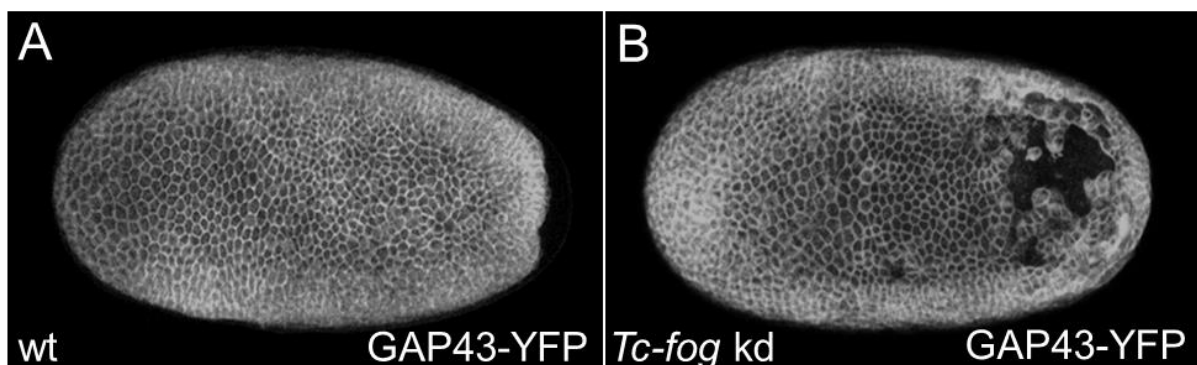


Figure 3.4: Fog signaling is involved in germ rudiment formation of *Tribolium castaneum*

(A) Wildtype embryo injected with H_2O and the membrane marker GAP43-YFP. (B) Embryo injected with *Tc-fog* RNAi and GAP43-YFP. Holes are visible in the posterior part of the blastoderm. (pictures provided by Matthew A. Benton)

In *Tribolium* the cells of the blastoderm undergo some cell shape changes prior to gastrulation. The embryonic cells start to contract and become columnar, while the serosa cells started to flatten and become squamous (Benton et al., 2013; Handel et al., 2005; Handel et al., 2000). This explains the extension of some of the holes during early condensation of the germ rudiment (Fig. 3.4 A and B).

Interestingly, knockdown experiments in the *Gryllus bimaculatus*, result in the same phenotype upon *cta* and *mist* knockdown (Fig. 3.5 A and B, unpublished data by Matthias Pechmann). *Tribolium* as well as *Gryllus* are more basally branching insects compared to *Drosophila*. Thus, it is likely that the role of Fog signaling in coordinating embryo condensation represents an ancestral process.

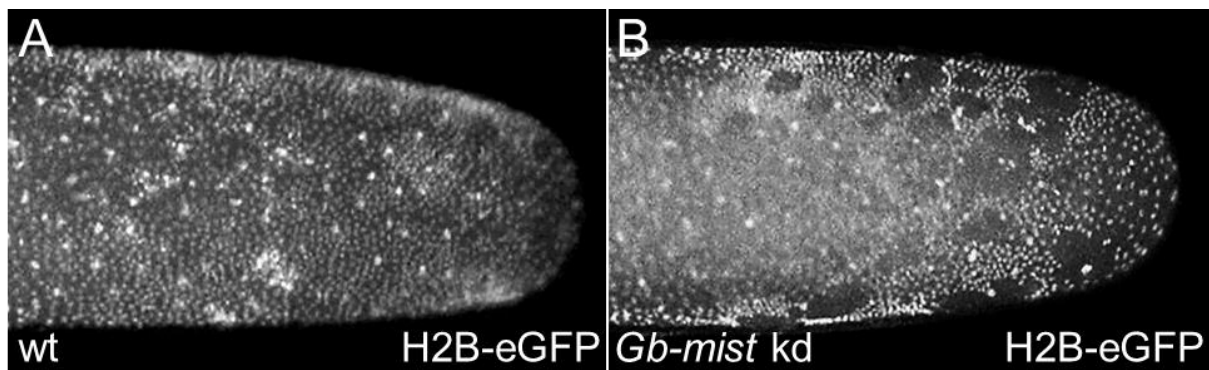


Figure 3.5: Fog signaling is involved in germ rudiment formation of *Gryllus bimaculatus*

Females of a H2B-eGFP line expressing nuclear eGFP were used for dsRNA injection. (A) Control embryo. (B) Embryo injected with *Gb-fog* RNAi embryo showing a disintegrating blastoderm with numerous holes. (pictures provided by Matthias Pechmann)

6.7 Conclusion

In *Drosophila* Fog signaling is involved in tissue internalization during gastrulation, like internalization of the mesoderm and the posterior midgut primordium. By activating the GPCR Mist, the G α -subunit Concertina (Cta) and RhoGEF2, Fog signaling controls rearrangements of the actomyosin network, resulting in apical constrictions and thus bending of epithelial sheets (Dawes-Hoang et al., 2005; Manning and Rogers, 2014). The loss of pathway components results in defects in ventral furrow formation. However, the mesoderm still gets internalized, indicating that Fog signaling is important but not absolutely essential for mesoderm invagination (Costa et al., 1994).

Although pathway homologs were identified in the genomes of many different winged insects, recent comparative studies in the more basally branching fly *Chironomus*, in which Fog signaling plays only a minor role in mesoderm internalization, indicate that Fog signaling was recruited to increase the speed of gastrulation (Urbansky et al., 2016). This could be an adaptation to the very fast embryonic development of highly derived long-germ insects like *Drosophila melanogaster*.

This work focused on Fog signaling in the red flour beetle *Tribolium castaneum* which possesses a more ancestral mode of embryogenesis. The observations in embryos deficient of Fog signaling components showed that Fog signaling is also involved in mesoderm internalization and invagination of posterior endoderm homologous to the PMG primordium. This suggests indeed a conserved role of Fog signaling during gastrulation outside of dipterans. However, the defects in early morphogenetic movements after loss of *Tc-fog* are more multifaceted. *Tc-fog* is required for formation of the posterior amniotic fold as well as the positioning of the primordial germ cells. Furthermore, the presented data suggest an involvement of Fog signaling in cell shape changes other than apical constrictions, like the transition from a cuboidal to a flat squamous shape of extraembryonic cells during serosa spreading. In addition, cellularization defects in blastoderm embryos of *Tribolium* and *Gryllus* indicate an additional conservation of Fog signaling in stabilizing the cytoskeleton during formation of the blastoderm.

Material & Methods

7 Strains

The San Bernadino wildtype strain was used for RNAi injections and as wild-type control, if not specified otherwise. For selected experiments, different transgenic lines like pBA19 ("muscle-line") (Lorenzen et al., 2003), G04609 ("heart-line") (Koelzer et al., 2014), a nGFP strain (Sarrazin et al., 2012) and a Life-actin GFP line (Tania Vazques, van der Zee lab; unpublished) were used.

8 Animal keeping and embryo collection

The beetles are kept in boxes containing a mixture of 75% wheat flour "Extra" type 405 (Diamant Mehl) and 25% dark wheat flour type 1050 (Diamant Mehl) mixed with 25 g/kg dry yeast. To avoid fungal infestation, the flour is complemented with 0.3 g/kg fungicide (Fumagilin B, Medivet Pharmaceuticals Ltd). The animals are kept at 30°C, which ensures a generation cycle of around 30 days (Bucher, 2009).

For the collection of eggs, the beetles are transferred to special wheat flour ("Instant" Diamant Mehl, type 405). This flour has a grain size suited for efficient egg collection. Around 30 minutes after transfer to new flour, the females start to lay eggs. A certain stage of embryos is obtained as follows: After a specific egg-laying period the beetles are transferred to new flour and the eggs are further incubated at 30°C for several hours (minimum age) on fresh flour before they are collected (total time - 0.5 h = maximum age). Adult beetles are separated from flour and eggs by using sieves with a mesh size of 710 µm. The eggs are separated from the flour by using sieves with a mesh size of 300 µm.

For constant access to young beetles with high egg lay (EL) rates, one EL per week was set up. 1.2 g embryos were transferred to a box containing 1250 g of mixed flour. After 4 weeks the pupae can be sorted (males/females) for RNAi experiments. A turn-over of the stock was done every 3 months. Beetles from every-week-egg lays were collected and 23 g were transferred into new boxes containing 900 g of mixed flour.

9 Total RNA isolation

For the isolation of total RNA, *Tribolium* eggs are collected in a defined stage, dependent on subsequent experiments. Due to problems with the quality of isolated *Tribolium* RNA, the manufacture's protocol using TRIzol (Life Technologies) was modified (Stappert et al., 2016).

First, the eggs were washed with water followed by two minutes incubation in 50% DanKlorix (Colgate-Palmolive). To remove all remaining Klorix solution, they were again rinsed with clear water. The eggs were transferred into a 1.5ml RNase-free reaction tube and shock frozen in liquid nitrogen (-80°C) for later processing or treated with TRIzol for direct RNA isolation. The eggs were homogenized in 500 µl TRIzol using a pestle. It should be noticed that working on ice is important to avoid degradation of the RNA. After centrifugation for 10 min (12,000 x g at 4°C) the supernatant was transferred into a new reaction tube and mixed with additional 500 µl TRIzol (total volume of 1ml). The samples were incubated for 5 min at room temperature before 100 µl chloroform were added. The tubes were shaken thoroughly by hand for 15 seconds and incubated for 2-3 minutes at RT. The phases were separated by 15 minutes centrifugation at 4°C (12,000 x g). The upper aqueous phase (containing the RNA) was transferred into a new reaction tube and the contained RNA was precipitated by adding 40 µl 3M NaAc pH5.2 and 800µl room temperature 100% EtOH followed by incubation for at least 30 min at -80°C. After centrifugation (20 min, full speed at 4°C), the RNA pellet was purified from contaminations (TRIzol or polysaccharides from flour) by different washing steps. 800 µl 3M NaAc pH5.2 were added and samples were incubated for 5 minutes at RT. After centrifugation (15 min, full speed, 4°C) the pellet was washed with 800 µl room temperature 70% EtOH, followed again by incubation for 5 minutes at RT and centrifugation (15 min, full speed, 4°C). The washing steps were repeated before the pellet was resuspended in 21 µl RNase-free H₂O. The concentration and 260/280 and 260/230 ratios were checked on a NanoDrop2000 (Thermo Scientific). The samples were stored at -80°C.

10 cDNA synthesis

Complementary DNA (cDNA) is synthesized from RNA by the enzyme reverse transcriptase and was used as template for probe and dsRNA synthesis as well as qRT-PCR. Due to an optimized protocol for generation of first-strand cDNA for qRT-PCR, the SuperScript VILO cDNA Synthesis Kit (Life Technologies) was used according to the manufacture's manual.

11 Primer design

Primers are required to amplify DNA by PCR. Primers are DNA oligonucleotides, which bind to the DNA which should be amplified. Polymerases can bind to the primers and copy the sequence selected by a forward (5') and a reverse primer (3'). The online application Primer3 version 0.4.0 (<http://bioinfo.ut.ee/primer3-0.4.0/>) (Untergasser et al., 2012) was used for primer design. For *in-situ* probes or dsRNA synthesis the fragment size was set to 500 bp to 800 bp. The primer size was set to 20-24 bp. Furthermore, the primers should show a low self- and cross-complementarity and the GC content should be <50%. The suggested primers were tested for specificity by BLASTing them to the *Tribolium* genome. Appropriate primers should bind to a unique sequence without any mismatches. The primer design for the *in-situ* hybridization screen and dsRNA synthesis of the differential expression analysis was based on the *Tribolium* Tcas 3.0 annotation/ OGS 2 (<http://bioinf.uni-greifswald.de/gb2/gbrowse/tribolium/>). The primers used for analysis of the Fog signaling pathway were designed by using the new *T. castaneum* genome assembly Tcas 5.2/ OGS 3. All primers used in this work are listed in the Appendix A, B, C and G.

12 Standard Polymerase Chain Reaction (PCR)

Polymerase Chain reaction is a method for *in vitro* amplification of a selected piece of DNA using Taq polymerase (Mullis, 1990). Taq polymerase is derived from the thermophilic bacterium *Thermus aquaticus* and is able to resist the high temperatures that are required for denaturation of double stranded DNA (dsDNA) into single stranded DNA (ssDNA). Denaturation takes place at 94°C. Primers are used to specify the target DNA and to enable binding of the polymerase. For amplification of a specific DNA fragment, two primers (5' and 3') are needed. Annealing of the primers to single DNA strands takes place at 55-65°C. Too low temperatures result in unspecific binding of the primers. The last step enables efficient binding of polymerase to the primers and elongation of the complement strand. Elongation of the new strand takes place at 72°C. To efficiently amplify the DNA, all three steps are repeated ~35 times.

Reaction mix for standard PCR

10 µl Red Taq mix, Sigma
7 µl H₂O
1 µl cDNA
1 µl specific 5' primer (10 µM)
1 µl specific 3' primer (10 µM)

Cycler program for standard PCR

Denaturation	5 min	94°C	} 35x
Denaturation	30 sec	94°C	
Annealing	30 sec	55-57°C	
Elongation	1 min	72°C	
Elongation	5 min	72°C	

13 Gel electrophoresis

To confirm the presence and correct size of PCR products, 5 µL of the reaction was run on a 1% agarose gel run in 0.5x TRIS-Acetate-EDTA-Buffer (TAE) at 135 V. To visualize the DNA, 1-2 drops of 0.025% ethidium bromide solution per 50 ml agarose were used. The size of the bands was determined using 2.5 µL of the Smart Ladder MW 1700-10 (Eurogentec).

50 x TAE
2 M TRIS
0.05 M EDTA
In H₂O (adjusted to pH 8.0)

14 *In-situ* hybridization (ISH)

In-situ hybridization is a method to detect the presence and location of mRNA in different tissues. The gene specific mRNA is hybridized with a complementary mRNA-probe. The probe is for example labeled with Digoxigenin (DIG) which is detected by using an anti-DIG antibody (anti-DIG-AB). The enzyme alkaline phosphatase is conjugated with the anti-DIG-AB and converts a substrate like NBT/BCIP (nitro blue tetrazolium chloride/5-bromo-4-chlor-3-indolyl-phosphate) into a purple dye. The staining indicates the spatial expression of the gene of interest.

14.1 Generation of mRNA probes

14.1.1 Two-step Polymerase Chain Reaction

A two-step polymerase chain reaction (PCR) strategy was used to amplify DNA as template for antisense mRNA probe synthesis. To detect complementary mRNA in subsequent *in-situ* hybridizations (ISH), the DNA template was equipped with a T7 promotor. To amplify DNA of the gene of interest, first a standard PCR (denaturation at 94°C, annealing at 57°C, elongation at 72°C, 35 cycles) using cDNA as template was performed. A linker sequence was attached to the gene specific primers used for the 1. PCR. A second PCR was performed using only one of the gene specific primers (3' for sense/5' for antisense) and one T7 universal primer that contains the T7 promotor sequence and is able to bind to the linker sequence which was attached during the 1. PCR. The universal primer binds to a specific sequence which is attached to the 5' end of the gene specific primer (T7 linker) and was amplified during the first PCR. Cycling parameters for the second PCR reaction are the same as for the first PCR. The amplicon from the second PCR is used as template for RNA probe synthesis.

Reaction mix for sense probe

10 µl Red Taq mix, Sigma
7 µl H₂O
1 µl cDNA
1 µl 5' T7 universal primer (10 µM)
1 µl specific 3' primer (10 µM)

Reaction mix for antisense probe

10 µl Red Taq mix, Sigma
7 µl H₂O
1 µl cDNA
1 µl specific 5' primer (10 µM)
1 µl 3' T7 universal primer (10 µM)

Linker sequences attached to the gene specific primers

5' T7 linker: ggccgcgg

3' T7 linker: cccggggc

5' T7 universal primer: gagaattc taatacgactcactatag ggccgcgg

3' T7 universal primer: agggatcc taatacgactcactataggg cccggggc

14.1.2 Probe synthesis

To label the probe during synthesis UTP-Digoxigenin (DIG) (Roche) was used. 3 µl of the amplicon from the second PCR were mixed with 7 µl of T7 master mix and incubated for 4 hours at 37°C. The reaction was stopped by adding 15 µl H₂O and 25 µl 2x Stop solution (0.2 M NaAc, 1% HAc; pH 6.0). For precipitation 2.5 µl tRNA (20 mg/ml; Roche), 5 µl LiCl (4M) and 150 µl 100% EtOH were added. The probes were incubated for at least 30 minutes at -20°C followed by a full speed centrifugation at room temperature for 30 minutes. The RNA pellet was dried for 5 minutes before it was resuspended in 40 µl 50% formamide, 2x SSC. The probes were stored at -20°C. The correct size of the probes was tested on a 1% agarose gel.

T7 master mix

3.5 µl RNase-free H₂O
0.25 µl RNase inhibitor
1 µl 10x T7 reaction buffer
1 µl DIG labelling mix
1 µl T7 polymerase

14.2 Embryo fixation

Tribolium eggs were rinsed with tap water to remove dirt and left-over flour. For dechorionization the eggs were put for 2 min in 50% DanKlorix (Colgate-Palmolive). The Klorix was then thoroughly washed away with tap water. To fix the embryos, they were incubated in fixation solution (2 ml 10% formaldehyde, 3 ml PBS, 5 ml heptane), shaking at 120 rpm, for 45 min to 1.5 h. The embryos were devitellinized by methanol (MeOH) shock or by hand dissection. The embryos can be stored at -20°C.

14.3 Detection of mRNA expression

Embryos were transferred from MeOH into PBST (first 2:1, then 1:2 MeOH:PBST), washed with PBST (2 times, 5 min each), fixed in 5% PFA/PBST for 30 min. The PFA was washed away with 1xPBST (four times, 5 min each). The embryos were slowly transferred into hybridization solution I (first 1:1 hyb sol I:1xPBST for 10 min, then 100% hyb sol I for 10 min) and then pre-hybridized in hybridization solution II at 65°C for 1 h. 4 µl probe, specific for the mRNA of interest, was diluted in 196 µl hybridization solution II and incubated with the embryos overnight at 60 °C while rotating. The probe was washed away by washing four times for 5 min, and four times for 30 min with hybridization solution I at 60 °C. The embryos were then transferred into PBST (first 2:1, then 1:2, hyb sol I:1xPBST, at 60 °C) and washed for 10 min with PBST (room temperature). For blocking, embryos were incubated two times for 30 min in PBST that contains bovine serum albumin (BSA, 100 µl/ml) and normal goat serum (NGS, 30 µl/ml). Then, anti-digoxigenin antibody coupled with alkaline phosphatase was added in a final concentration of 1:4000 and incubated with the embryos overnight at 4 °C while rotating. The next day the embryos were rinsed by washing three times for 5 min and three times for 15 min with PBST and three times for 5 min with AP-buffer. For the color reaction 8 µl NBT/BCIP (nitro blue tetrazolium chloride/5bromo-4chlor-3indolyl-phosphate; Roche) solution in 400 µl AP-buffer were added to the embryos. The color reaction was observed and stopped by washing three times with PBST when background staining started to develop. The staining was then fixed by incubating the embryos for 30 min in 5% PFA in PBST. Background staining was in some cases removed by incubating the embryos for ≥20 min in 100% ethanol (EtOH). The EtOH was washed away by two to three washes with 1xPBST. The embryos were embedded into VECTASHIELD Mounting Medium with DAPI (Vector Laboratories).

10x PBS (Phosphate Buffered Saline)

dissolve in 800 ml H₂O

80 g NaCl

2 g KCl

14.4 g Na₂HPO₄

2.4 g KH₂PO₄

Adjust to pH 7.4

fill up to 1 l with millipore H₂O (autoclave)

1x PBST

5 ml 10x PBS

500 ml 20% Tween

fill up to 50 ml with millipore H₂O

Hybridization Solution I

25 ml formamide

12.5 ml 20xSSC

50 µl heparine (50 mg/ml)

250 µl 20% Tween20

fill up to 50 ml with millipore H₂O

Hybridization Solution II

25 ml formamide

12.5 ml 20xSSC

50 µl heparine (50 mg/ml)

250 µl 20% Tween20

500 µl salmon sperm (100 mg/ml)

fill up to 50 ml with millipore H₂O

AP-buffer

1 ml TRIS-HCl (pH 9.5)

500 µl 1M MgCl₂

200 µl 5M NaCl

50 µl 20% Tween20

fill up to 50 ml with millipore H₂O

Blocking Solution

100 µl BSA (1 mg/ml in PBS)

.30 µl NGS (60 mg/ml)

fill up to 1 ml with 1xPBST

15 Double *in-situ* hybridization (dISH)

This protocol was modified from (Schinko et al., 2009). The amount of each probe to use is a critical variable that must be optimized for every probe preparation. DIG-labeled probes detected by NBT/BCIP are more sensitive than fluorescein-labeled probes detected by INT/BCIP. Thus, best results can be expected by detect the stronger signal first, using a fluorescein-labeled probe visualized by NBT/BCIP (Roche) color reaction. Second, the weaker signal should be detected by a DIG-labeled probe stained by FAST Red (Roche). Fast red staining is both, colormetric (red) and fluorescent (orange).

Day 1 of the double *in-situ* hybridization protocol is similar to day 1 of the standard ISH protocol (see above). However, both mRNA probes (2 µl each) were mixed and diluted in 196 µl hybridization solution II and incubated with the embryos overnight at 60 °C while rotating.

Also the second day resembles mainly the protocol for single ISH. Dilute the antibody for the first staining (anti-DIG-AP) was diluted 1:2000 in blocking solution. 500 µl of diluted antibody was added to the embryos. The samples were incubated over night at 4°C (or for 1 h at room temperature) on a rotator.

As mentioned above, best results were achieved by staining with NBT/BCIP first. Thus, the next day the embryos were rinsed by washing three times for 5 min and three times for 15 min with PBST and three times for 5 min with AP-buffer (see single ISH protocol). 8 µl NBT/BCIP solution were diluted in 400 µl AP-buffer and were added to the embryos. The reaction was stopped by both, a decrease in pH and dilution of the staining buffer. The alkaline phosphatase was deactivated by washing the embryos three times for 20 min in glycine-HCl (100 mM glycine-HCl, pH 2.3) on a rotator. Afterwards the inactivation buffer (IB) was removed by washing the embryos three times 20 min in 1xPBST. To remove the unspecific background staining, the embryos can be incubated for 15-30 min in 100% EtOH on a rotator, followed by a slow retransfer into PBST. After another round of blocking (2x 30 min, rotator) on room temperature, the second antibody was added. If the DIG-labeled probe was used as the first stain, then use the fluorescein-labeled probe here. Dilute the antibody for the second staining (anti-fluorescein-AP) was diluted 1:2000 in blocking solution and 500 µl of the diluted antibody was added to the embryos. The embryos were incubated in the dark over night at 4°C or for 1 h at room temperature on a rotator.

The second color reaction was performed on day 4. The embryos were washed three times for 5 min and three times for 15 min with PBST. Afterwards, the embryos were prepared for the staining by washing them three times for 10 min in 0.1 M Tris-HCl (pH 8.0) solution. For staining, 1 Fast Red tablet was dissolved in 2 ml of 0.1 M Tris-HCl solution (pH 8.0). The samples should be incubated in the dark at room temperature until the staining is strong and distinct. If the staining is weak or absent after 3 h, continue staining overnight at 4°C. The color reaction is stopped by washing the embryos 3 times 10 min in PBST. EtOH should not be used to remove Fast Red background staining, as also the specific staining would be removed! The embryos were mounted with VECTASHIELD Mounting Medium with DAPI (Vector Laboratories).

Inactivation buffer (100 mM glycine-HCl)

11.1 g Glycine-HCl
800 ml millipore H₂O
adjust to pH 2.3
fill up to 1 l with millipore H₂O

16 Fluorescence staining

16.1 Phalloidin staining

Dechorionated, fixed embryos (not treated with methanol) were devitellinized by hand and washed in PBST (3 times, 5 min each). The embryos were post-fixed in 350 μ l 5% PFA/PBST for 20 min. The PFA was removed by five 5 min washes with PBST. After 1 h incubation in 500 μ l blocking solution (100 μ l BSA (100 μ g/ml), 250 μ l NGS (30 μ l/ml), 5 μ l 20% Tween, 5 ml 1xPBS), Alexa Fluor 555/568 Phalloidin (Molecular Probes, life technologies) was added (1:50 in blocking solution) and the embryos were incubated over night at 4°C. Phalloidin was removed by washes in PBST (5 times, 10 min each). The embryos were covered with VECTASHIELD Mounting Medium with DAPI or for fluorescent staining (Vector Laboratories).

For Phalloidin staining on cryosections it should be noticed that best results were generated by performing the Phalloidin staining protocol directly on the sections. Therefore, a humidity chamber covered with aluminum foil (light protection) was used. To ensure a proper humidity and to suck up the used solutions the bottom of the chamber was covered with paper towels. To avoid contact of the samples with the already used solutions, the slides were placed on a grid (see Fig. A). During the washing steps the chamber was placed on a shaker. The sections were then covered in VECTASHIELD Mounting Medium for fluorescence staining (Vector Laboratories). One spacer on each side was used to avoid destruction of the samples by the coverslip.

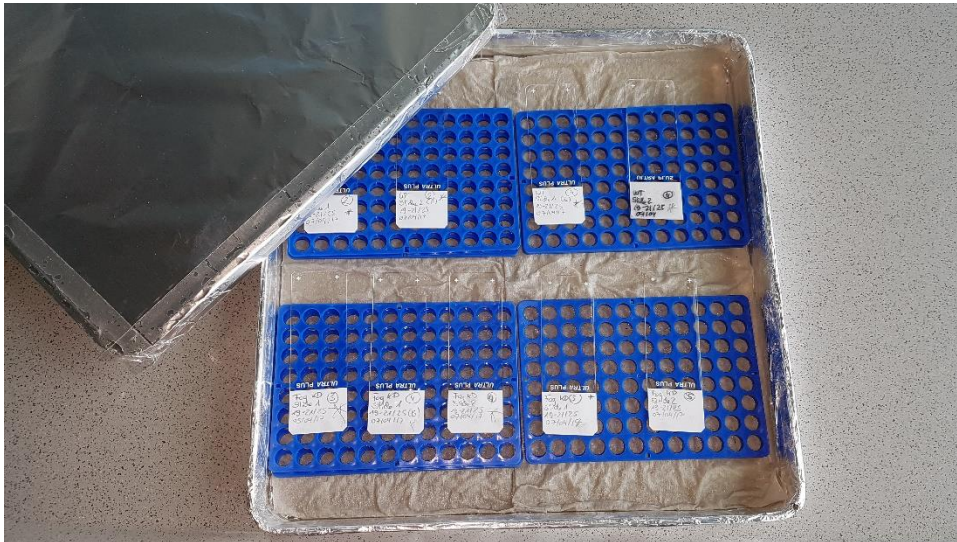


Figure A: Humidity chamber for Phalloidin staining on cryosections.

The samples are protected from light by covering the chamber in aluminum foil. The humidity is kept by paper towels soaked with the washing solutions. The samples are placed on a slightly higher grid to avoid contamination with already used solutions.

16.2 Nuclear staining

16.2.1 DAPI staining

Dechorionated, fixed embryos were transferred from methanol to PBST (PBS supplemented with 1 % Tween20) and washed three times for 5 min with PBST. Then, the embryos were embedded in VECTASHIELD Mounting Medium with DAPI (4',6-Diamidin-2-phenylindol) (Vector Laboratories).

16.2.2 Sytox staining

Dechorionated and fixed embryos were stained by ~30 min incubation in PBST with 1:5000 Sytox Green (Thermo Fisher Scientific). During the staining the embryos should be kept in the dark at 4°C. After several washing steps with PBST, the embryos can be mounted in VECTASHIELD Mounting Medium for fluorescence staining (Vector Laboratories). For nuclear staining of cryosections, the protocol was performed on slides in a humidity chamber (see Phalloidin staining).

17 Generation of knockdown embryos by RNA interference (RNAi)

RNA interference is a natural defense mechanism against RNA-viruses. Furthermore, it is involved in gene regulation and transposal control. In developmental biology it used as a popular tool for transient gene knockdown. dsRNA that is present in cells silences gene expression by degradation of mRNA. Long dsRNA from an exogenous source like viruses is cut by Dicer, an RNase III enzyme, into small fragments (Miller et al., 2012). The produced small interfering RNA (siRNA) is incorporated into the RNA-induced silencing complex (RISC) which binds mRNA complementary to the siRNA and causes mRNA cleavage through the action of the catalytic Argonaute proteins (Hammond et al., 2001). The cleavage of mRNA reduces the amount of mRNA available for translation and thus phenocopies a loss of function mutation (Hammond et al., 2001; Miller et al., 2012). This mechanism can be experimentally employed for the specific knockdown of target genes by inserting long dsRNA molecules (about 200 bp to 1.5 kb) into cells, whereas the dsRNA molecules correspond to part of the coding region of the respective target gene.

17.1 Production of double-stranded RNA (dsRNA)

17.1.1 2. PCR for amplification of a dsRNA template

Similar to the generation of RNA probes for *in-situ* hybridization we used a PCR-based approach for dsRNA synthesis. The linker sequences attached to the fragments during the first PCR serve as binding sites for the T7 universal primer. In contrast to the second PCRs used for probe synthesis, generation of dsRNA requires both T7 3' and T7 5' primers. Cycling parameters for the PCR reaction are the same as used for standard PCR. The amplicons had a size between 500 bp and 800 bp.

17.1.2 dsRNA synthesis

For synthesis of dsRNA the MEGAscript T7 Kit (Life Technologies) was used. 12 µl of the T7 master mix is added to 8 µl template from the second PCR. The reaction mix is placed on 37°C for 4 h or overnight. To stop the reaction 115 µl RNase-free water and 15 µl ammonium acetate stop solution were added before the dsRNA was purified by adding 150 µl phenol:chloroform. The reaction was vortexed for 1 minute followed by 5 minutes centrifugation (5000 rpm). The upper, aqueous layer was transferred into a new tube avoiding the interface. dsRNA was precipitated by adding 150 µl isopropanol followed by incubation for at least 30 minutes at 80°C. The sample was spun at full speed in a refrigerated centrifuge (4°C) for 15 minutes before the supernatant was decanted and the dsRNA pellet was

washed with 300 μ l 70% ethanol. After another full speed centrifugation for 5 minutes at 4°C the pellet dried for 5 minutes before it was resuspended in 21 μ l RNase-free H₂O. To check the quality of the dsRNA, 1 μ l of the dsRNA can be separated by gel electrophoresis. If multiple bands are observed, the reaction can be boiled (96°C, 30 sec) to resolve secondary structures. The concentration of the dsRNA was checked with a NanoDrop 2000 (Thermo Scientific).

18 Adult or pupal injections (pRNAi)

Two possibilities for parental RNAi (pRNAi) in beetles were used: Either the injection into female pupae or the injection into virgin adult females (Bucher et al., 2002; Posnien et al., 2009). It should be noticed that knockdown of some genes results in sterility of the beetles, if they are injected as pupae. If sterility occurs, it is advisable to inject into adult females or to lower the concentration of the dsRNA. The pupae or adult females (adults were first anesthetized on ice) were fixed with their abdomen on double sided tape (Doppelklebeband Fotostrip, transparent 05338, Tesa). The dsRNA was diluted to a final concentration of 1 μ g/ μ l. For better visualization of the injected volume dsRNA solution can be mixed with phenol red (1 μ l in 10 μ l dsRNA). For injection of the dsRNA, thin glass needles were generated from capillaries (Hilgenberg) by a laser needle puller (Sutter Instrument Co. Model P-2000). The dsRNA was loaded to the needle with microloader tips (Eppendorf). The tip of the needle was opened using a razor blade. After one day of regeneration time, injected females were pooled with males at a ratio of 4:1. The RNAi effect can last from a few days to several weeks and can be checked by DAPI staining, ISH or qRT-PCR. To account for any bias caused by the injection procedure itself (increase of death rate or number of embryos showing defects or the upregulation of immune- and stress-related genes), dsRNA of an exogenous gene (e.g. *dsRed* or *eGFP*) can be used as control. However, the results of our differential transcriptome analysis suggest that there is no significant upregulation of RNAi-related genes or genes involved in immune- and stress response caused by the injection procedure itself (Stappert et al., 2016). Thus, injection of H₂O or using an equal amount of uninjected wildtype beetles should be sufficient as control.

Settings for needle puller

Heat = 400
Filament = 4
Velocity = 60
Delay = 255
Pull = 150

19 Embryonic injections (eRNAi)

Especially for genes showing a sterility effect upon dsRNA injection into female pupae or even adult beetles, it might be necessary to generate knockdowns by embryonic injection (Schinko et al., 2009). Furthermore, eRNAi can be used for timed gene knockdown in a specific embryonic stage and thus for analysis of a specific part of the phenotype (Horn and Panfilio, 2016). The following protocol was adapted from the embryonic injections protocol by (Benton et al., 2013). As the needles (Hilgenberg) for embryonic injections need to be shorter and less flexible than for pupal or adult injections, a different program for pulling the needles was used (see below). Afterwards the needles were opened by polishing them for 15 to 30 min on a grinder (Narishige, EG-44). The opened needle was cleaned by rinsing it with some EtOH (if the EtOH gets sucked up into the tip, the needle is open). The embryos were dechorionated by washing them three times with 25% DanKlorix for 2bmin followed by careful washing with tap water. For the subsequent injection procedure, the embryos were lined up in with the anterior facing the edge of the slide. Due to the evaporation of the water surrounding the embryos, they stick to the slide. To avoid dehydration of the embryos and for subsequent live-imaging, the embryos were covered with halocarbon oil 700 (Sigma; CAS 9002-83-9). If the embryos should be fixed and devitellinized by MeOH shock (for staining), they were lined up on parafilm and were not covered with oil. After injection of the embryos, the parafilm were cut into stripes transferred into reaction tubes containing fixation solution. After 25 min fixation at room temperature, the parafilm dissolved and the embryos could be treated with MEOH.

Settings for needle puller

Heat = 325
Filament = 4
Velocity = 50
Delay = 255
Pull = 150

Settings for microinjector

Time = 0.5-1.00
Pressure = 30-60 (highly dependent on needle)
Balance = 0.5 (const. pressure)
→ settings should be adjusted for each needle

20 Cuticle preparation

Cuticle preparations of larva shortly after hatching, is a simple method to analyze morphological defects after gene knockdown by pRNAi. Eggs were collected and incubated for 72 h at 30°C. The dechorionated embryos were embedded in Hoyer's medium 1:1 mixed with lactic acid. Careful pressure on the coverslip helps to ensure that the Hoyer's is also reaching unhatched larva in the eggs. After one night at 60°C the larval tissue is digested and just the cuticles are left. The cuticles were visualized using the Zeiss Axioplan2 microscope (dark field).

Hoyer's medium

0.6 g/ml Arabic gum
1.2 M chloral hydrate
217 mM glycerol

21 Cryosections

The embedding agar (2 g agarose and 15 g sucrose in 100 ml 1xPBS) was melted using the microwave. The embryos were then embedded in the agarose in a petri dish (make sure that the agar surrounds the embryo from all sides!). After the agarose cooled down, blocks of agarose containing the embryos (1.0 cm x 0.5 cm x 0.5 cm) were cut out. To make the cells more permeable, the embedded embryos were incubated overnight in sucrose solution (15 g sucrose in 50 ml 1xPBS). In addition, the treatment of the embryos with sucrose solution helps to attach the embryo to the agarose. The tissue specimen was bound to the specimen block by using Tissue-Tek O.C.T.TM Compound (Sakura). After shock freezing the samples in -80°C isopentane, the embryos were sliced at -20°C in intervals of 30 µm (Leica CM 1850 Cryostat) and transferred to Superfrost Ultra Plus microscope slides (Thermo Scientific). The sections were dried overnight at room temperature and were stored on RT or at -20°C for long term storage.

Embedding medium

2 g agarose
15 g sucrose
in 100 ml 1xPBS
heated in microwave

Sucrose solution

15 g sucrose
in 50 ml 1xPBS

22 Microscopy

All embryos were covered with a coverslip using two spacers (18x18 mm coverslips cut in half). Pictures of non-fluorescent ISH stainings were taken with a “SteREO Lumar.V12” stereomicroscope (Zeiss) or a AxioPlan2 microscope (Zeiss) operated by the AxioVision 4.8.2.0 software. Pictures of embryos stained with fluorescent dyes (Sytox Green, Phalloidin) were taken using an “Axio Imager 2” microscope equipped with an “ApoTome 2” (Zeiss). The Z stacks were combined to a projection using the Zen2 Blue software, AxioVision 4.8.2.0 or Image J. Pictures of cross- and longitudinal sections stained with Phalloidin and Sytox Green were imaged using the Zeiss LSM700 with Imager.M2 and analyzed with the Zen 2 Black Software.

All pictures were processed using Adobe Photoshop CS4 for brightness and contrast as well as black or white balance. Changes were always applied to the whole picture.

23 Live-imaging

Eggs for live-imaging were treated very gently especially during chorion removal as described in section 8.2. Keep the eggs in tap water afterwards to avoid desiccation. For mounting, the eggs were placed with a fine brush from the water surface onto a coverslip and lined up in a row. After approximately 2 minutes air-drying the embryos stick to the glass and can be covered with halocarbon oil 700 (Sigma; CAS 9002-83-9). For subsequent imaging the coverslip with the embryos was attached to a slide using two spacers (18x18 mm coverslips cut in half). Embryogenesis was visualized at room temperature using the Zeiss AxioImager.Z2 in combination with an Apotome.2 module and a movable stage (Zen 2 Blue) or the Applied Precision DeltaVision RT microscope.

References

- Adams, M.D., Celniker, S.E., 2000. The genome sequence of *Drosophila melanogaster*. *Science* 287, 2185-2195.
- Anderson, D. T. (1972) The development of hemimetabolous insects. In S. J.Counce and C. H.Waddington (eds): *Developmental Systems: Insects*. Vol. 1. London: Academic Press, pp. 95–163.
- E. Bock „Bildung und Differenzierung der Keimblätter bei *Chrysopa perla*“ (1939) *Z. Morph. Ökol. Tiere* 35: 615-702.
- Aranda, M., Marques-Souza, H., Bayer, T., Tautz, D., 2008. The role of the segmentation gene hairy in *Tribolium*. *Dev Genes Evol* 218, 465-477.
- Barrett, K., Leptin, M., Settleman, J., 1997. The Rho GTPase and a putative RhoGEF mediate a signaling pathway for the cell shape changes in *Drosophila gastrulation*. *Cell* 91, 905-915.
- Beermann, A., Schroder, R., 2008. Sites of Fgf signalling and perception during embryogenesis of the beetle *Tribolium castaneum*. *Dev Genes Evol* 218, 153-167.
- Beiman, M., Shilo, B.Z., Volk, T., 1996. Heartless, a *Drosophila* FGF receptor homolog, is essential for cell migration and establishment of several mesodermal lineages. *Genes Dev* 10, 2993-3002.
- Benton, M.A., Akam, M., Pavlopoulos, A., 2013. Cell and tissue dynamics during *Tribolium* embryogenesis revealed by versatile fluorescence labeling approaches. *Development* 140, 3210-3220.
- Benton, M.A., Kenny, N.J., Conrads, K.H., Roth, S., Lynch, J.A., 2016. Deep, Staged Transcriptomic Resources for the Novel Coleopteran Models *Atrachya menetriesi* and *Callosobruchus maculatus*. *PLoS One* 11, e0167431.
- Berghammer, A.J., Weber, M., Trauner, J., Klingler, M., 2009. Red flour beetle (*Tribolium*) germline transformation and insertional mutagenesis. *Cold Spring Harb Protoc* 2009, pdb prot5259.
- Berns, N., Kusch, T., Schroder, R., Reuter, R., 2008. Expression, function and regulation of Brachyenteron in the short germband insect *Tribolium castaneum*. *Dev Genes Evol* 218, 169-179.
- Bonn, S., Furlong, E.E., 2008. cis-Regulatory networks during development: a view of *Drosophila*. *Curr Opin Genet Dev* 18, 513-520.
- Bottcher, R.T., Niehrs, C., 2005. Fibroblast growth factor signaling during early vertebrate development. *Endocr Rev* 26, 63-77.
- Brigaud, I., Duteyrat, J.L., Chlasta, J., Le Bail, S., Couderc, J.L., Grammont, M., 2015. Transforming Growth Factor beta/activin signalling induces epithelial cell flattening during *Drosophila* oogenesis. *Biol Open* 4, 345-354.
- Brody, T., Cravchik, A., 2000. *Drosophila melanogaster* G protein-coupled receptors. *J Cell Biol* 150, F83-88.
- Broihier, H.T., Moore, L.A., Van Doren, M., Newman, S., Lehmann, R., 1998. zfh-1 is required for germ cell migration and gonadal mesoderm development in *Drosophila*. *Development* 125, 655-666.

- Brown, S.J., Patel, N.H., Denell, R.E., 1994. Embryonic expression of the single *Tribolium* engrailed homolog. *Developmental genetics* 15, 7-18.
- Bucher, G., 2009. The beetle book. Protocol Collection, 1-34.
- Bucher, G., Scholten, J., Klingler, M., 2002. Parental RNAi in *Tribolium* (Coleoptera). *Curr Biol* 12, R85-86.
- Busby, M.A., Stewart, C., Miller, C.A., Grzeda, K.R., Marth, G.T., 2013. Scotty: a web tool for designing RNA-Seq experiments to measure differential gene expression. *Bioinformatics* 29, 656-657.
- Caamano, J., Hunter, C.A., 2002. NF-kappaB family of transcription factors: central regulators of innate and adaptive immune functions. *Clin Microbiol Rev* 15, 414-429.
- Carroll, S.B., 2005. Evolution at two levels: on genes and form. *PLoS Biol* 3, e245.
- Casal, J., Leptin, M., 1996. Identification of novel genes in *Drosophila* reveals the complex regulation of early gene activity in the mesoderm. *Proc Natl Acad Sci U S A* 93, 10327-10332.
- Chang, Z., Price, B.D., Bockheim, S., Boedigheimer, M.J., Smith, R., Laughon, A., 1993. Molecular and genetic characterization of the *Drosophila* tartan gene. *Dev Biol* 160, 315-332.
- Chen, G., Handel, K., Roth, S., 2000. The maternal NF-kappaB/dorsal gradient of *Tribolium castaneum*: dynamics of early dorsoventral patterning in a short-germ beetle. *Development* 127, 5145-5156.
- Choe, C.P., Brown, S.J., 2007. Evolutionary flexibility of pair-rule patterning revealed by functional analysis of secondary pair-rule genes, paired and sloppy-paired in the short-germ insect, *Tribolium castaneum*. *Dev Biol* 302, 281-294.
- Coffman, C.R., 2003. Cell migration and programmed cell death of *Drosophila* germ cells. *Annals of the New York Academy of Sciences* 995, 117-126.
- Conesa, A., Madrigal, P., Tarazona, S., Gomez-Cabrero, D., Cervera, A., McPherson, A., Szczesniak, M.W., Gaffney, D.J., Elo, L.L., Zhang, X., Mortazavi, A., 2016. A survey of best practices for RNA-seq data analysis. *Genome Biol* 17, 13.
- Conrads, K.H., Master Thesis 2015. Analysis of Fog signaling in *Nasonia vitripennis*. University of Cologne.
- Costa, M., Wilson, E.T., Wieschaus, E., 1994. A putative cell signal encoded by the folded gastrulation gene coordinates cell shape changes during *Drosophila* gastrulation. *Cell* 76, 1075-1089.
- Dassen, M., Bachelor Thesis 2016. Investigation of potential dorso-ventral patterning genes in *Tribolium castaneum*.
- Davis, G.K., Jaramillo, C.A., Patel, N.H., 2001. Pax group III genes and the evolution of insect pair-rule patterning. *Development* 128, 3445-3458.
- Dawes-Hoang, R.E., Parmar, K.M., Christiansen, A.E., Phelps, C.B., Brand, A.H., Wieschaus, E.F., 2005. folded gastrulation, cell shape change and the control of myosin localization. *Development* 132, 4165-4178.

- De Renzis, S., Yu, J., Zinzen, R., Wieschaus, E., 2006. Dorsal-ventral pattern of Delta trafficking is established by a Snail-Tom-Neuralized pathway. *Dev Cell* 10, 257-264.
- De Robertis, E.M., Kuroda, H., 2004. Dorsal-ventral patterning and neural induction in *Xenopus* embryos. *Annu Rev Cell Dev Biol* 20, 285-308.
- Ephrussi, A., Lehmann, R., 1992. Induction of germ cell formation by oskar. *Nature* 358, 387-392.
- Ewen-Campen, B., Srouji, J.R., Schwager, E.E., Extavour, C.G., 2012. Oskar predates the evolution of germ plasm in insects. *Curr Biol* 22, 2278-2283.
- Extavour, C.G., Akam, M., 2003. Mechanisms of germ cell specification across the metazoans: epigenesis and preformation. *Development* 130, 5869-5884.
- Fleig, R., Walldorf, U., Gehring, W.J., Sander, K., 1988. *In situ* localization of the transcripts of a homeobox gene in the honeybee *Apis mellifera* L. (Hymenoptera). *Roux Arch Dev Biol* 197, 269-274.
- Fleig, R., K. Sander, (1986) „Embryogenesis of the honeybee *Apis mellifera* L. (Hymenoptera: Apidae): a SEM-study“ *Int. J. Insect Morph. Embryol.* 15, 449-462.
- Fleig, R., K Sander, “Honeybee morphogenesis: Embryonic cell movements shape the larval body” (1988) *Development* 103: 525-534.
- Fonseca, R.N., Lynch, J.A., Roth, S., 2009. Evolution of axis formation: mRNA localization, regulatory circuits and posterior specification in non-model arthropods. *Curr Opin Genet Dev* 19, 404-411.
- Fortini, M.E., Lai, Z.C., Rubin, G.M., 1991. The *Drosophila* Zfh-1 and Zfh-2 Genes Encode Novel Proteins Containing Both Zinc-Finger and Homeodomain Motifs. *Mechanisms of Development* 34, 113-122.
- Frey, N., Master Thesis 2013. "Identification of new dorso-ventral patterning genes by differential transcriptome analyses in *Tribolium castaneum*".
- Fuse, N., Yu, F., Hirose, S., 2013. Gprk2 adjusts Fog signaling to organize cell movements in *Drosophila* gastrulation. *Development* 140, 4246-4255.
- Gilles, A.F., Averof, M., 2014. Functional genetics for all: engineered nucleases, CRISPR and the gene editing revolution. *Evodevo* 5, 43.
- Gilles, A.F., Schinko, J.B., Averof, M., 2015. Efficient CRISPR-mediated gene targeting and transgene replacement in the beetle *Tribolium castaneum*. *Development* 142, 2832-2839.
- Gisselbrecht, S., Skeath, J.B., Doe, C.Q., Michelson, A.M., 1996. heartless encodes a fibroblast growth factor receptor (DFR1/DFGF-R2) involved in the directional migration of early mesodermal cells in the *Drosophila* embryo. *Genes Dev* 10, 3003-3017.
- Goltsev, Y., Fuse, N., Frasch, M., Zinzen, R.P., Lanzaro, G., Levine, M., 2007. Evolution of the dorsal-ventral patterning network in the mosquito, *Anopheles gambiae*. *Development* 134, 2415-2424.
- Gould, A.P., Brookman, J.J., Strutt, D.I., White, R.A., 1990. Targets of homeotic gene control in *Drosophila*. *Nature* 348, 308-312.

- Hacker, U., Perrimon, N., 1998. DRhoGEF2 encodes a member of the Dbl family of oncogenes and controls cell shape changes during gastrulation in *Drosophila*. *Genes Dev* 12, 274-284.
- Hammond, S.M., Boettcher, S., Caudy, A.A., Kobayashi, R., Hannon, G.J., 2001. Argonaute2, a link between genetic and biochemical analyses of RNAi. *Science* 293, 1146-1150.
- Handel, K., Basal, A., Fan, X., Roth, S., 2005. *Tribolium castaneum* twist: gastrulation and mesoderm formation in a short-germ beetle. *Dev Genes Evol* 215, 13-31.
- Handel, K., Grunfelder, C.G., Roth, S., Sander, K., 2000. *Tribolium* embryogenesis: a SEM study of cell shapes and movements from blastoderm to serosal closure. *Dev Genes Evol* 210, 167-179.
- Hilbrant, M., Horn, T., Koelzer, S., Panfilio, K.A., 2016. The beetle amnion and serosa functionally interact as apposed epithelia. *Elife* 5.
- Hong, J.W., Hendrix, D.A., Papatsenko, D., Levine, M.S., 2008. How the Dorsal gradient works: insights from postgenome technologies. *Proc Natl Acad Sci U S A* 105, 20072-20076.
- Horn, T., Panfilio, K.A., 2016. Novel functions for Dorsocross in epithelial morphogenesis in the beetle *Tribolium castaneum*. *Development* 143, 3002-3011.
- Imam, F., Sutherland, D., Huang, W., Krasnow, M.A., 1999. stumps, a *Drosophila* gene required for fibroblast growth factor (FGF)-directed migrations of tracheal and mesodermal cells. *Genetics* 152, 307-318.
- Jacobs, C.G., Rezende, G.L., Lamers, G.E., van der Zee, M., 2013. The extraembryonic serosa protects the insect egg against desiccation. *Proc Biol Sci* 280, 20131082.
- Jiang, J., Kosman, D., Ip, Y.T., Levine, M., 1991. The dorsal morphogen gradient regulates the mesoderm determinant twist in early *Drosophila* embryos. *Genes Dev* 5, 1881-1891.
- Johannsen, O.A., Butt, F.H., (1941) "Embryology of insects and myriapods" McGraw-Hill, New York
- Jura, C., (1972) "Development of apterygote insects." *Developmental systems: Insects* pp. 49-94.
- Kerridge, S., Munjal, A., Philippe, J.M., Jha, A., de las Bayonas, A.G., Saurin, A.J., Lecuit, T., 2016. Modular activation of Rho1 by GPCR signalling imparts polarized myosin II activation during morphogenesis. *Nat Cell Biol* 18, 261-270.
- Kispert, A., Herrmann, B.G., Leptin, M., Reuter, R., 1994. Homologs of the mouse Brachyury gene are involved in the specification of posterior terminal structures in *Drosophila*, *Tribolium*, and *Locusta*. *Genes Dev* 8, 2137-2150.
- Klambt, C., Glazer, L., Shilo, B.Z., 1992. breathless, a *Drosophila* FGF receptor homolog, is essential for migration of tracheal and specific midline glial cells. *Genes Dev* 6, 1668-1678.
- Knust, E., Schrons, H., Grawe, F., Campos-Ortega, J.A., 1992. Seven genes of the Enhancer of split complex of *Drosophila melanogaster* encode helix-loop-helix proteins. *Genetics* 132, 505-518.
- Koelzer, S., Kolsch, Y., Panfilio, K.A., 2014. Visualizing late insect embryogenesis: extraembryonic and mesodermal enhancer trap expression in the beetle *Tribolium castaneum*. *PLoS One* 9, e103967.

- Kolsch, V., Seher, T., Fernandez-Ballester, G.J., Serrano, L., Leptin, M., 2007. Control of *Drosophila* gastrulation by apical localization of adherens junctions and RhoGEF2. *Science* 315, 384-386.
- Kusch, T., Reuter, R., 1999. Functions for *Drosophila* brachyenteron and forkhead in mesoderm specification and cell signalling. *Development* 126, 3991-4003.
- Lai, Z.C., Fortini, M.E., Rubin, G.M., 1991. The embryonic expression patterns of *zfh-1* and *zfh-2*, two *Drosophila* genes encoding novel zinc-finger homeodomain proteins. *Mech Dev* 34, 123-134.
- Lai, Z.C., Rushton, E., Bate, M., Rubin, G.M., 1993. Loss of function of the *Drosophila* *zfh-1* gene results in abnormal development of mesodermally derived tissues. *Proc Natl Acad Sci U S A* 90, 4122-4126.
- Lemaitre, B., Nicolas, E., Michaut, L., Reichhart, J.M., Hoffmann, J.A., 1996. The dorsoventral regulatory gene cassette *spatzle/Toll/cactus* controls the potent antifungal response in *Drosophila* adults. *Cell* 86, 973-983.
- Lengyel, J.A., Iwaki, D.D., 2002. It takes guts: the *Drosophila* hindgut as a model system for organogenesis. *Dev Biol* 243, 1-19.
- Leptin, M., 1991. *twist* and *snail* as positive and negative regulators during *Drosophila* mesoderm development. *Genes Dev* 5, 1568-1576.
- Leptin, M., 1994. Morphogenesis. Control of epithelial cell shape changes. *Curr Biol* 4, 709-712.
- Leptin, M., 1999. Gastrulation in *Drosophila*: the logic and the cellular mechanisms. *EMBO J* 18, 3187-3192.
- Leptin, M., Grunewald, B., 1990. Cell shape changes during gastrulation in *Drosophila*. *Development* 110, 73-84.
- Levine, M., Davidson, E.H., 2005. Gene regulatory networks for development. *Proc Natl Acad Sci U S A* 102, 4936-4942.
- Lorenzen, G., Capko, J., 2003. Steps to increase the profitability of your practice. *J Med Pract Manage* 18, 235-238.
- Lorenzen, M.D., Berghammer, A.J., Brown, S.J., Denell, R.E., Klingler, M., Beeman, R.W., 2003. piggyBac-mediated germline transformation in the beetle *Tribolium castaneum*. *Insect Mol Biol* 12, 433-440.
- Lynch, J.A., El-Sherif, E., Brown, S.J., 2012. Comparisons of the embryonic development of *Drosophila*, *Nasonia*, and *Tribolium*. *Wiley Interdiscip Rev Dev Biol* 1, 16-39.
- Lynch, J.A., Ozuak, O., Khila, A., Abouheif, E., Desplan, C., Roth, S., 2011. The phylogenetic origin of *oskar* coincided with the origin of maternally provisioned germ plasm and pole cells at the base of the Holometabola. *PLoS Genet* 7, e1002029.
- Lynch, J.A., Roth, S., 2011. The evolution of dorsal-ventral patterning mechanisms in insects. *Genes Dev* 25, 107-118.
- Manning, A.J., Peters, K.A., Peifer, M., Rogers, S.L., 2013. Regulation of epithelial morphogenesis by the G protein-coupled receptor *mist* and its ligand *fog*. *Sci Signal* 6, ra98.

- Manning, A.J., Rogers, S.L., 2014. The Fog signaling pathway: insights into signaling in morphogenesis. *Dev Biol* 394, 6-14.
- Marlow, F., 2015. Primordial Germ Cell Specification and Migration. *F1000Res* 4.
- Martin, A.C., Kaschube, M., Wieschaus, E.F., 2009. Pulsed contractions of an actin-myosin network drive apical constriction. *Nature* 457, 495-499.
- Milan, M., Weihe, U., Perez, L., Cohen, S.M., 2001. The LRR proteins capricious and Tartan mediate cell interactions during DV boundary formation in the *Drosophila* wing. *Cell* 106, 785-794.
- Miller, S.C., Miyata, K., Brown, S.J., Tomoyasu, Y., 2012. Dissecting systemic RNA interference in the red flour beetle *Tribolium castaneum*: parameters affecting the efficiency of RNAi. *PLoS One* 7, e47431.
- Misof, B., Liu, S., Meusemann, K., Peters, R.S., Donath, A., 2014. Phylogenomics resolves the timing and pattern of insect evolution. *Science* 346, 763-767.
- Morisato, D., 2001. Spatzle regulates the shape of the Dorsal gradient in the *Drosophila* embryo. *Development* 128, 2309-2319.
- Morize, P., Christiansen, A.E., Costa, M., Parks, S., Wieschaus, E., 1998. Hyperactivation of the folded gastrulation pathway induces specific cell shape changes. *Development* 125, 589-597.
- Moussian, B., Roth, S., 2005. Dorsoventral axis formation in the *Drosophila* embryo--shaping and transducing a morphogen gradient. *Curr Biol* 15, R887-899.
- Muha, V., Muller, H.A., 2013. Functions and Mechanisms of Fibroblast Growth Factor (FGF) Signalling in *Drosophila melanogaster*. *Int J Mol Sci* 14, 5920-5937.
- Mullis, K.B., 1990. Target amplification for DNA analysis by the polymerase chain reaction. *Ann Biol Clin (Paris)* 48, 579-582.
- Nikolaidou, K.K., Barrett, K., 2004. A Rho GTPase signaling pathway is used reiteratively in epithelial folding and potentially selects the outcome of Rho activation. *Curr Biol* 14, 1822-1826.
- Nilson, L.A., Schupbach, T., 1998. Localized requirements for windbeutel and pipe reveal a dorsoventral prepattern within the follicular epithelium of the *Drosophila* ovary. *Cell* 93, 253-262.
- Nunes da Fonseca, R., van der Zee, M., Roth, S., 2010. Evolution of extracellular Dpp modulators in insects: The roles of tolloid and twisted-gastrulation in dorsoventral patterning of the *Tribolium* embryo. *Dev Biol* 345, 80-93.
- Nunes da Fonseca, R., von Levetzow, C., Kalscheuer, P., Basal, A., van der Zee, M., Roth, S., 2008. Self-regulatory circuits in dorsoventral axis formation of the short-germ beetle *Tribolium castaneum*. *Dev Cell* 14, 605-615.
- Ozuak, O., Buchta, T., Roth, S., Lynch, J.A., 2014. Dorsoventral polarity of the *Nasonia* embryo primarily relies on a BMP gradient formed without input from Toll. *Curr Biol* 24, 2393-2398.
- Panfilio, K.A., 2008. Extraembryonic development in insects and the acrobatics of blastokinesis. *Dev Biol* 313, 471-491.

- Panfilio, K.A., Oberhofer, G., Roth, S., 2013. High plasticity in epithelial morphogenesis during insect dorsal closure. *Biol Open* 2, 1108-1118.
- Parks, S., Wieschaus, E., 1991. The *Drosophila* gastrulation gene *concertina* encodes a G alpha-like protein. *Cell* 64, 447-458.
- Patil, V.S., Anand, A., Chakrabarti, A., Kai, T., 2014. The Tudor domain protein Tapas, a homolog of the vertebrate Tdrd7, functions in the piRNA pathway to regulate retrotransposons in germline of *Drosophila melanogaster*. *BMC Biol* 12, 61.
- Pavlopoulos, A., Berghammer, A.J., Averof, M., Klingler, M., 2004. Efficient transformation of the beetle *Tribolium castaneum* using the Minos transposable element: quantitative and qualitative analysis of genomic integration events. *Genetics* 167, 737-746.
- Peri, F., Roth, S., 2000. Combined activities of Gurken and decapentaplegic specify dorsal chorion structures of the *Drosophila* egg. *Development* 127, 841-850.
- Peter, I.S., Davidson, E.H., 2011. Evolution of gene regulatory networks controlling body plan development. *Cell* 144, 970-985.
- Pope, K.L., Harris, T.J., 2008. Control of cell flattening and junctional remodeling during squamous epithelial morphogenesis in *Drosophila*. *Development* 135, 2227-2238.
- Posnien, N., Schinko, J., Grossmann, D., Shippy, T.D., Konopova, B., Bucher, G., 2009. RNAi in the red flour beetle (*Tribolium*). *Cold Spring Harb Protoc* 2009, pdb prot5256.
- Quan, H., Lynch, J.A., 2016. The evolution of insect germline specification strategies. *Curr Opin Insect Sci* 13, 99-105.
- Reeves, G.T., Stathopoulos, A., 2009. Graded dorsal and differential gene regulation in the *Drosophila* embryo. *Cold Spring Harbor perspectives in biology* 1, a000836.
- Reeves, G.T., Trisnadi, N., Truong, T.V., Nahmad, M., Katz, S., Stathopoulos, A., 2012. Dorsal-ventral gene expression in the *Drosophila* embryo reflects the dynamics and precision of the dorsal nuclear gradient. *Dev Cell* 22, 544-557.
- Rickoll, W.L., Counce, S.J., 1980. Morphogenesis in the embryo of *Drosophila melanogaster* - Germ band extension. *Wilehm Roux Arch Dev Biol* 188, 163-177.
- Rocke, D.M., Ruan, L., Gossett, J.J., Durbin-Johnson, B., Aviran, S., 2015. Controlling False Positive Rates in Methods for Differential Gene Expression Analysis using RNA-Seq Data. *bioRxiv*.
- Rosetto, M., Engstrom, Y., Baldari, C.T., Telford, J.L., Hultmark, D., 1995. Signals from the IL-1 receptor homolog, Toll, can activate an immune response in a *Drosophila* hemocyte cell line. *Biochem Biophys Res Commun* 209, 111-116.
- Roth, S., 2003. The origin of dorsoventral polarity in *Drosophila*. *Philos Trans R Soc Lond B Biol Sci* 358, 1317-1329; discussion 1329.
- Roth, S., 2004. Gastrulation: From cells to Embryo. edited by Claudio Stern, Cold Spring Harbor Laboratory Press, „Gastrulation in other insects“, Pages 105-119.

- Roth, S., Hiromi, Y., Godt, D., Nusslein-Volhard, C., 1991. *cactus*, a maternal gene required for proper formation of the dorsoventral morphogen gradient in *Drosophila* embryos. *Development* 112, 371-388.
- Roth, S., Lynch, J.A., 2009. Symmetry breaking during *Drosophila* oogenesis. *Cold Spring Harbor perspectives in biology* 1, a001891.
- Rouso, T., Lynch, J., Yogev, S., Roth, S., Schejter, E.D., Shilo, B.Z., 2010. Generation of distinct signaling modes via diversification of the *Egfr* ligand-processing cassette. *Development* 137, 3427-3437.
- Sachs, L., Chen, Y.T., Drechsler, A., Lynch, J.A., Panfilio, K.A., Lassig, M., Berg, J., Roth, S., 2015. Dynamic BMP signaling polarized by Toll patterns the dorsoventral axis in a hemimetabolous insect. *Elife* 4, e05502.
- Sandmann, T., Girardot, C., Brehme, M., Tongprasit, W., Stolc, V., Furlong, E.E., 2007. A core transcriptional network for early mesoderm development in *Drosophila melanogaster*. *Genes Dev* 21, 436-449.
- Sarrazin, A.F., Peel, A.D., Averof, M., 2012. A segmentation clock with two-segment periodicity in insects. *Science* 336, 338-341.
- Sawyer, J.M., Harrell, J.R., Shemer, G., Sullivan-Brown, J., Roh-Johnson, M., Goldstein, B., 2010. Apical constriction: a cell shape change that can drive morphogenesis. *Dev Biol* 341, 5-19.
- Schinko, J., Posnien, N., Kittelmann, S., Koniszewski, N., Bucher, G., 2009. Single and double whole-mount in situ hybridization in red flour beetle (*Tribolium*) embryos. *Cold Spring Harb Protoc* 2009, pdb prot5258.
- Schroder, R., 2006. *vasa* mRNA accumulates at the posterior pole during blastoderm formation in the flour beetle *Tribolium castaneum*. *Dev Genes Evol* 216, 277-283.
- Schroder, R., Eckert, C., Wolff, C., Tautz, D., 2000. Conserved and divergent aspects of terminal patterning in the beetle *Tribolium castaneum*. *Proc Natl Acad Sci U S A* 97, 6591-6596.
- Schupbach, T., Roth, S., 1994. Dorsoventral patterning in *Drosophila* oogenesis. *Curr Opin Genet Dev* 4, 502-507.
- Schupbach, T., Wieschaus, E., 1989. Female sterile mutations on the second chromosome of *Drosophila melanogaster*. I. Maternal effect mutations. *Genetics* 121, 101-117.
- Sharma, R., Beer, K., Iwanov, K., Schmohl, F., Beckmann, P.I., Schroder, R., 2015. The single *fgf* receptor gene in the beetle *Tribolium castaneum* codes for two isoforms that integrate FGF8- and Branchless-dependent signals. *Dev Biol* 402, 264-275.
- Sims, D., Sudbery, I., Illott, N.E., Heger, A., Ponting, C.P., 2014. Sequencing depth and coverage: key considerations in genomic analyses. *Nature reviews. Genetics* 15, 121-132.
- Singer, J.B., Harbecke, R., Kusch, T., Reuter, R., Lengyel, J.A., 1996. *Drosophila* brachyenteron regulates gene activity and morphogenesis in the gut. *Development* 122, 3707-3718.
- Sommer, R.J., 2009. The future of evo-devo: model systems and evolutionary theory. *Nature reviews. Genetics* 10, 416-422.

- Sommer, R.J., Tautz, D., 1994. Expression patterns of twist and snail in *Tribolium* (Coleoptera) suggest a homologous formation of mesoderm in long and short germ band insects. *Developmental genetics* 15, 32-37.
- Soneson, C., Delorenzi, M., 2013. A comparison of methods for differential expression analysis of RNA-seq data. *BMC Bioinformatics* 14, 91.
- Sonnenblick, B.P., 1941. Germ Cell Movements and Sex Differentiation of the Gonads in the *Drosophila* Embryo. *Proc Natl Acad Sci U S A* 27, 484-489.
- Stanley, M.G., AW 1970. The embryonic development of *Tribolium confusum*. *Ann Entomol Soc Am* 63, 1248–1256.
- Stappert, D., PhD Thesis 2014. Two novel, complementary next generation sequencing approaches to reveal the dorso-ventral gene regulatory network of *Tribolium castaneum*
- Stappert, D., Frey, N., von Levetzow, C., Roth, S., 2016. Genome-wide identification of *Tribolium* dorsoventral patterning genes. *Development* 143, 2443-2454.
- Stathopoulos, A., Levine, M., 2002. Dorsal gradient networks in the *Drosophila* embryo. *Dev Biol* 246, 57-67.
- Stathopoulos, A., Levine, M., 2005. Localized repressors delineate the neurogenic ectoderm in the early *Drosophila* embryo. *Dev Biol* 280, 482-493.
- Stern, D.L., 2010. *Evolution, Development, & The Predictable Genome*. Roberts and Company Publishers.
- Suzuki, M., Morita, H., Ueno, N., 2012. Molecular mechanisms of cell shape changes that contribute to vertebrate neural tube closure. *Dev Growth Differ* 54, 266-276.
- Sweeton, D., Parks, S., Costa, M., Wieschaus, E., 1991. Gastrulation in *Drosophila*: the formation of the ventral furrow and posterior midgut invaginations. *Development* 112, 775-789.
- Szuperak, M., Salah, S., Meyer, E.J., Nagarajan, U., Ikmi, A., Gibson, M.C., 2011. Feedback regulation of *Drosophila* BMP signaling by the novel extracellular protein larval translucida. *Development* 138, 715-724.
- Tautz, D., Sommer, R.J., 1995. Evolution of segmentation genes in insects. *Trends Genet* 11, 23-27.
- Trauner, J., Schinko, J., Lorenzen, M.D., Shippy, T.D., Wimmer, E.A., Beeman, R.W., Klingler, M., Bucher, G., Brown, S.J., 2009. Large-scale insertional mutagenesis of a coleopteran stored grain pest, the red flour beetle *Tribolium castaneum*, identifies embryonic lethal mutations and enhancer traps. *BMC Biol* 7, 73.
- Turner, F.R., Mahowald, A.P., 1976. Scanning electron microscopy of *Drosophila* embryogenesis. 1. The structure of the egg envelopes and the formation of the cellular blastoderm. *Dev Biol* 50, 95-108.
- Urbano, J.M., Torgler, C.N., Molnar, C., Tepass, U., Lopez-Varea, A., Brown, N.H., de Celis, J.F., Martin-Bermudo, M.D., 2009. *Drosophila* laminins act as key regulators of basement membrane assembly and morphogenesis. *Development* 136, 4165-4176.

- Urbansky, S., Gonzalez Avalos, P., Wosch, M., Lemke, S., 2016. Folded gastrulation and T48 drive the evolution of coordinated mesoderm internalization in flies. *Elife* 5.
- van der Zee, M., Berns, N., Roth, S., 2005. Distinct functions of the *Tribolium* *zerknüllt* genes in serosa specification and dorsal closure. *Curr Biol* 15, 624-636.
- van der Zee, M., Stockhammer, O., von Levetzow, C., Nunes da Fonseca, R., Roth, S., 2006. Sog/Chordin is required for ventral-to-dorsal Dpp/BMP transport and head formation in a short germ insect. *Proc Natl Acad Sci U S A* 103, 16307-16312.
- Vassin, H., Bremer, K.A., Knust, E., Campos-Ortega, J.A., 1987. The neurogenic gene Delta of *Drosophila melanogaster* is expressed in neurogenic territories and encodes a putative transmembrane protein with EGF-like repeats. *EMBO J* 6, 3431-3440.
- Venter, J.C., di Porzio, U., Robinson, D.A., Shreeve, S.M., Lai, J., Kerlavage, A.R., Fracek, S.P., Jr., Lentes, K.U., Fraser, C.M., 1988. Evolution of neurotransmitter receptor systems. *Prog Neurobiol* 30, 105-169.
- Vincent, S., Wilson, R., Coelho, C., Affolter, M., Leptin, M., 1998. The *Drosophila* protein Dof is specifically required for FGF signaling. *Molecular Cell* 2, 515-525.
- von Levetzow, C., PhD Thesis 2008. Konservierte und divergente Aspekte der twist-, snail- und concertina-Funktion im Käfer *Tribolium castaneum* University of Cologne.
- Waterhouse, R.M., Zdobnov, E.M., Tegenfeldt, F., Li, J., Kriventseva, E.V., 2011. OrthoDB: the hierarchical catalog of eukaryotic orthologs in 2011. *Nucleic Acids Res* 39, D283-288.
- Wech, I., Bray, S., Delidakis, C., Preiss, A., 1999. Distinct expression patterns of different enhancer of split bHLH genes during embryogenesis of *Drosophila melanogaster*. *Dev Genes Evol* 209, 370-375.
- Wheeler, S.R., Carrico, M.L., Wilson, B.A., Brown, S.J., Skeath, J.B., 2003. The expression and function of the achaete-scute genes in *Tribolium castaneum* reveals conservation and variation in neural pattern formation and cell fate specification. *Development* 130, 4373-4381.
- Wilson, M.J., Kenny, N.J., Dearden, P.K., 2014. Components of the dorsal-ventral pathway also contribute to anterior-posterior patterning in honeybee embryos (*Apis mellifera*). *Evodevo* 5, 11.
- Wolff, C., Schroder, R., Schulz, C., Tautz, D., Klingler, M., 1998. Regulation of the *Tribolium* homologues of caudal and hunchback in *Drosophila*: evidence for maternal gradient systems in a short germ embryo. *Development* 125, 3645-3654.
- Wu, L.H., Lengyel, J.A., 1998. Role of caudal in hindgut specification and gastrulation suggests homology between *Drosophila* amnioproctodeal invagination and vertebrate blastopore. *Development* 125, 2433-2442.
- Xiang, S.Y., Dusaban, S.S., Brown, J.H., 2013. Lysophospholipid receptor activation of RhoA and lipid signaling pathways. *Biochim Biophys Acta* 1831, 213-222.
- Xie, G., Zhang, H., Du, G., Huang, Q., Liang, X., Ma, J., Jiao, R., 2012. Uif, a large transmembrane protein with EGF-like repeats, can antagonize Notch signaling in *Drosophila*. *PLoS One* 7, e36362.
- Zhang, L., Ward, R.E.t., 2009. uninflatable encodes a novel ectodermal apical surface protein required for tracheal inflation in *Drosophila*. *Dev Biol* 336, 201-212.

Appendix A: Primerlist RNA-Seq

The list contains the primer sequences of genes for generation of the initial knockdown samples for RNA-sequencing and of marker genes used for characterization of the respective knockdown phenotypes. Primers containing the linker sequences and both T7 universal primers were used for RNA-probe synthesis and generation of dsRNA for injections.

Nr.	Gene	Sequence
1	5' T7 linker	ggccgcgg
2	3' T7 linker	cccggggc
3	5' T7 universal primer	gagaattc taatcgactcactatag ggccgcgg
4	3' T7 universal primer	agggatcc taatcgactcactataggg cccggggc
5	<i>dsRed_fwd</i>	ggccgcggTGGTGTAGTCCTCGTTGTGG
6	<i>dsRed_rev</i>	cccggggcAGTTCATGCGCTTCAAGGTG
7	<i>TC000176 (Toll)_fwd</i>	ggccgcggAACCCGAAGCGTTTTATGTC
8	<i>TC000176 (Toll)_rev</i>	cccggggcTACGTCCAGTTTCCGATGAG
9	<i>TC014598 (twist)_fwd</i>	ggccgcggGCTGATGGACCTGACCAACT
10	<i>TC014598 (twist)_rev</i>	cccggggcCTCCAATCACCTCCATCC
11	<i>TC008466 (dpp)_fwd</i>	ggccgcggAGATCGACACTGTTGCCCTTTT
12	<i>TC008466 (dpp)_rev</i>	cccggggcAGATGGTTGGTTTTGGGGTCTTG
13	<i>TC012650 (sog)_fwd</i>	ggccgcggTACCGAAACCTGGAGTGCGTGT
14	<i>TC012650 (sog)_rev</i>	cccggggcCCTTCCAGTCGCCACTACAT
15	<i>TC010407 (pannier)_fwd</i>	ggccgcggGTCAAAACTGCCACCCTGTT
16	<i>TC010407 (pannier)_rev</i>	cccggggcCCGGTACAACCAAAAGTGCT
17	<i>TC008433 (achaete-scute homolog) fwd</i>	ggccgcggGTCATCCAGAGCAAACGACC
18	<i>TC008433 (achaete-scute homolog)_rev</i>	cccggggcTCGGGACTTTTCGGTTCGTA
19	<i>TC006788 (gooseberry)_fwd</i>	ggccgcggACGTTGGAAGTTGAGGCAAG
20	<i>TC006788 (gooseberry)_rev</i>	cccggggcACCAGCGAAAAGGCTGTAAT
21	<i>TC009896 (engrailed)_fwd</i>	ggccgcggCAAAAGGGCCAAAATCAAAA
22	<i>TC009896 (engrailed)_rev</i>	cccggggcAAAAATCCCGTGTCTTGAC

Appendix B: Genes differentially expressed upon *Tc-dpp* kd and *Tc-sog* kd

Genes detected as up- or downregulated upon *Tc-dpp* kd and *Tc-sog* kd with a false positive rate of 1% (FDR01) and 5% (FDR05). The list contains the official TC-identifier, information about up- or downregulation in the different knockdown conditions and *Drosophila* orthologs of the respective genes. Furthermore, the primer sequences and expression patterns are listed.

	Nr.	Gene	<i>Tc-twist</i> kd vs. wt	<i>Tc-Toll</i> kd vs. wt	potential <i>Drosophila</i> homolog	5' Primer (fwd)	3' Primer (rev)	Expression Pattern
FDR01	1	TC001715	down	up	<i>windpipe</i>	ggccgcgAGTGTGATGAGGGAAGTGG	cccggggcTGACGCTTTGATCGTCACTC	serosa, prim pit, uniform in germband, serosal window free!
	2	TC006222	down	up	<i>dimmed</i>	ggccgcgGATGTGGAGGTGGAGGACAT	cccggggcGCGTTCCTCTTGTTGTTTTTC	first uniform, later anterior serosa, germband uniform, serosal window
	3	TC006771	down	up	<i>downstream of receptor kinase</i>	ggccgcgAGATGGAAGCTTGGAACGA	cccggggcTCCAAGTTGCTCCTGCTTT	first nothing, later serosa + prim. pit, germband nothing
	4	TC008855	down	up	<i>Dopamine transporter</i>	ggccgcgGTAGAGCGAAACCGACGAAG	cccggggcTAGCTGCATTCGGGTATC	nothing
	5	TC010157	down	up	<i>Succinyl coenzyme A synthetase α subunit</i>	ggccgcgCATCAACCTGCAGAAGCAAA	cccggggcCGTATGTCGCTCAAGAAAA	serosa (stronger dorsal), serosal window!!!
	6	TC010855	down	up	<i>epidermal retinal dehydrogenase 2 (LOC660853)</i>	ggccgcgACCCCAAAGCTTACGCTAT	cccggggcGCGCTTTCATGATGGATTTT	serosa, uniform in germband (very weak!!!)
	7	TC014139	down	up	<i>n.a.</i>	ggccgcgCGAAAGAAGCCCAAGACTG	cccggggcCCAGTTGGGATCACTCTGGT	uniform, later serosa, germband uniform
	8	TC015188	down	up	<i>waterproof</i>	ggccgcgTTGATCGAACAAACGAGCAG	cccggggcGACAACACATCCCCAAATC	serosa
	9	TC015379	down	up	<i>n.a.</i>	ggccgcgTTCTGCAGACATGGAAGCAC	cccggggcTCAGCGTAACCTTCGCTTT	serosa, serosal window!!!
	10	TC015392	down	up	<i>n.a.</i>	ggccgcgCCAGACAAAGGACTTGGA	cccggggcTCCAATCCGAACAACCTCTC	serosa
	11	TC004745	up	down	<i>patched</i>	ggccgcgGGCAAGTTCTCTTCGTGAG	cccggggcCCTCCTGTGCGAACTTCTC	stronger at headregion, segment. in germband, strong in head
	12	TC007409	up	down	<i>twi of eyeless</i>	ggccgcgCCCAGAACGAGAGCGTCTAC	cccggggcCCCAGACATCGAACTGTAGGT	x
	13	TC010596	up	down	<i>prospero</i>	ggccgcgCAGGTCTTCTCGCCTACAG	cccggggcGCCTGTCTGGCTACTTCTC	stronger at headregions + most ventral regions free, points in germband
	14	TC014658	up	down	<i>tartan</i>	ggccgcgCAAGGGACTTGCAATTGT	cccggggcTTGCTCAACCAGAGCAAAATG	stronger at headregion, strong in head + 2 spots in growth zone
FDR 05	1	TC002459	down	up	<i>CG3165</i>	ggccgcgATTAGTCCCGAAGCCACCTC	cccggggcCCGCACAAGTGACTAGCATC	serosa
	2	TC004480	down	up	<i>n.a.</i>	ggccgcgCGAGCAGACATTTCTTGAGG	cccggggcTGGTAATTAAGCGGTACC	x
	3	TC004902	down	up	<i>n.a.</i>	ggccgcgACTGGAATGCAGATTCCGA	cccggggcGCACGACACAGATCAATT	x
	4	TC008024	down	up	<i>vir-1 - virus-induced RNA 1 (CG31764)</i>	ggccgcgAGGTGGCGGTATTGTGATA	cccggggcCGTCGGTAATACCTGATTGAC	twi domain weaker, growth zone
	5	TC009479	down	up	<i>n.a.</i>	ggccgcgCACCTCTGCACCATCTACA	cccggggcTCCATTTCTCAAGCCGAAC	serosa
	6	TC010590	down	up	<i>Rcd6 - Reduction in Cnn dots 6 (CG11175)</i>	ggccgcgTCTTTGTCTCATCGCCTGGA	cccggggcTCGGGATAATGCGCTACTT	serosa
	7	TC013334	down	up	<i>n.a.</i>	ggccgcgTCCCCAATCAGAACCCTCAC	cccggggcCCGCTTGTCAAACTGGC	x
	8	TC012208	down	up	<i>n.a.</i>	ggccgcgCAGTCTTCTCGTGGTA	cccggggcGTGTGTCCCTCAACTTGC	weak in twi domain
	9	TC014534	down	up	<i>chemosensory protein 7</i>	ggccgcgTTCGGCCGCTGAAACAAAT	cccggggcCGTTTCTGTACTGACCCTGT	weak uniform
	10	TC001270	up	down	<i>knot</i>	ggccgcgTCTCGAGTACCTTTGAC	cccggggcGGTGTTCCTGTTCTGTTCCC	S/E border
	11	TC004474	up	down	<i>Toll 7</i>	ggccgcgACACGTTCTCGACAAGACT	cccggggcAGTGGGAGTTGACGACAAT	stripes in early embryo
	12	TC000871	up	down	<i>uninflatable</i>	ggccgcgCAGATGCGACAAAGAGGACG	cccggggcCGTAAGCGGGGACATTAATA	lateral stripes in early embryo, later stronger in head and growth zone
	13	TC011763	up	down	<i>empty spiracles</i>	ggccgcgGCTTCTCCATCGACTCCATC	cccggggcTGCTCCACTTGTGACGTG	embryo uniform, germband uniform
	14	TC001364	up	down	<i>hedgehog</i>	ggccgcgATCGCTCGAAATACGGAATG	cccggggcAAAGTCCGCCGTAGCATAAA	AP-pattern

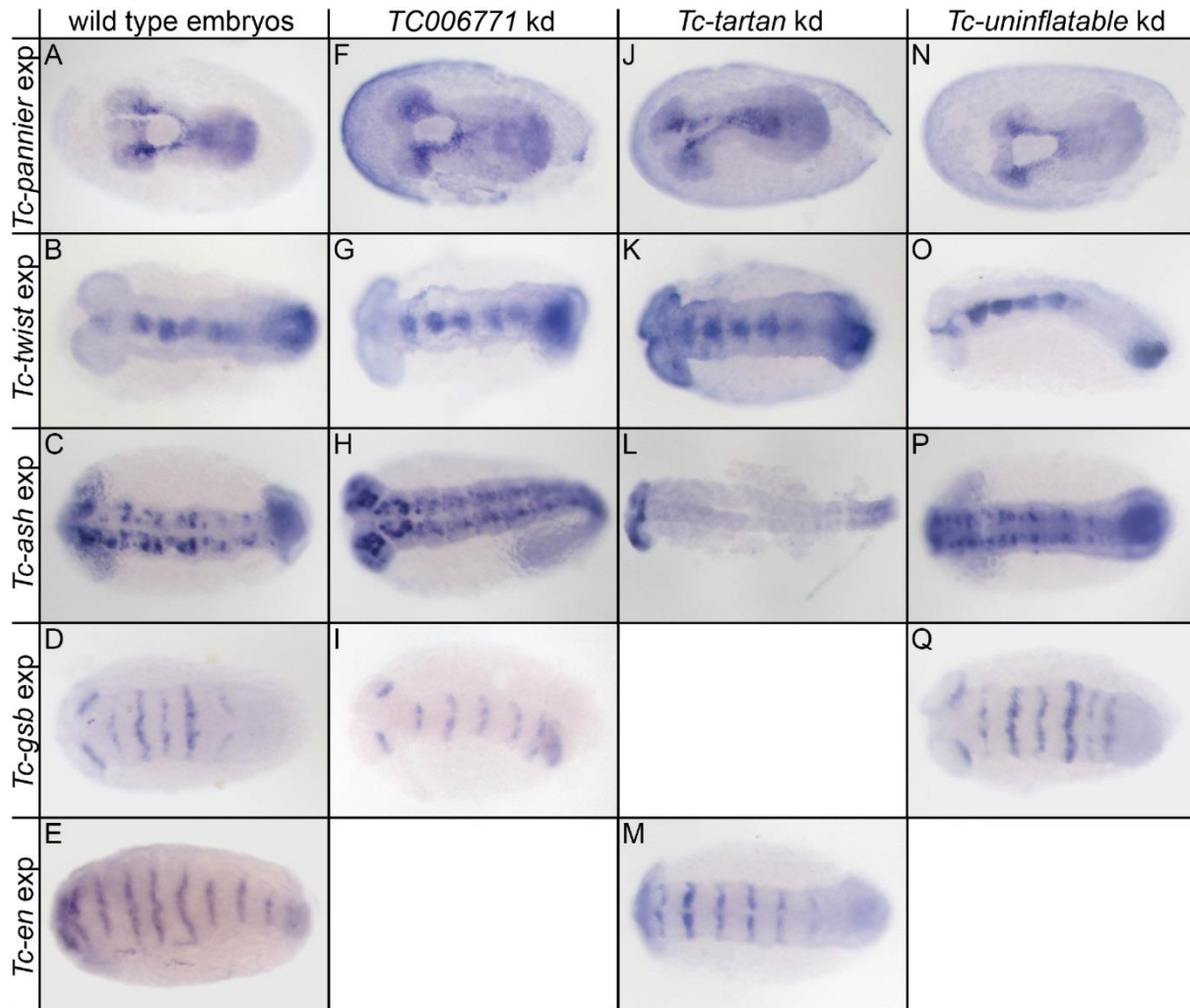
Appendix C: Genes differentially expressed upon *Tc-twist* vs *Tc-Toll* knockdown

Genes detected as up- or downregulated upon *Tc-twist* kd and *Tc-Toll* kd with a false positive rate of 1% (FDR01) and 5% (FDR05). The list contains the official TC-identifier, information about up- or downregulation in the different knockdown conditions and *Drosophila* orthologs of the respective genes. Furthermore, the primer sequences and expression patterns are listed.

Nr.	Gene	<i>Tc-twist</i> kd vs. wt	<i>Tc-Toll</i> kd vs. wt	potential <i>Drosophila</i> homolog	5' Primer (fwd)	3' Primer (rev)	Expression Pattern	
FDR01	1	TC001667	down	down	<i>inflated/integrin αP2</i>	ggccgcgACCAACACACGCTACAACCA	cccggggcAGTACGACGCCACAAGG	ventral stripe at gastrulation, later along midline
	2	TC002003	down	down	<i>cactus</i>	ggccgcgCACCTGTTGAAACACCAACG	cccggggcTCGCTGACTCGTCTCTGA	ventral midline
	3	TC004114	down	down	<i>delta</i>	ggccgcgCCTGTTGAATGGCGTACT	cccggggcTTCGACTCGGAGGACTCT	ventral (haben wir bestimmt irgendwo)
	4	TC004713	down	down	<i>heartless</i>	ggccgcgGTACCCAAAACCCAGATT	cccggggcGCTGTTTACCTGCATTTT	ventral stripe, later two stripes along midline
	5	TC005328	down	down	<i>n.a.</i>	ggccgcgGATAAAGAGGGCCAGAG	cccggggcGCATTGCTGACGAGACAT	prim. pit, gastrulation, growth zone
	6	TC005541	down	down	<i>E(spl)my-HLH/ E(spl)3</i>	ggccgcgGAAGTGATGAAGCCGATGT	cccggggcTGGTCAAGTGCACACT	two stripes (prim pit stage), later two spots head
	7	TC006580	down	down	<i>E(spl)my-HLH/E(spl) 1</i>	ggccgcgAAGAGCCAGCCGATCT	cccggggcACCAGCCCTCCACAT	two stripes (prim pit stage), later two spots head
	8	TC008064	down	down	<i>sloppy-paired 2</i>	ggccgcgAATAACTCTCTACTACGTTTTT	cccggggcCACAGTGACAGTTTGAGGAG	AP pattern
	9	TC011323	down	down	<i>dof/stumps</i>	ggccgcgTATCACCAGAAAGATCG	cccggggcTCTCCTCACTCTGCCACT	ventral stripe, midline germband
	10	TC014474	down	down	<i>escargot/snail</i>	ggccgcgGTGCAAATGCTGGAGACAT	cccggggcGCAGTGGGACACAATACT	ventral stripe
	11	TC014598	down	down	<i>twist</i>	ggccgcgGCTGATGGACTGACCAACT	cccggggcCTCAATCACCTCCATCC	ventral stripe, later along midline
	12	TC010105	down	down	<i>lethal (2) essential for life</i>	ggccgcgGGACGATGACGACTTCCACT	cccggggcGGTGTTCGACTTTGGGTTG	artifacts
	13	TC010461	down	down	<i>n.a.</i>	ggccgcgCCGAACGAACCTACGACAAT	cccggggcGAATTCGGTGTCTGACTT	nothing
	14	TC003461	down	down	<i>Laminin A</i>	ggccgcgTAACGGGAGTTTTGTCAGG	cccggggcATTGCGGATCCTACGTGTTT	x
	15	TC003606	down	down	<i>n.a.</i>	ggccgcgATCGTGTGATGGTGTGA	cccggggcTGTACACATAAGGATCCATGTCC	nothing
	16	TC007056	down	down	<i>n.a.</i>	ggccgcgGTCATCCAGCAGTGAAGAA	cccggggcTCTTCGGCAAAAATTGCT	nothing
	17	TC009862	down	down	<i>n.a.</i>	ggccgcgCAACCAACCAACCAAGTCT	cccggggcAAAAGTCGAAGGCGTTAAA	x
	18	TC010195	down	down	<i>Papilin</i>	ggccgcgGGGTGCAACATCACAACCTG	cccggggcCCTTCGGTTTGACACAAGT	x
	19	TC013142	down	down	<i>Jhl-21</i>	ggccgcgGCCTCTGGATCGCTACTG	cccggggcCCGCCACAGAAAACCATAAT	artifacts
	20	TC000319	up	up	<i>n.a.</i>	ggccgcgACACGAGTTTTACCGTTGG	cccggggcGAGAAATGCATTGCAGACA	maternal, pot. embryo not serosa
	21	TC006513	up	up	<i>foraging</i>	ggccgcgAATTGTCAAAGACCGCAAC	cccggggcCTCCAGACAGCTCTCCATC	maternal
	22	TC015747	up	up	<i>pollux</i>	ggccgcgCAGACGCAATTTAGCCATA	cccggggcTGCAATTTCTCTCCATCC	nothing
	23	TC000089	down	up	<i>n.a.</i>	ggccgcgGGAACGTCCTCCGTTACAA	cccggggcGACGAGATGAACCTTTTGG	nothing
	24	TC000611	down	up	<i>similar to CG3823 CG3823-PA (LOC657947)</i>	ggccgcgGACATCGGAAAAATCCGAGA	cccggggcGGGAAATGTTGAGAATGTGG	nothing
	25	TC004948	down	up	<i>similar to peroxiredoxin (LOC656825)</i>	ggccgcgCAAGGCGCAAAATGGGTAGT	cccggggcCCAGGGCATTGTAACCTTGT	nothing
	26	TC005503	down	up	<i>similar to AGAP011121-PA (LOC654889)</i>	ggccgcgCCCAGAGGCTACTGTCCAAA	cccggggcTCCAGGCTCCACATGACTG	nothing
	27	TC006631	down	up	<i>sodium-dependent phosphate transporter</i>	ggccgcgTTTACGTTTTGGGGCTTTG	cccggggcACTATGGCAATGGTGAACA	nothing
	28	TC007255	down	up	<i>similar to AGAP000696-PA, transcript variant 1</i>	ggccgcgTGTGCTTTCTGTAGCATCG	cccggggcCTTAGGGTGGTGGTTGTG	nothing
	29	TC008197	down	up	<i>similar to SET domain containing 3 (LOC664524)</i>	ggccgcgCCAAGGAGGATCATGGAA	cccggggcCATGCTGTGAAGTGCAGCT	pot. serosa, stronger dorsal, segmental stripes in germband
	30	TC008400	down	up	<i>similar to Cuticular protein 100A CG12045-PA</i>	ggccgcgGCAGTTTGTCTGTTTTGGT	cccggggcGCAAAGCGTATTGCTCACA	serosa
	31	TC011140	down	up	<i>Cpap3-a1</i>	ggccgcgGTGCAAGGAGAACTTTG	cccggggcCTTGCTGTTTAGCAGGAG	nothing

	32	TC011602	down	up	<i>similar to GA14337-PA (LOC662721)</i>	ggccgcggAAAGGAGGGTGGGCTTAC	cccggggcGTTGCTGCAAGTTGTTGACG	nothing
	33	TC012828	down	up	<i>similar to Cuticular protein 92F CG5494-PA</i>	ggccgcggTCGCACTGGTCATTATCCAA	cccggggcCCATCATGTCCAATCACAGC	artifacts
	34	TC014517	down	up	<i>similar to conserved hypothetical protein (LOC660482)</i>	ggccgcggACCGCACAAAAAGTCAATC	cccggggcCGAGTCATAACAGCCCCATA	artifacts
	35	TC015517	down	up	<i>similar to take-out-like carrier protein JHBP-1 (LOC663271)</i>	ggccgcggCGCCCAGAAATTAATAATGT	cccggggcTCAGCTGTTCTTACCGTTG	uniform
	36	TC015555	down	up	<i>n.a.</i>	ggccgcggTTGTCGTTCAAGTGCAGAC	cccggggcTTGCCAAATTCACCTTTT	nothing
	37	TC015564	down	up	<i>similar to CG2837 CG2837-PD (LOC660047)</i>	ggccgcggTGGTGTCCACTGTTGATTG	cccggggcGTCGTTGCTTCACTCGTTT	nothing
	38	TC016034	down	up	<i>similar to conserved hypothetical protein (LOC100141613)</i>	ggccgcggATCACGCAGAGAAGCAAGT	cccggggcGGTGGGAACGATAAGTCT	x
FDR 05	1	TC000216	down	down	<i>neuralized</i>	ggccgcggCGACTCCAATTTCTGCTCG	cccggggcCCGCACATATAAAGGACGGC	<i>ventral stripe (twi domain), germband uniform</i>
	2	TC000920	down	down	<i>deformed</i>	ggccgcggCGTGGCGAGTTAATTGAGGG	cccggggcAATTGGCATCTTCGAGTCGC	<i>ventral stripe + 2 stripes in head region, 2 stripes in germband</i>
	3	TC001169	down	down	<i>Cpap 3-c5</i>	ggccgcggGCAGGCCGATTGAAGTTGAT	cccggggcGTTTGTGCGACTTCCAGT	x
	4	TC005184	down	down	<i>Lan B1</i>	ggccgcggGCTTTTGAGCCCTGTACAT	cccggggcTGCAGAAATGTCAAGGGCC	<i>ventral stripe, later along midline</i>
	5	TC006788	down	down	<i>gooseberry</i>	ggccgcggACGTTGGAAGTTGAGGCAAG	cccggggcACCAGCGAAAAGGCTGTAAT	x
	6	TC000035	down	down	<i>n.a.</i>	ggccgcggTTCCTGCAAATACCCGGAT	cccggggcTCAGTCAGTGTGGCATGTT	<i>twi domain free (very dynamic!?)</i>
	7	TC000922	down	down	<i>zen2</i>	ggccgcggAACGCCAGTTTTCAACAA	cccggggcCTCATCCTTACCACCACCT	<i>serosa</i>
	8	TC001270	down	down	<i>knot</i>	ggccgcggTCTCGGAGTACCTTTGAC	cccggggcGGTGTTCGTTCTGTTCC	<i>S/E border</i>
	9	TC001364	down	down	<i>hedgehog</i>	ggccgcggATCGCTCGAAATACGGAATG	cccggggcAAAGTCCGCCGTAGCATAAA	<i>AP-pattern</i>
	10	TC006750	down	down	<i>multiple edematous wings/integrin αPS1</i>	ggccgcggCGAAATCGAAACACCAAGC	cccggggcATCGTTAAAAATCGTGCCG	<i>germband uniform</i>
	11	TC006882	down	down	<i>n.a.</i>	ggccgcggTGGCATCGAGTGTGAGTTCT	cccggggcGCGAGCTTGGTCACATACAG	x
	12	TC008062	down	down	<i>sloppy-paired</i>	ggccgcggACTAATCCTGGCCTGTCTCT	cccggggcACTTAAGTTGTCCGGATGG	<i>AP-pattern</i>
	13	TC009157	down	down	<i>dystroglycan</i>	ggccgcggACCACCACTACTGTAAGCCC	cccggggcGGTTGAAATGGCACCAGGAG	<i>ventral twi domain, germband midline</i>
	14	TC011114	down	down	<i>Zn finger homeodomain 1</i>	ggccgcggCGCCTTCAACGTACATGAT	cccggggcGACCTTCGCTGTTCTGTGT	<i>early posterior spot, ventral stripe at gastrulation</i>
	15	TC004491	up	up	<i>fumble</i>	ggccgcggGACATCACCAAGACGAGGC	cccggggcGCTGTAGCGACCAAAATCTC	nothing
	16	TC009220	up	up	<i>n.a.</i>	ggccgcggTGCAGAACCTCATCGACGAT	cccggggcGACTTTCTCTCCGTCTCCC	<i>uniform, uniform in germband</i>
	17	TC011870	up	up	<i>kayak</i>	ggccgcggGGTTTCGTTCCACTCTAGT	cccggggcAATTCGGTGTCAAGGCTTC	<i>overstained</i>
	18	TC007256	down	up	<i>n.a.</i>	ggccgcggCCTCTTACAGAACTGGAGG	cccggggcACACACATAACACAACGCT	x
	19	TC010980	down	up	<i>n.a.</i>	ggccgcggTGGAAATGTCGGCCGATATGA	cccggggcTTGCCAAACCAATACCAGC	x
	20	TC030077	down	up	<i>serpin 5</i>	ggccgcggGCGCTCGAAATCGGAAAT	cccggggcTTGACTTTCTTGTGCGGAC	<i>serosa</i>

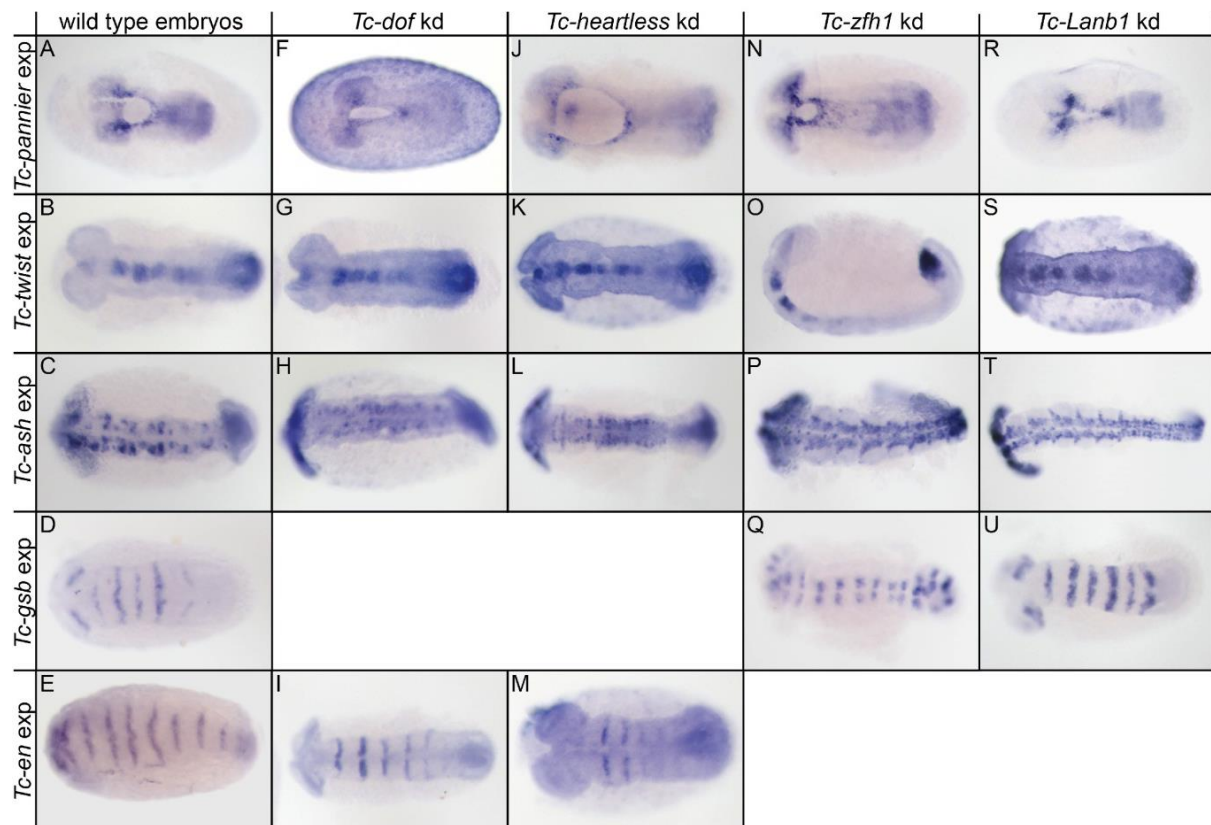
Appendix D: Marker gene expression in *Tc-sog* and *Tc-dpp* knockdown embryos



Marker gene expression after RNAi for genes differentially regulated upon *Tc-sog* and *Tc-dpp* knockdown

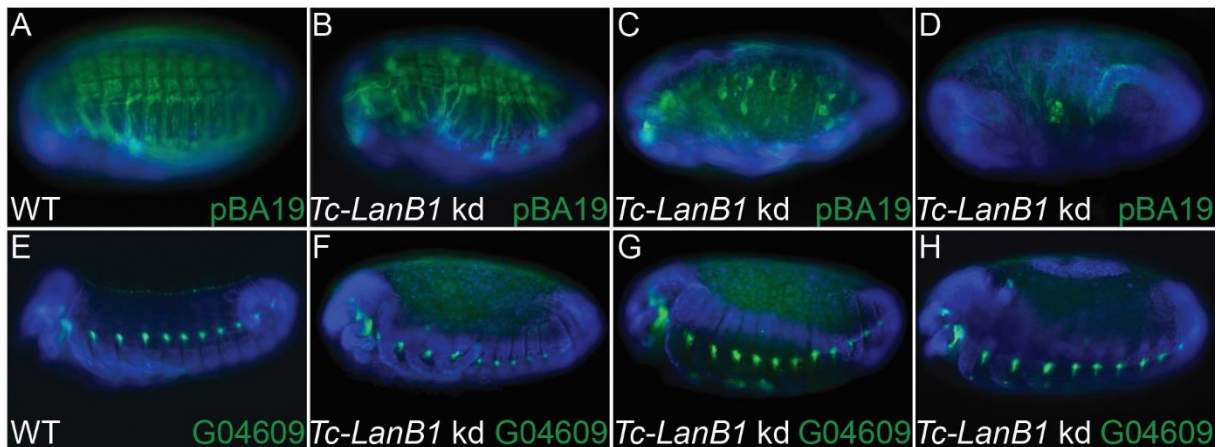
(A-E) wildtype embryos. (F-I) *TC006771* kd embryos. (J-M) *TC014658/Tc-tartan* kd embryos. (N-Q) *TC000871/Tc-uninflatable* kd embryos. (A, F, J, N) Expression of amnion marker *Tc-pannier* at serosal window stage. (B, G, K, O) Expression of mesodermal marker *Tc-twist* during germ band extension. (C, H, L, P) Expression of neuronal precursor marker *Tc-achaete-scute homolog* during germ band extension. (D, I, Q) Expression of segmental marker *Tc-gooseberry* during germ band extension. (E, M) Expression of segmental marker *Tc-engrailed* during germ band extension. Expression patterns in all kd embryos are wildtype-like with the following exception: (L) The expression of *Tc-achaete-scute homolog* is only visible in the head and the posterior end of elongated germ band embryos upon *TC014658/Tc-tartan* kd. All panels show ISHs and ventral surface views of embryos with the anterior pole pointing to the left. exp - expression; kd - knock down; *Tc-ash* - *Tc-achaete-scute homolog*; *Tc-gsb* - *Tc-gooseberry*; *Tc-en* - *Tc-engrailed*.

Appendix E: Marker gene expression in *Tc-Toll* and *Tc-twist* knockdown embryos



Marker gene expression after RNAi for genes differentially regulated upon *Tc-Toll* and *Tc-twist* knockdown. (A-E) wildtype embryos. (F-I) *TC011323/Tc-dof* kd embryos. (J-M) *TC004713/Tc-heartless* kd embryos. (N-Q) *TC011114/Tc-Zinc finger homeodomain 1 (Tc-zfh1)* kd embryos. (R-U) *TC005184/Tc-LanB1* kd embryos. (A, F, J, N, R) Expression of amnion marker *Tc-pannier* at serosal window stage. (B, G, K, O, S) Expression of mesodermal marker *Tc-twist* during germ band extension. (C, H, L, P, T) Expression of neuronal precursor marker *Tc-achaete-scute homolog* during germ band extension. (D, Q, U) Expression of segmental marker *Tc-gooseberry* during germ band extension. (E, I, M) Expression of segmental marker *Tc-engrailed* during germ band extension. Expression patterns in all kd embryos are wild type-like with following exception: (O) *Tc-twist* expression is missing from a large portion of the trunk in *TC011114/Tc-zfh1* kd embryos. All panels show ISHs and ventral surface views of embryos with the anterior pole pointing to the left with the exception of (O) showing a lateral view. exp - expression; kd - knock down; *Tc-ash*- *Tc-achaete-scute homolog*; *Tc-gsb* - *Tc-gooseberry*; *Tc-en* - *Tc-engrailed*.

Appendix F: Varsity in knockdown strength of *Tc-LanB1*



Knockdown of *Tc-LanB1* leads to loss of mesodermal derived tissues.

(A-D) pBA19 enhancer trap line which expresses EGFP in muscles (blue counterstaining is DAPI) (Lorenzen et al., 2003). (A) Wild type pBA19 embryo. The body wall muscles are labeled by EGFP. (B-D) *Tc-LanB1* knockdown. (B) Mild phenotype showing partial loss and irregular shape of the muscles. (C) Intermediate *Tc-LanB1* kd phenotype. The number of muscles fibers is strongly reduced, remaining muscles have a more spherical shape compared to wild type. (D) Strong *Tc-LanB1* kd phenotype. The muscles are almost completely lost. (E-H) Embryos of the enhancer trap line G04609. The cardioblast cell row (the presumptive heart) expresses EGFP (blue counterstaining is DAPI) (Koelzer et al., 2014; Trauner et al., 2009). (E) Wild type embryo of the G04609 line. (F-H) Different stages of G04609 embryos upon *Tc-LanB1* kd (F = youngest embryo, before serosal rupture; G = oldest embryo, after serosal rupture) show loss of the cardioblast cell row. kd: knockdown DAPI: 4',6-diamidino-2-phenylindole for nuclear staining.

Appendix G: Primerlist Fog signaling

The list contains the primer sequences which were used to analyze the Fog signaling pathway in *Tribolium*. Primers containing the linker sequences and both T7 universal primers were used for RNA-probe synthesis and generation of dsRNA for injections. The primer in red were used to create non-overlapping fragments.

Nr.	Gene	Primer Name/Number	Sequence	
1	cta	359_TC034430_for	ggccgcggTCAAGCTGTGGCGGGATAG	
2		360_TC034430_rev	cccggggcCAGTGGATGTTCTGTCTCGGGATT	
3		1151_TC034430 (cta) fwd_new	ggccgcggAATCCCGAGACGAACATCCA	
4		1152_TC034430 (cta) rev_new	cccggggcTTACATAAGAACCCGGCGGA	
5	fog	fog_fwd_ROD	CACCGACAAGGACGTGGCGATTGT	
6		fog_rev_ROD	AATCCTCCTCCAGAAGAGCG	
7		953_TC006723_fwd	ggccgcggCCCGCATCCATAATTGTGTT	
8		954_TC006723_rev	cccggggcAGAAGAGCGCCTCACCATC	
9		1141_TC006723_fwd 2.0	ggccgcggTAATCACCGTTGCATCTTGC	
10		1142_TC006723_rev 2.0	cccggggcATCGTGGTCACTTCCACCTC	
11		1153_TC006723 (fog) fwd_new	ggccgcggCCAGTACAGAAGGTGGGGAG	
12		1154_TC006723 (fog) fwd_new	cccggggcACCTAACAGTCGAACAAAAGGT	
13		mist	955_TC010654_fwd 1	ggccgcggACAAAAATGGGAGCTTGTGG
14			956_TC010654_rev 1	cccggggcGGAGAAAGTTGGAGCTGTCTG
15	957_TC010654_fwd 2		ggccgcggGCCTTCTTCTGGCTCAACAC	
16	958_TC010654_rev 2		cccggggcAAGACCCTTGAAGCAGTT	
17	1155_TC010654 (mist) fwd_new		ggccgcggATGACGGCTGTTAGGGTGAA	
18	1156_TC010654 (mist) rev_new		cccggggcGACACAGCGATTGAGAAGCA	
19	smog	1097_1_TC013504 (smog) fwd	ggccgcggCGATCCTGGAACGATCCTA	
20		1098_1_TC013504 (smog) rev	cccggggcTGCAGATGGTTTTGCTCTTG	
21		1157_TC013504 (smog) fwd_new	ggccgcggGCCCCGTCTTACTTTGACCAC	
22		1158_TC013504 (smog) rev_new	cccggggcTCTCTGCGAGCCGAACATAT	
23	T48	T48_Conny_fwd	ATTCGCCCCGAAAGACGAGACT	
24		T48_Conny_rev	CACTCTGAATCCGCAGTGAA	
25		3 A11_T48_fwd	ggccgcggGCCCCAAAGGATGTATCAAA	
26		4 A11_T48_fwd	cccggggcGAGTGGCATGAAGTGCAGAA	
27		1159_TC033934 (T48) fwd_new	ggccgcggTTATAAAGACTGAGGCCCGCA	
28		1160_TC033934 (T48) rev_new	cccggggcCTTTGGGGCCACATTCAGG	
29		1161_TC033934 (T48) fwd_iBeetle	ggccgcggCGACACGCGCTACATTCATT	
30		1162_TC033934 (T48) rev_iBeetle	cccggggcAACAGCACCACAATGTCCAC	

Appendix H: Movies

- 1) Life-Act_wildtype
- 2) Life-Act_*Tc-cta* knockdown
- 3) Life-Act_*Tc-fog* knockdown
- 4) nGFP_wildtype
- 5) nGFP_*Tc-Toll+Tc-fog* double knockdown

Acknowledgements

First and foremost, I would like to thank my supervisor Prof. Dr. Siegfried Roth. Thank you, Siegfried, for giving me freedom and guidance at the same time. For your constrictive criticism and general help during the last years and during writing up this work.

Of course, I would also like to thank the other members of my committee, Dr. Michael Kroiher and Prof. Dr. Ute Höcker. Also Dr. Kristen Panfilio, who was open to numerous discussions during my PhD.

Thanks to Oliver and Stefan, what would be science without the help of our technicians!

Kai, thank you a thousand times for the tons of sweets which served as energy source and soul food! You saved many lives ;-)

Thank you, Salim, you are one of the friendliest persons I've ever met. Stay as open minded as you are and never stop laughing!

Danka and Dennis, I can't find words for both of you! You guys know how to make a normal day special! Thank you for all the professional discussions as well as discussions about the latest Ikea or Aldi product lines ;-) But most important: for your honest friendship!!!

I would like to thank two special men, which always encourage me: Dominik and Thorsten.

Dominik, you took care of me from my first day on. You, guided me through my Bachelor Thesis, my Master Thesis and the first year of my PhD. You taught me all your little tricks to make lab work highly efficient. Thank you very much.

Thorsten, we spend a long time in this lab. You taught me everything about live-imaging. We worked, we discussed, we laughed, and we traveled. Thanks for many amazing hours and your integrity!

Thank you to all former and current members of the lab Waldemar, Rodrigo, Jeremy, Buru, Matt, Matthias and Fabian for being part of this little family.

Of course, I want to thank all my friends and family members who supported me during the last 10 years. Danke Mama, danke Papa! Diese Arbeit ist auch für euch. Danke Sarah, Melanie und Dominic! Ihr seid einfach total verrückt und habt es immer geschafft mich für ein paar Tage alles andere vergessen zu lassen. Ihr seid die Besten!

Last, but most important: Thank you Manuel. We shared our lives for the last 17 years. We went to school, moved to a new city, helped each other during our studies and through the PhD. And still I am not tiered of you! We share our love for science and you are supporting me no matter what I do. I just want to say once more: I love you!

Erklärung zur Dissertation

Ich versichere, dass ich die von mir vorgelegte Dissertation selbständig angefertigt, die benutzten Quellen und Hilfsmittel vollständig angegeben und die Stellen der Arbeit – einschließlich Tabellen, Karten und Abbildungen -, die anderen Werken im Wortlaut oder dem Sinn nach entnommen sind, in jedem Einzelfall als Entlehnung kenntlich gemacht habe; dass diese Dissertation noch keiner anderen Fakultät oder Universität zur Prüfung vorgelegen hat; dass sie – abgesehen von unten angegebenen Teilpublikationen – noch nicht veröffentlicht worden ist sowie, dass ich eine solche Veröffentlichung vor Abschluss des Promotionsverfahrens nicht vornehmen werde. Die Bestimmungen dieser Promotionsordnung sind mir bekannt. Die von mir vorgelegte Dissertation ist von Prof. Dr. Siegfried Roth betreut worden.

Köln, den 13.10.2017

Nadine Frey

Teilpublikation:

Stappert D & Frey N, von Levetzow C, Roth S (2016).

Genome-wide identification of *Tribolium* dorsoventral patterning genes.
Development. 2016 Jul 1;143(13):2443-54. doi: 10.1242/dev.130641.

Lebenslauf

PERSÖNLICHE INFORMATIONEN

Name: Nadine Frey
Geburtstag: 10.10.1986
Geburtsort: Lindau / Bodensee
Nationalität: deutsch

SCHULBILDUNG

09.1993 – 08.1997 **Grundschule Lindau (Aeschach)**

09.1997 - 06.2008 **Abitur at Bodensee-Gymnasium, Lindau**
Leistungskurs: Biologie, Deutsch
Weitere Prüfungsfächer: Englisch, Religion

STUDIENVERLAUF

10.2008 - 09.2011 **B.Sc. in Biologie an der Universität zu Köln**
Bachelor Arbeit: "Conservation of a protein cascade between Nudel and Spätzle - An important step in dorsoventral patterning of *Tribolium castaneum*"

10.2011 - 09.2013 **M.Sc. in "Biological Science" an der Universität zu Köln**
Master Arbeit: "Identification of new dorsoventral patterning genes by differential transcriptome analyses in *Tribolium castaneum*"

PROMOTION

Seit 01.2014 **Promotion an der Universität zu Köln**
Institut für Entwicklungsbiologie
Betreuer: Prof. Dr. Siegfried Roth

PUBLIKATIONEN

Stappert D & **Frey N**, von Levetzow C, Roth S (2016).
Genome-wide identification of *Tribolium* dorsoventral patterning genes. Development. 2016 Jul 1;143(13):2443-54. doi: 10.1242/dev.130641.

Benton MA, Pechmann M, **Frey N**, Stappert D, Conrads KH, Chen YT, Stamatakis E, Pavlopoulos A, Roth S. (2016). *Toll* genes have an ancestral role in axis elongation. Current Biology. 2016;26:1609–1615.doi: 10.1016/j.cub.2016.04.055